Università degli Studi di Bologna

Dipartimento di Elettronica Informatica e Sistemistica

Dottorato di Ricerca in Ingegneria Elettronica ed Informatica

XI Ciclo

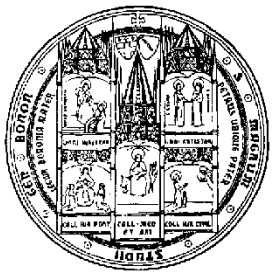

Similarity Search in Multimedia Databases

Tesi di:
Ing. Marco Patella

Coordinatore:
Chiar.mo Prof. Ing. Fabio Filicori

Relatore:
Chiar.mo Prof. Ing. Paolo Tiberio

Relatore Esterno:
Chiar.mo Prof. Ing. Paolo Ciaccia

"What is understood need not be discussed"
Loren Adams

Contents

Chapter 1

Introduction

This thesis presents an approach to similarity search in Multimedia Databases (MMDBs). Altough the terms *multimedia* and *database* have very precise meanings, the concept of *multimedia database* means different things to different people. This should not be so surprising to the reader, since the term *multimedia* implies so many different concepts. We therefore begin our dissertation by precisely defining the scope of our work.

Definition 1.1 (Multimedia database)
A *multimedia database* is a system able to store and retrieve objects made up of text, images, sounds, animations, voice, video, etc. □

The wide range of applications for MMDBs leads to a number of different problems with respect to traditional database systems, which only consider textual and numerical attributes. These problems include:

- data modeling;
- support for different data types;
- efficient data storing;
- data compressing techniques;
- index structures for non-traditional data types;
- query optimization;
- presentation of objects of different types.

1.1 Motivation

In this work, we focus on the task of *querying* and *retrieving* multimedia objects from a MMDB.

Usually, MM systems provide two different modalities to retrieve stored objects:

Browsing. Starting from a set of *high-level* objects, the user can browse and navigate through stored objects to locate those he/she is interested in. Hypermedia systems use *anchors* to allow the navigation through different MM objects.

Querying. If the user is interested in a set of objects all satisfying a particular property, he/she can issue a query to the system, indicating the values of objects' attributes or features. The query is expressed by means of a query language or of a visual query environment; then, the system has to compile, optimize and process the query in order to present the result to the user.

In this work, we will concentrate on the latter retrieval modality.

As for traditional databases, the search process has to be

1. *efficient*, i.e. the time needed to process a query should be in the number of milliseconds/seconds, and

2. *complete*, i.e. all the objects satisfying the query should appear in the result set (no false dismissals are allowed).

It has to be noted that, when querying traditional DBs, the fundamental search operation is that of *matching*. In MMDBs, however, the complexity of stored objects requires for richer search operations. The most common solution is to define a notion of *similarity* between objects, allowing the user to issue *similarity queries* (Chapter 2).

The great heterogeneity of MM data types calls for the specification of access structures able to perform efficient and complete similarity search for a wide range of applications (Chapters 3, 4, and 5). For query optimization purposes, efficient cost models have to be developed for these access structures, in order to predict the cost of accessing them during the search phase (Chapter 6).

Finally, it has to be noted that the traditional approach of querying a DB, i.e. the user issues a query that specifies all the attributes the user is interested in, is not appropriate for MMDBs. Often, the user can use the result of a query to specify a different query, thus activating a *relevance feedback* process. Furthermore, the user can specify different query attributes. Therefore, a MMDB has to deal with *complex* queries (Chapter 7).

1.2 Summary of Contributions

The contributions of this thesis in effective and efficient similarity search are as follows: In this thesis we

1. present a new index structure, the M-tree, for indexing a generic metric space,
2. develop a novel approach to derive cost models to predict performance of metric trees, and
3. present an extension for distance-based access methods to deal with *complex* similarity queries.

1.3 Thesis Outline

This thesis is organized as follows:

- In Chapter 2 we explore the concept of similarity, reasoning about the way the user perceives similarity between stimuli. We then show how the human brain process of similarity assessment can be modeled by means of a metric space, assuming that similar stimuli correspond to "close" objects of such a space. We also introduce two types of similarity queries, namely range and k-nearest neighbors queries.
- In Chapter 3 we deal with the problem of efficient processing of (simple) similarity queries. We start by reviewing existing access methods able to index points in vector spaces (Spatial Access Methods), and we continue by presenting structures able to index objects drawn from generic metric spaces (metric trees).
- In Chapter 4, after showing the major drawbacks presented by existing access methods, and introduce the M-tree, a novel paged dynamic metric tree. We detail algorithms for insertion of objects and split management, which keep the M-tree always balanced. Algorithms for similarity queries are also described. Results from extensive experimentation are reported, considering as performance criteria both I/O and CPU costs.
- In Chapter 5, we present an algorithm for loading the M-tree when the whole dataset is available in advance. The purpose of such algorithm is to speed-up the creation of the tree. Experimental results show that the presented algorithm can significantly improve the index' performance with respect to standard insertion methods, and its performance is comparable to that of other metric trees.

- In Chapter 6 we consider the problem of estimating costs for similarity query processing. Existing cost models for SAMs are reviewed in order to show how their approaches cannot be applied to the generic case of metric spaces. We then introduce the concept of *distance distribution* as the basis for our approach, and consequently develop a concrete cost model for the M-tree. This cost model is experimentally validated, and we show how the same approach can be applied to derive a cost model for the vp-tree access method. Finally, we extend the presented cost model for the M-tree into a *query-sensitive* cost model, i.e. a model which takes into account the "position" of the query object inside the metric space.

- In Chapter 7 we extend our scenario to complex similarity queries, i.e. queries consisting of more than one similarity predicate. Again, we review existing approaches, indicating their major drawbacks. Then, we introduce our approach showing how distance-based access methods, like the M-tree, can be extended to efficiently process single-feature complex similarity queries — queries whose predicates all refer to a single feature. The flexibility of our approach is demonstrated by considering three different similarity languages, and extending the M-tree. Our approach is then experimentally evaluated, evidencing how it can outperform state-of-the-art search algorithms. Finally, we step on to multi-feature queries, showing how the results obtained for single-feature queries can also be exploited in this more general case, provided that access methods "powerful enough" for the value domains at hand exist.

- In Chapter 8, we present a brief discussion on the major limitations of the M-tree access method and show how the structure can be extended in order to overcome such restrictions. In particular, the M-tree is generalized to a new access structure, the M^2-tree, able to index objects drawn from the "product" of multiple domains.

- In Chapter 9, we conclude our work and present some open problems that we plan to investigate in future research.

- Appendix A presents a detailed description of M-tree implementation, showing how the code can be customized for specific applications.

- Finally, in Appendix B, we briefly present a prototype application, using the concepts presented in Chapters 2, 3, 4, and 7, for image retrieval by color content.

Chapter 2

Similarity and Distance

In classical database systems, where most of the attributes are either textual or numerical, the fundamental search operation is *matching*: Given a query object, the system has to determine which DB object is the "same", in some sense, as the query. The result of this type of queries is, typically, a set of objects (the objects in the DB whose attributes match those specified in the query).

In MMDBMSs, however, this kind of operation is not appropriate — with the complexity of multimedia objects, matching is not expressive enough. What is usually needed is a notion of *similarity*: The user could query the DBMS to assess the similarity between each object in the DB and the given query object. In such scenario, the result of a query is a list, where all the DB objects are sorted by decreasing values of similarity with respect to the query object.

Example 2.1
Consider a painting database, where the user can retrieve images by means of a `painter` textual attribute and using a *Query-by-sketch* modality. Now, suppose the user wants to retrieve, say, van Gogh's *Wheat Field Under Threatening Skies* (Figure 2.1 (a)). The user knows that the bottom part of the image consists of a yellow stripe and that there is a dark blue sky background. Thus, he/she draws a sketch as shown in Figure 2.1 (b). If, however, the sketch query is given to the system, the user is returned all the paintings in the DB, sorted for their similarity against the sketched image. If the DB contains several images similar to the query, the user may need to browse the list in order to find the correct painting.[1]

In order to restrict the search, the user could specify the name of the author by issuing a query like

```
painter = 'van Gogh'
```

[1]This could be the case, since wheat fields are a common subject of paintings.

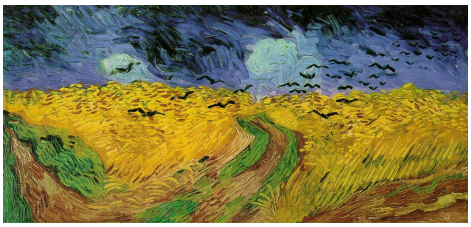

(a)

(b)

Figure 2.1: Van Gogh's *Wheat Field Under Threatening Skies* (a) and the sketch of a query to retrieve it (b).

Now the result of the query is a set of all van Gogh's paintings. Again, since van Gogh was a very prolific painter, the result set can consist of several images, that the user will have to browse.

What the user has in mind, however, is a query like this:

```
(painter = 'van Gogh') and (image = sketch)
```

In this case, the system has to combine a set with a list: What is the result of such a query? Obviously, the user wants to be returned with a list of all van Gogh's paintings sorted with respect to their similarity with the sketched image. If, however, the query is a more complicated one, the answer may not be so intuitive.[2] We will precise these concepts later in Chapter 7. □

2.1 Similarity Search

We now formalize the basic similarity operations that a typical MMDBMS has to deal with. In the following, for the sake of simplicity, we suppose that the database scheme consists of a single collection $\mathcal{C}$ of objects. We will, thus, ignore the actual implementation of $\mathcal{C}$, which, for our purposes, can be represented by a relation, a class, etc., or as a combination of such schemes. Objects (tuples) of $\mathcal{C}$ can be compared by means of a set of relevant features $\mathcal{F}$.[3] The values of each feature $F \in \mathcal{F}$ belong to a domain $\mathcal{D} = dom(F)$.

2.1.1 Similarity Queries

We consider similarity predicates p all having the form $F \sim v$, where $F \in \mathcal{F}$ is a feature, $v \in \mathcal{D}$ is a constant value (the query value), and $\sim$ is a similarity operator. When applied

[2] As an example, consider the query obtained by substituting the `and` operator with an `or` in the previous query.

[3] For instance, images can be compared using attributes like color, texture, shape, etc.

to an object $O \in \mathcal{C}$, the predicate p returns a score (grade) $s(p, O.F) \in [0, 1]$, assessing the similarity (with respect to feature F) of object O to the query value v. Evaluating a predicate p on all the objects of $\mathcal{C}$, thus, yields a "graded set" $\{(O, s(p, O.F)) : O \in \mathcal{C}\}$. For instance, evaluating the predicate `color` $\sim$ `'red'` on an image DB means to assign to each image in the collection a score assessing its "redness". We can also think of a graded set returned by a similarity predicate as corresponding to a sorted list, where the objects of the collection $\mathcal{C}$ are sorted by their grades, i.e. by their similarity to the query value.

The two basic form of similarity queries that we consider are *range* and *nearest neighbors* queries.

Definition 2.1 (Range query)
Given a predicate $p : F \sim v$ and a minimum similarity threshold α, the (simple) *range query* $\texttt{range}(p, \alpha, \mathcal{C})$ selects all the objects in $\mathcal{C}$, along with their scores, such that $s(p, O.F) \geq \alpha$, that is, all the objects whose grade with respect to p is not less than α. □

Definition 2.2 (Nearest neighbors query)
Given a predicate $p : F \sim v$ and an integer $k \geq 1$, the (simple) *nearest neighbor query* $\texttt{NN}(p, k, \mathcal{C})$ selects the k objects in $\mathcal{C}$, along with their scores, having the highest grades with respect to p, with ties arbitrarily broken. □

2.2 Similarity Theories

The concept of similarity has been widely investigated throughout the last century, both in the field of psychology and in that of computer science, attempting to define a theory consistent with the huge amount of experimental data. An important point, discovered by computer scientists only in recent times [SJ98], is the discrepancy between the concepts of similarity in psychology and in computer science. In computer science, usually, the similarity has the target of *recognizing an object under conditions of uncertainty*. There is an object and a model of the same object: The system has to assess if the actual appearance of the object, different from the appearance of the model due to noise, distortion, etc., is consistent with the model itself. Computer scientists, thus, have to define the class of possible transformations that an object can undergo.

The human concept of similarity is completely different: Human mind has to assess the similarity between *different* objects. Thus, there is no way to define a number of deformations to transform an object into another one.

It is, therefore, possible, for computer scientists, to assess the similarity between two rotated images of a cube, since it is easy to model all the possible rotations of a cube in

the space, but the task of assessing the similarity between a cube and a tetrahedron is a difficult one. And an even more difficult task is that of assessing if the image of a cube is more similar to that of a tetrahedron or to that of a sphere.

The concept of similarity for our scenario is that of psychologists, since we want our system to model the behavior of human mind in comparing perceptual stimuli. Therefore, in the following, we will briefly review some of the similarity theories presented by psychologists. Our goal is to obtain a concept of similarity sufficiently "close" to that of human mind, but also useful for the purposes of searching in a database.

Psychologists usually distinguish between *perceived similarity* and *judged similarity* [SJ98]. The judged similarity between two stimuli is usually defined as a real value in the interval $[0, 1]$, such that stimuli judged very similar by human mind have high judged values. The most common definition of perceived similarity in psychology is that of a *distance* function d assessing the dissimilarity between objects in a psychological space. If A, B and C are objects and S_A, S_B and S_C are the stimuli of such objects in a perceptual space, usual features of d are the following (*metric axioms*):

$$d(S_A, S_A) = d(S_B, S_B) \qquad \text{(constancy of self-similarity)} \tag{2.1}$$

$$d(S_A, S_B) \geq d(S_A, S_A) \qquad (S_A \neq S_B) \qquad \text{(minimality)} \tag{2.2}$$

$$d(S_A, S_B) = d(S_B, S_A) \qquad \text{(symmetry)} \tag{2.3}$$

$$d(S_A, S_B) + d(S_B, S_C) \geq d(S_A, S_C) \qquad \text{(triangle inequality)} \tag{2.4}$$

Each of the previous properties, however, has been subject of debate by different similarity theories. The axiom 2.1 of constancy of self-similarity has been refuted by theories proposing that the dissimilarity between two stimuli in the perceptual space also depends on the spatial density of objects around each stimulus, that is, human mind gives higher self-similarity to stimuli that can be easily confused with other ones. The distance function between stimuli S_A and S_B, thus, can be defined as:

$$d(S_A, S_B) = \phi(S_A, S_B) + \alpha h(S_A) + \beta h(S_B) \tag{2.5}$$

where $\phi(S_A, S_B)$ is a function that satisfies the metric axioms and $h(S)$ is the density of stimuli around S. If $\phi(S_A, S_A) = 0$, it is

$$d(S_A, S_A) = (\alpha + \beta) h(S_A) \tag{2.6}$$

thus self-similarity is not a constant and depends linearly on the density of stimuli around the stimulus itself. This model emphasizes the fact that stimuli in "highly populated" areas of the space have a higher self-similarity, because human mind seems to someway "prototypize" such stimuli more than others.

Axiom 2.2 of minimality of the distance function has been refuted by different theories of perception. These theories assert that sometimes an object is identified as another object more frequently than it is identified as itself. Argumentations of such theories, however, seem very feeble, thus the axiom of minimality appears to be well-founded to be included in our considered similarity theory.

Axiom 2.3 states that the distance between stimuli is symmetrical. A number of theories refuted this assumption, showing asymmetries between stimuli due to their different "saliency". What is observed is that, in general, the less salient stimulus is more similar to the more salient than vice versa. The model of Equation 2.5 accounts for violation of the symmetry assumption whenever $\alpha \neq \beta$.

The last axiom 2.4 of triangle inequality is the most attacked assumption. It is, however, the fundamental property that, as we will see in Chapter 4, allows us to organize the collection of objects $\mathcal{C}$ to search it efficiently.

As we have seen, all of the four basic assumptions for the distance function are (at least) questionable. Our model of similarity, however, should be both *effective* (in the sense that should effectively mimic the behavior of human mind in assessing similarity between two stimuli) and *efficient* (in the sense that should efficiently organize the perceptual space in order to answer to similarity queries). This tradeoff between effectiveness and efficiency led us to consider only distance functions that satisfy all of the four metric axioms.

A last remark should be pointed out: The two kinds of similarity — judged and perceived — are, obviously, inversely related, in the sense that high values of perceived distance between two stimuli correspond to low values of judged similarity, and vice versa. It should also be noted that only the judged similarity between two stimuli can be accessed through experimentation.

2.3 Metric Spaces

Taking into account the considerations of Section 2.2, our scenario is the following: The similarity $s(v_x, v_y)$ between two feature values $v_x, v_y \in \mathcal{D}$ is assessed by means of a distance function d, satisfying the metric axioms, and of a correspondence function h, transforming distance values (perceived similarities) into (judged) similarity scores. More precisely:

Definition 2.3 (Metric)
A *metric function* is a non-negative function $d : \mathcal{D}^2 \rightarrow \Re_0^+$ such that, for each $v_x, v_y, v_z \in$

$\mathcal{D}$, the following axioms are satisfied:

$$d(v_x, v_x) = 0 \qquad \text{(non-negativity)} \tag{2.7}$$

$$d(v_x, v_y) > 0 \qquad (v_x \neq v_y) \qquad \text{(positivity)} \tag{2.8}$$

$$d(v_x, v_y) = d(v_y, v_x) \qquad \text{(symmetry)} \tag{2.9}$$

$$d(v_x, v_z) + d(v_z, v_y) \geq d(v_x, v_y) \qquad \text{(triangle inequality)} \tag{2.10}$$

□

Relevant examples of metrics include, among others:

Example 2.2
The Minkowski (L_p) metrics over n-dimensional vector spaces, defined as $L_p(v_x, v_y) = (\sum_{j=1}^{n} (|v_x[j] - v_y[j]|^p)^{1/p}$ $(p \geq 1)$. Special cases of such metrics are the Euclidean (L_2) and the Manhattan — or "city-block" — (L_1) distances. When $p \to \infty$, we obtain the L_∞ metric defined as $L_\infty(v_x, v_y) = \max_{j=1}^{n} \{|v_x[j] - v_y[j]|\}$. □

Example 2.3
The Levenshtein (*edit*) distance over strings, $d_E(s, t)$, which counts the minimum number of edit operations (insertions, deletions, substitutions) needed to transform string s into string t. □

Example 2.4
The Hausdorff metric over sets of points, which is used to compare 2-D shapes and is defined as:

$$d_H(O_x, O_y) = \max\{\delta(O_x, O_y), h(O_y, O_x)\}$$

where $\delta(O_x, O_y) = \max_i \min_j L_p(O_{x,i}, O_{y,j})$ is the maximum L_p distance between a point of O_x and any point of O_y. □

Example 2.5
The normalized overlap distance for set similarity, defined as

$$d_{no}(O_x, O_y) = 1 - \frac{\|O_x \cap O_y\|}{\|O_x \cup O_y\|}$$

□

Example 2.6
Quadratic-form distance functions are widely used in comparing images by means of their color histograms [FEF+94, SK97]. In these cases, in fact, color histograms are represented by n-dimensional points, but a Minkowski metric is not suitable for comparing such

vectors, since there is a correlation between the components (e.g. the color red is more similar than the color green to the color orange).

The quadratic-form distance between histograms h_x and h_y is given by:

$$d_Q(h_x, h_y) = \sqrt{(h_x - h_y)^T A (h_x - h_y)}$$

where element $A_{i,j}$ of the matrix denotes the similarity between the i-th and the j-th colors of the histograms. □

The feature domain $\mathcal{D}$ and the metric d define a *metric space* $\mathcal{M} = (\mathcal{D}, d)$. For our purposes, it is also convenient to assume that such a metric space is bounded, that is, exists a finite $d^+ \in \Re_0^+$ such that, for every $v_x, v_y \in \mathcal{D}$, it is $d(v_x, v_y) \leq d^+$. This last assumption is not essential, and we will only use it in Chapter 6.

In such a scenario, similarity queries defined in Section 2.1.1 can be rewritten as:

Definition 2.4 (Range query)
Given a collection $\mathcal{C}$, a query value $Q \in \mathcal{D}$, and a maximum distance threshold r_Q, the (simple) *range query* $\texttt{range}(Q, r_Q, \mathcal{C})$ selects all the objects in $\mathcal{C}$ such that $d(O, Q) \leq r_Q$, that is, all the objects whose distance from Q does not exceed r_Q. □

Definition 2.5 (Nearest neighbors query)
Given a collection $\mathcal{C}$, a query value $Q \in \mathcal{D}$, and an integer $k \geq 1$, the (simple) *nearest neighbors* query $\texttt{NN}(Q, k, \mathcal{C})$ selects the k closest to Q objects in $\mathcal{C}$, with ties arbitrarily broken. □

The analogy between the definitions of similarity queries and distance queries is evident. These two parallel definitions manifest the correspondence between *judged similarity*, used in similarity queries, and *perceived similarity*, used in distance queries. As we saw in Section 2.2, there is an inverse relationship between these two concepts. This kind of relationship is, in our scenario, materialized in the following

Definition 2.6 (Correspondence function)
A (distance to similarity) *correspondence function* is a function $h : \Re_0^+ \to [0, 1]$ having the following properties:

$$h(0) = 1 \tag{2.11}$$

$$x_1 \leq x_2 \Rightarrow h(x_1) \geq h(x_2) \quad \forall x_1, x_2 \in \Re_0^+ \tag{2.12}$$

□

Intuitively, a correspondence function inversely relates similarity and distance (high distance values correspond to dissimilar objects and, thus, to low similarity scores) and assigns the maximum similarity in case of 0 distance (exact-match).

2.4 Examples

In this Section we will review several approaches to similarity search in a variety of different environments.

2.4.1 Image Retrieval

As we saw in Chapter 1, the use of textual descriptors to search through image databases is largely inadequate. Usually, Image Storage and Retrieval (ISR) systems provide access to content of images by means of image-analysis tools, extracting features like color, shape and texture. Several systems, like Photobook [PPS96] from MIT, QBIC [FSN+95] from IBM, Chabot [OS95], Virage [HGH+96], and VisualSEEk [SC96], all use Content Based Visual Queries (CBVQs) to search in an image database. All these systems use feature-based approaches to index images information.

Color Representation

The distribution of colors in an image is usually represented by an histogram. Each pixel of an image $I[x, y]$ consists of three *color channels* $I = (I_R, I_G, I_B)$, representing red, green, and blue components. These channels are transformed, by way of a *transformation matrix* T_c, into the natural components of color perception, that is, hue, brightness, and saturation. Finally, the three latter channels are quantized, through a quantization matrix Q_c, into a space consisting of a finite number M of colors. The m-th component of the histogram, $h_c[m]$ is given by:

$$h_c[m] = \sum_x \sum_y \begin{cases} 1 & \text{if } Q_c(T_c I[x, y]) = m \\ 0 & \text{otherwise} \end{cases} \tag{2.13}$$

Each image is, therefore, represented by a point in a M-dimensional space. To compare histograms of different images, we can use a metric on such a space. Used metrics include the Manhattan distance L_1, the Euclidean distance L_2, and the histogram quadratic distance d_Q of Example 2.6.

In [SO95], the authors propose an alternate method of color indexing. A 9-dimensional vector, consisting of mean, variance, and skewness of the hue, saturation, and brightness components for all the pixels, is extracted from each image. A method for preserving color locality by dividing each image in 5 regions of fixed size and position, and by computing the 9-dimensional vector for each of the 5 regions, thus obtaining a 45-dimensional vector for each image, is also considered. On these vector, a weighted L_1 metric (with weights empirically computed) is then used to compare images. Though the authors claim that

their method is more efficient than others in finding images with the same content of the query image, in [Smi97] it is shown that the simpler metrics (i.e. L_1 and L_2) provide consistently better performance in retrieving images by color content.

In Appendix B, we describe a sample application of our approach to image retrieval by color content.

Texture Representation

Textures are homogeneous patterns or spatial arrangements of pixels that cannot be sufficiently described by regional intensity or color features. Texture for an image can be represented, as for color, by an histogram. Image texture is first decomposed into nine spatial-frequency subbands, by way of a wavelet filter bank. Then, a texture channel generator is used to produce nine channels, starting from the nine subbands. Again, these texture channels can be transformed (by way of a transformation matrix T_t) and quantized (by way of a quantization matrix Q_t) to produce the final histogram representing the image.

It is beyond the scope of this thesis to describe the mathematical tools used to produce the texture channels from the original image. The only point that we like to emphasize is that the histogram transformation is, typically, applied in order to provide invariance with respect to rotation and scaling of the image.

The representation of texture as an histogram allows us to use, for texture similarity, the same metrics used for color similarity. In particular, in [Smi97] it is shown that L_1 and L_2 metrics perform extremely well in retrieving images having texture similar to that of the query image.

2.4.2 Content-Based Retrieval of Audio Data

Sounds are usually described by psychophysiologists using pitch, loudness, duration, and timbre. While the former three physiological stimuli can be effectively modeled by measurable acoustic features, the timbre feature collects all those acoustic qualities of a sound that cannot be represented by pitch, loudness and duration. In the light of what we expressed in Section 2.2, the timbre feature has to be broken up into its principal components. Salient elements of timbre include the amplitude and the spectral envelope, the harmonicity, etc.

In [WBKW96], only four features — loudness, pitch, brightness, and bandwidth — are used to classify and index sounds. However, since sounds have a duration, it is not sufficient to use only a single value, since above features can vary over time. The average value, the variance of the value over the duration of the signal, and the autocorrelation of

the trajectory over a small lag are computed for each of the four features and form, along with the sound duration, the 13-dimensional vector used to index the sound space. The vectors representing the relevant classes of sounds are then selected by an human expert. The metric used in [WBKW96] to classify the sounds is a quadratic form distance having the form:

$$d_S(x, y) = \sqrt{(x - y)^T R(x - y)}$$

where the matrix R is the inverse of the covariance matrix computed for the vectors representing the classes. If the feature vector elements are reasonably independent of each other, the off-diagonal elements of R can be ignored in the distance computations, thus the metric assumes the form of a weighted L_2 metric.

2.4.3 Face Recognition

Human and machine recognition of faces is a topic that has been subject of investigation by psychophysicists over the last twenty years. The main issues of debate between scientists are the following:

Is face recognition a dedicated process? That is, does exists a face recognition system within the human brain? The existence of such system is supported by several experiments (e.g. the fact that humans have difficulty in recognizing familiar faces when these are presented upside down), thus experts usually agree on this topic.

Is face recognition the result of global or feature analysis? Most studies suggest that human mind recognizes faces by using distinctive features (e.g. a big nose, distant eyes, flapping ears, etc.). However, it is not clear what features are the most distinctive for human recognition of faces.

What is the role of gender and/or race in the process of face recognition? It is well known that humans recognize people from their own race better than people from different races. It is also suspected that the recognition of male faces is slightly different from that of female ones.

All these theories produced a number of different machine recognition systems. Several approaches extract a number of numerical features from the face image (i.e. nose length and width, mouth width and height, face width, chin radius, etc.) all normalized by the interocular distance, in order to provide invariance to image scaling [BP93, KK72, Kan77]. These features form a multi-dimensional vector that is used to represent the corresponding

face. On this multi-dimensional vector space, a simple Manhattan or Euclidean metric is then used to index the face space.

Another approach to face recognition uses the eigenvectors of the covariance matrix of the set of database faces to find the principal components of the faces distribution [TP91]. The basic idea of this approach is the following: A face image of $N * N$ pixels may be considered as a vector of dimension N^2, thus a typical image is represented by a point in a very high-dimensional space. Since face images are very similar in configuration, they will be clustered in a relatively small area of the overall space, and, therefore, can be described as points in a lower-dimensional subspace. The goal of Principal Component Analysis (PCA), or Karhunen-Loeve (KL) expansion, is to find a suitable representation for this subspace. Tipically, this is obtianed by extracting the k most significant eigenvectors of the covariance matrix corresponding to the original face images. The value of the subspace dimensionality, k, has to be high enough to be able to preserve the subspace topology (i.e. different images are to be mapped to different points), but low enough to obtain a compact representation of the subspace. Given the k most significant eigenvectors, the so-called *eigenfaces*, each image is transformed to a point in the "face space" by projecting the face onto the subspace defined by the eigenfaces. Usually the system uses an Euclidean distance L_2 as the metric in the face subspace. The system can now recognize faces by using two distances:

- the distance ϵ between the image and its projection onto eigenfaces, describing the distance of the image to the face space, and
- the minimum distance ϵ_k between the projection of the image and a point in the subspace, corresponding to a face in the original dataset.

If the image is distant from the face space, then it is assumed that the image is not a face. If the face is near to the face space and sufficiently near to a face image, then an individual is recognized, otherwise the image is identified as the face of an unknown person. Both recognizing tasks — that of recognizing the image as a face and that of recognizing a face as a known person — use a threshold θ to define the maximum distance to the face space and to an individual face.

2.4.4 Genomic Databases

A genomic database collects nucleotide sequences, i.e. DNA strings. Each string is composed from a four-character alphabet of *nucleotide bases*, usually represented with letters A, C, G, and T. An important kind of queries that can be issued to the system is the

local sequence alignment [WZ96]. Locally aligned DNA sequences are likely to behave in a similar way. The score of local alignment for two DNA sequences x and y is given by:

$$s(x, y) = \max_i \{c \cdot length_i - gaps_i\} \tag{2.14}$$

where c is a predefined constant, $length_i$ is the total length of alignment i, and $gaps_i$ is a non-negative function that accounts for the gaps in the i-th alignment.

What is usually requested to the system is a set of sequences having a local alignment score with respect to the query sequence q not lower than a given threshold σ, that is:

$$\{x : s(x, q) \geq \sigma\} \tag{2.15}$$

For all the sequences satisfying Equation 2.15, it exists an alignment j such that

$$c \cdot length_j \geq \sigma \tag{2.16}$$

The number of characters in the gaps is given by

$$\|x\| + \|q\| - 2 \cdot length_j \tag{2.17}$$

where $\|\cdot\|$ indicates the length of the string. The number of gaps is greater than or equal to the edit distance between the sequences, i.e. $d_E(x, q)$, when substitutions of characters are not allowed. Thus, from Equations 2.15, 2.16, and 2.17, follows:

$$d_E(x, q) \leq \|x\| + \|q\| - 2\sigma/c \tag{2.18}$$

A local alignment query, therefore, can be transformed into a distance range query with non-constant radius $r = \|x\| + \|q\| - 2\sigma/c$ [CA97].

Chapter 3

Indexing

In the previous Chapter, we discussed about the way of representing MM objects in order to support similarity queries. We presented a generic approach, the feature extraction technique, that can be used by a system to assess the similarity between two objects, by exploiting a distance function. Now, we are faced with the problem of how to efficiently deal with similarity queries.

If our MMDB has a relatively small size, e.g. in the order of hundreds of objects, and the similarity function is computationally unexpensive, a sequential scan of the entire database, followed by a similarity assessment, can be an adequate solution. However, as the size of the database grows, or if the evaluation of similarity between two objects is a non-trivial operation, the sequential scan of the database is not a reasonable arrangement. What is needed is a way to filter out objects that are non-relevant to the query, without dismissing relevant ones. Classical DBMSs use access methods, like indices and other structures, to search through the objects of the database. Quoting from [SZ+96],

> ... Query processing will have to be extended to cover more data types than those handled in today's database products. For example, queries involving sequences (e.g. time series) are becoming more important. Optimization over these structures will require new indexing methods and new query processing strategies.

We have, hence, to find an access method suitable to index MM objects in the considered similarity environment.

The requirements of modern multimedia applications call for access methods having some fundamental features:

Dynamicity. The access structure has to support insertion and deletions of objects from the database.

Scalability. Since the typical size of modern multimedia data repositories is in the order of millions of objects, the access method should perform well also when the size of the database grows.

Efficiency. Unlike typical access structures, which only try to minimize the number of disk I/Os, indices for similarity search also have to take into account CPU costs, since the task of computing the similarity between two objects can be computationally very expensive.

Independence of the data. The access structure should have good performance for all possible data distributions.

Use of secondary storage. Due to the huge amount of data, it is not conceivable to store the entire dataset in main memory. The access structure, therefore, should be able to efficiently exploit secondary (and possibly tertiary) storage devices.

In the previous Chapter, we assumed that our concept of similarity can be modeled by means of a distance function on a suitable metric space. We also saw, through several examples, that this metric space is, in most cases, indeed a vector space, on which a simple L_p metric is used. In this scenario, similarity queries assume the form of *spatial queries*. In order to deal with similarity queries in such spaces, an access method should implement a clustering method — for grouping together similar objects — and a way to represent such clusters for indexing purposes. This means that access structures used to index classical tabular data, like *B-trees*, are not suitable to our goals. This is due to the lack of ordering techniques, among multidimensional points, preserving space proximity. If we try to extend one-dimensional access methods to multi-dimensional data, by sequentially applying a structure to each dimension, the overall approach would be quite inefficient. This is because each access method has to be independently traversed. The potentially high selectivity on each dimension, therefore, cannot be exploited to restrict the search in the remaining ones.

To support spatial search operation, what is needed is a *multidimensional* (or *spatial*) *access method*. In recent times, a plethora of such methods has been proposed, each claiming superior performance and/or generality with respect to others (for a survey, see [Sam89, GG96]). In the following, we will review some of these Spatial Access Methods, showing how they can be used to answer similarity queries.

3.1 Spatial Access Methods

Spatial Access Methods (SAMs) are access structures created to index points and extended objects (such as polyhedra) in a multidimensional vector space.[1] Usually, points corresponding to data objects are stored in *buckets*, each corresponding to a disk page. Each bucket also defines a subspace of the overall vector space; such subspaces are often refferred to as *regions*. In order to access the data buckets, a *directory*, corresponding to a search tree or to a sort of hashing scheme, is provided. The directory implementation and the region splitting algorithm are the distinctive characteristics that differentiate between SAMs. In [SK88], the authors propose a classification taxonomy of SAMs, based on the characteristics of the regions. Regions may:

- have rectilinear or arbitrarily polyhedral shape,
- cover the entire multidimensional space or just those parts containing data points, and
- overlap or be pairwise disjoint.

Common spatial database search operations include [GG96]:

Exact Match Queries. Find all the objects equal to the query object Q.

Point Queries. Find all the objects overlapping the query point Q.

Region Queries. Find all the objects with at least one point in common with the query region Q.

Window Queries. Find all the objects with at least one point in common with the hyper-rectangular query Q.

Containment Queries. Find all the objects containing the query region Q.

Enclosure Queries. Find all the objects enclosing the query region Q.

Adjacency Queries. Find all the objects adjacent to the query region Q.

Nearest Neighbor Queries. Find all the objects with a minimum distance from the query object Q.

[1] Since stimuli are represented by points in a perceptual vector space, in the following we will ignore extended objects, considering only punctual objects.

A study of topological relations that can be exploited in order to deal with such queries with R-trees and similar access structures can be found in [PTSE95]. For our purposes, however, the only interesting search operations that have to be supported by a SAM are those defined in Section 2.3, i.e. range (window) and nearest neighbors queries. It is easy to see (Figure 3.1) that a range query $\texttt{range}(Q, r_Q, \mathcal{C})$ defines a region of the space, centered on the query value and whose shape depends on the used metric.[2] For example, range queries correspond to (hyper-)diamonds for the L_1 metric, to (hyper-)spheres for L_2, and to (hyper-)cubes for L_∞.

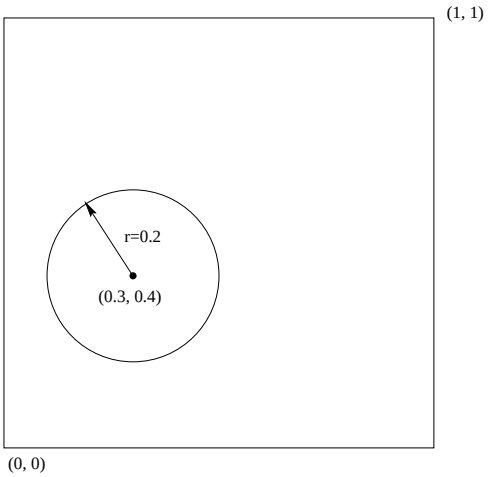

Figure 3.1: The range query $\texttt{range}((0.3, 0.4), 0.2)$ in the real plane with the Euclidean L_2 metric.

In order to answer to such queries, we have to return all the objects in $\mathcal{C}$ corresponding to points inside the query region. For this goal, all the buckets whose region overlaps the query region have to be accessed, and the points contained herein checked. The purpose of the directory of the index structure, therefore, is to minimize the number of accessed pages (and of computed distances as well) for accessing all and only those buckets overlapping the query region.

In the following, we will concentrate on data-partitioning indices, i.e. access structures dividing the data space according to the distribution of data points, and, in particular, on the R-tree-like family. The motivation for this choice is the superior search performance of such indices with respect to space-partitioning methods that divide the data space along predetermined hyper-planes, like the quadtree [FB74] and the grid-file [NHS84].

[2]Nearest neighbor queries, as we will see later in Chapter 4, can be represented as range queries with a variable radius.

3.1.1 The R-tree and Related Structures

The R-tree [Gut84] indexes D-dimensional points by way of a height-balanced hierarchy of nested hyper-rectangles. Each node N of the tree corresponds to a disk page and to a D-dimensional box I_N. The semantics of such boxes is the following:

- If N is a leaf of the tree, I_N corresponds to the Minimum Bounding Box (MBB) of the points stored in N, i.e. the smallest hyper-rectangle that spatially contains all the data points stored in the node itself.
- If N is an internal node, I_N is the MBB of all the hyper-rectangles corresponding to the descendants of N.

Nodes at the same level of the tree may also overlap. Following the taxonomy of [SK88], R-trees have rectilinear regions that cover only those parts of the space containing data points and that may overlap.

Finally, a minimum and a maximum node utilization are present, such that if the number of objects within a node grows beyond the maximum threshold, a node split is triggered, whereas if the minimum threshold is reached, the node is deleted and its descendants are distributed among sibling nodes.

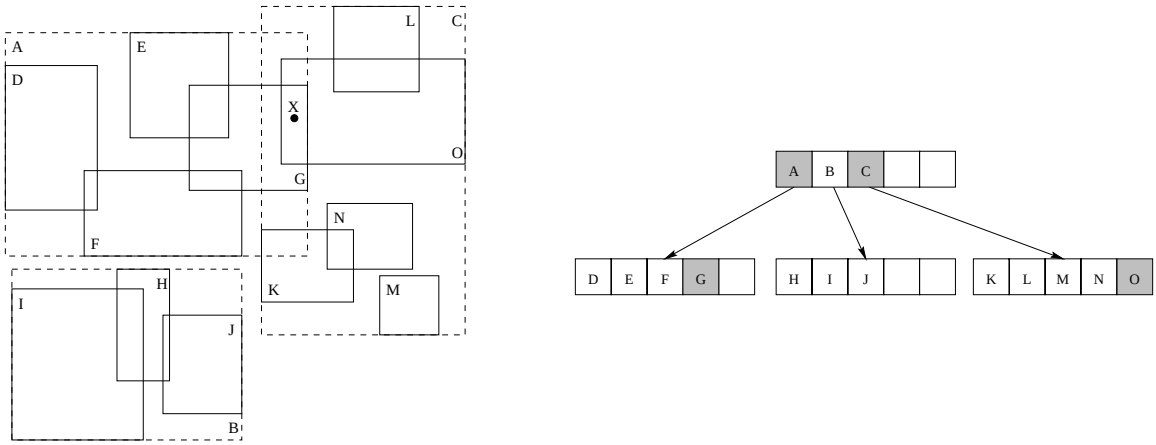

Figure 3.2: Searching in an R-tree. In order to retrieve point X, two different paths have to be traversed, A → G and C → O.

Searching in an R-tree is very easy. For a range query $\texttt{range}(Q, r_Q, \mathcal{C})$, we have to find those points of $\mathcal{C}$ contained within the region implicitly defined by the query. Such points are stored within those leaf nodes overlapping with the query region. At each level of the tree, therefore, all and only those nodes are accessed, whose region overlaps the query region. Due to the fact that node regions may overlap, even an exact match point

query, i.e. a range query with radius equal to zero, may lead to multiple search paths (see Figure 3.2). This fact, however, affects performance, introducing additional search costs.[3] In order to minimize search costs, in [Gut84] the author points out that the total volume covered by the index regions has to be minimized. This is because, during the search phase, a node is accessed only if its region overlaps the search region, thus smaller nodes have a lower probability to be accessed. The goal of minimizing regions' volume is pursued during both the insertion and the node splitting phases:

- When inserting a new point in the index, at each level a node is chosen, for which the least volume enlargement of the corresponding region is needed. In case of ties, the node corresponding to the smallest region is chosen.

- During splitting, the entries of the overflown node are to be divided into two nodes, with the goal of minimizing the volume of such nodes. Three algorithms are proposed: An exhaustive algorithm, considering all possible groupings and choosing the best one, and two quicker but non-optimal split algorithm, one having a quadratic complexity in the number of entries and one with linear complexity.

Another cause of inefficiency, not considered in [Gut84], is the overlap of node regions, leading to multiple paths searches. In [SRF87] the authors propose the R^+-tree, an R-tree-like structure that uses a clipping technique to overcome the problems caused by overlaps. The main idea is that objects intersecting with more than one index region have to be stored on multiple pages. The result of this technique is that a single path traversal of the tree is needed to search for each point query. In case of range queries, however, the index performance can even decrease, with respect to the original R-tree organization, due to the objects replication leading to lower storage utilizations.

Another variant of the R-tree, the R^*-tree, is proposed in [BKSS90]. Following a thorough study of R-tree performance with different data distributions, the authors propose two major modifications.

1. Instead of splitting an overflown node, the R^*-tree introduces the *forced reinsertion* technique: A number of entries is removed from the overflown node and reinserted into the tree at the same level of the overflown node. The goal of this technique is to achieve a dynamic reorganization of the tree. If a node is overflown after reinsertion, it is split.

2. The other modification concerns the splitting phase. The original R-tree policy only tries to minimize the overall regions volume. The authors introduce further objectives for their splitting algorithm:

[3] For SAMs, the only considered costs are typically I/O accesses.

- The overlap between node regions has to be minimized.
- The length of the regions' perimeter should be minimized.
- The volume covered by internal nodes has to be minimized.
- Storage utilization should be maximized.

Comparison of experimental results show that the R*-tree outperforms the R-tree as to search performance. This is the main reason for the world-wide success of this access structure, which has been used in several DBMSs for spatial data.

In [KF94], the authors propose a new structure, the *Hilbert* R-tree, achieving a better clustering of data within each node. This is obtained by using a space filling curve, namely the Hilbert curve, associating an Hilbert Value to each point, and storing, within each node N, the Largest Hilbert Value (LHV) of the data contained in the sub-tree rooted at N. LHV is then used during the insertion phase to find the most suitable leaf node in which the new entry is to be stored. Together with a revised split policy, the authors claim superior performance with respect to R*-tree.

The X-tree [BKK96] uses a different directory structure with respect to R-tree. The authors claim that the main problem for R-tree-like structures is the overlap of the bounding boxes in the directory, which grows as the dimensionality of the space increases. To avoid this problem, a new splitting algorithm is introduced to minimize the overlap, together with the concept of *super-nodes*, i.e. variable size directory nodes, that can be read faster with a sequential scan. The goal is to avoid splits of directory nodes that would result in high overlaps. If there is no "good" split for an overflown node, the node is not split and its size is extended by the size of a standard node. Experimental results show a significant improvement over R*-tree for space dimensionalities $D \geq 16$.

In [WJ96] the SS-tree is presented as a dynamic structure for similarity indexing. The main difference with R-tree is that the SS-tree uses bounding hyper-spheres rather than hyper-rectangles for the shape of nodes regions. Since a rectangle in a D-dimensional space is defined by $2D$ values, i.e. the position of a pair of opposite vertices, whereas a sphere is defined by the position of the center point and a radius, the fanout of a SS-tree is higher than that of a R-tree. This can lead to better performance in high dimensional spaces. However, search performance suffers from the high overlap between spheres and the high volume of nodes regions.

To overcome the problems of the SS-tree, in [KS97] the SR-tree is proposed, using intersections of spheres and rectangles as nodes regions. Each node, therefore, stores a bounding hyper-sphere and a bounding hyper-rectangle, and the actual node region is given by the intersection of the two. This reduces the overall volume of nodes regions

and the overlap in the directory, thus improving index performance during search phase. However, since each node should store the definition of both a rectangle and a sphere, the nodes fanout is considerably reduced, thus leading to a lower memory utilization.

3.1.2 The Curse of Dimensionality

All the presented methods for index multi-dimensional data have very bad performance in high-dimensional spaces, i.e. when the space dimensionality is higher than, say, 20. What is observed is that, even for range queries with very low selectivity, i.e. with very low volume, all of the index nodes are accessed. This effect has been named, by researchers in the area, the *curse of dimensionality*. In these cases, of course, a sequential scan of the entire database has to be preferred. In order to understand the reasons for this behavior, we first have to point out the fact that, for dimensions higher than 3, our intuition completely fails, since we have no geometric view of the space. As an example, consider the following situation:

Example 3.1
Suppose we have to draw, in the D-dimensional hyper-cube $[0,1]^D$, an hyper-sphere centered in the point $p = (0.3, 0.3, \ldots, 0.3)$ touching all the $(D-1)$-surfaces of the space. The smallest of such spheres will have radius 0.7. We want to know if the center point of the space $cp = (0.5, 0.5, \ldots, 0.5)$ is inside that sphere. Geometric intuition says that, since the sphere touches every surface of the space, the center point will be included in the hyper-sphere. For $D = 16$, however, it is $L_2(p, cp) = \sqrt{\sum_{i=1}^{16}(0.5 - 0.3)^2} = 0.8$, thus the center point of the space is outside of the sphere. □

In [BBK98] it is shown that one of the major problems of R-tree-like indices is their *balanced* split policy, It is known that, for low-dimensional spaces, it is advantageous to have hyper-cubic regions, in order to minimize their perimeter [BKSS90]. To achieve such goal, nodes are usually split in a balanced way, i.e. such that each new node contains almost half of the data stored in the overflown node. What is observed is that the data space cannot be split in every dimension. As an example, consider a 20-dimensional space with data points uniformly distributed: Splitting the space at least once in each dimension would lead to an index of $2^{20} \approx 1,000,000$ leaf pages containing 20,000,000 objects, supposing an average storage utilization of 20 entries per page. Thus, with less objects, the data space is split only on a number $D' < D$ of dimensions. Nodes regions are, therefore, extended to the whole $[0,1]$ interval in $D - D'$ dimensions. This is also a major flaw of space-partitioning methods: If the space is divided along a number of dimensions, the great majority of the partitions are empty.

Another problem is given by the relation existing between the dimensionality of the space and the radius of a range query. If we suppose an uniform distribution of data points in the D-dimensional space, in order to achieve a certain selectivity s for the query, the query radius r_Q has to be chosen accordingly. For example, if we consider the L_∞ metric, the query radius r_Q is given by

$$r_Q = \sqrt[D]{s}/2$$

Thus, the query region would be an hyper-cube with side length q equal to $2r_Q$. For $D = 20$ and $s = 0.01\%$, it is $q = 2r_Q = \sqrt[20]{0.0001} \approx 0.63$.

From the above consideration, it is easy to see that, in high-dimensional spaces, almost every reasonable range query has to touch every page of the index. In [BBK98] this effect is accurately modeled, showing that for $D > 10$ all of the pages of the index are accessed during a range search. In [WSB98] it is shown that data-partitioning methods based on hyper-rectangular regions, like R-tree and X-tree, and on hyper-spherical regions, like SS-tree, degenerate if the dimensionality is higher than a certain threshold $\bar{D}$. In this case, all of the index nodes are acessed and, of course, a sequential scan of the dataset has to be preferred. Analytical studies show that this threshold is reached for $\bar{D} \approx 20$.

Another reason for the difficult indexing of high-dimensional spaces is the fact that, for uniformly distributed datasets, almost every point is near a surface of the space. In Figure 3.3, the probability that a point is closer than x to any $(D-1)$-dimensional surface of the space, $\Pr(x)$, is plotted for different values of x as a function of D, for uniformly distributed points in the D-dimensional hyper-cube. This probability is given by the total volume of the space minus the volume of the hyper-cube obtained by subtracting x twice for each dimension, that is:

$$\Pr(x) = 1 - (1 - 2x)^D$$

The graph shows that this probability steadily increases for growing dimensionalities, e.g. for $x = 0.1$, it is $\Pr(x) = 97\%$ when $D = 16$. Hence, for $D = 16$, only 3 points out of 100 are farther than 0.1 to all the surfaces of the space. This suggests that, for high-dimensional spaces, an effective index structure should take this effect into account, proposing a different clustering technique for objects near the surface. In [BBK98] the pyramid-tree is introduced as a first step towards this direction.

3.2 Metric Trees

In the previous Section, we described Spatial Access Methods, showing how they can be used to index multi-dimensional vector spaces. Besides problems deriving from the

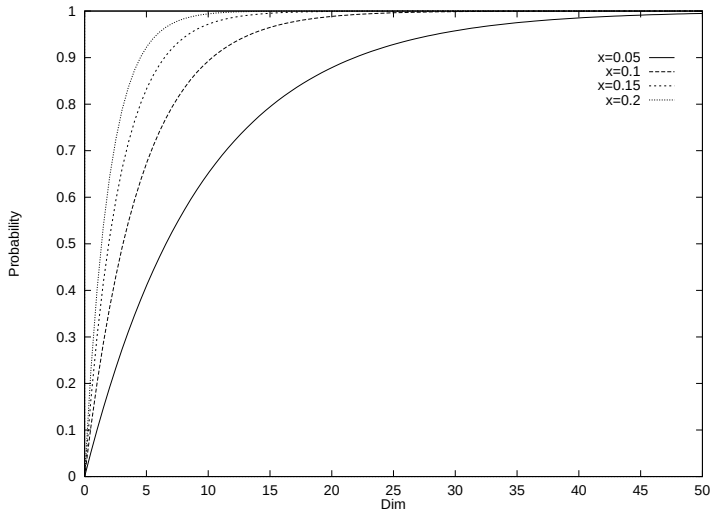

Figure 3.3: The probability $\Pr(x)$ that a point is closer than x to any surface of the space, as a function of the space dimensionality.

so called dimensionality curse, two major issues prevent the use of SAMs for generic similarity search environments:

1. We showed, in Section 3.1, that, in order to retrieve all the objects satisfying a generic range query, all of the index nodes overlapping the query region are to be accessed. Assessing if two regions overlap is an easy task if the used metric is a simple one, but can be very difficult if the metric is complex, e.g. a quadratic form distance.

2. SAMs can only index multi-dimensional vector spaces; thus, they are completely useless for those environments where similarity between objects is assessed by means of a non-vectorial distance function, e.g. for genomic databases (see Section 2.4.4).

3. When considering SAM performance, only I/O costs are considered, and CPU costs ignored, on the assumption that the comparison between two points is not computationally expensive. In cases where this assumption is not true, e.g. in very high dimensional spaces, the computation of the distance function cannot be ignored. An additional optimization is therefore needed, in order to minimize the number of computed distances.

The first of these problems can be overcome by using a *lower bounding distance function* [SK98].

Definition 3.1 (Lower bounding distance function)
If $d_O : \mathcal{D}^2 \rightarrow \Re_0^+$ is a (complex) distance function, we say that $d_f : \mathcal{D}^2 \rightarrow \Re_0^+$ is a *lower bounding distance function* of d_O ($d_f \leq d_O$), if d_f is an underestimate of d_O, that is:

$$d_f(v_x, v_y) \leq d_O(v_x, v_y) \qquad \forall v_x, v_y \in \mathcal{D}$$

□

The basic idea is to use a simple distance function (e.g. a Minkowski metric) as an approximation of the "real" distance function. In such cases, in order to answer to a range query, the index is searched using the lower bounding distance. Then, all and only those objects contained in the result of the query are exactly evaluated against the query value through a refinement filtering step, using the *real* distance.[4]

The lower bounding property is essential to prevent *false dismissals*, i.e. objects satisfying the query but not returned in the result. Of course, indexing the space is useful only if the lower bound is "tight", i.e. if the approximating distance is sufficiently close to the real distance for every pair of objects. Otherwise, the cardinality of the *candidates* set, i.e. the set returned by the index search phase, would be very high and the filtering step will compute the complex distance between the query value and almost all the objects of the dataset. Obviously, in this case a sequential scan of the database would be a quicker solution.

The second problem for SAMs can be solved in a similar manner. It is, however, very difficult to find a lower bounding distance function for arbitrarily complex metrics. Moreover, some metrics have to be mapped to very high-dimensional spaces, where SAMs are completely uneffective, as we saw in Section 3.1.2. As an example, consider the edit distance between strings. This metric can be approximated by a vector distance function in a space whose dimensionality is proportional to the length of the indexed strings. In genomic DBs, proteic sequences can be composed of hundreds of terms, thus the target vector space will have a *very* high dimensionality, well beyond the threshold for the usefulness of SAMs.

These considerations led to the development of *metric trees* [Uhl91]. A generic definition for a metric tree is the following:

Definition 3.2 (Metric tree)
A *metric tree* is an index structure having the following characteristics:

1. Leaf nodes store (pointers to) the data objects.

[4] A similar, but more complex, procedure is used for nearest neighbor queries; an optimal algorithm is presented in [SK98].

2. A region of the space is associated to each node.

3. The region associated with the root node corresponds to the whole space.

4. Regions associated to the children nodes of node N are enclosed in the region associated to node N.

5. The region associated with node N is such that all the objects stored in the sub-tree rooted at node N are contained within the region itself.

□

Regardless of the specific space partitioning algorithm, metric trees aim at grouping together objects that are close to each other and at separating distant objects.

Searching in a metric tree involves accessing all the nodes whose sub-tree could store objects contained in the region associated with the query. How this task has to be accomplished depends on the space decomposition of the considered metric tree.

In [Uhl91], the author points out two different decompositions of a metric space:

1. the *ball* decomposition, and

2. the *generalized hyperplane* decomposition.

In the ball decomposition, the space is dissected using a single object v. The regions associated with nodes correspond to spherical cuts around v. In the generalized hyperplane decomposition, the space is broken up using two different objects v_x and v_y. The generalized hyperplane (GH) between the two points is defined as the set of objects v satisfying the equation $d(v_x, v) = d(v_y, v)$. The two regions, thus, are defined as the set of points that are closer to one object than to the other. These two methods originated several index structures that we outline in the following sections.

3.2.1 The vp-tree

The *vantage-point tree*, proposed in [Yia93], is based on the ball decomposition strategy; therefore, the space is decomposed using spherical cuts around so-called *vantage points*. In a binary vp-tree, each internal node has the format $[O_v, \mu, ptr_l, ptr_r]$, where O_v is the vantage point (i.e. an object of the dataset chosen using a specific algorithm), μ is (an estimate of) the median of the distances between O_v and all the objects reachable from the node, and ptr_l and ptr_r are pointers to the left and right child, respectively. The left child of the node indexes the objects whose distance from O_v is less than or equal to μ, while the right child indexes the objects whose distance from O_v is greater than μ. The

same principle is recursively applied to the lower levels of the tree, leading to an almost balanced index.

The search algorithm for a range query $\texttt{range}(Q, r_Q, \mathcal{C})$ is the following:

1. If $d(Q, O_v) \leq r_Q$, then insert O_v in the result set.
2. If $d(Q, O_v) + r \geq \mu$, then recursively search in the node pointed by ptr_r (right branch).
3. If $d(Q, O_v) - r \leq \mu$, then recursively search in the node pointed by ptr_l (left branch).

In [Chi94] the vp-tree structure is enhanced to deal with nearest neighbor queries.

The binary vp-tree can be easily generalized into a multi-way vp-tree, having nodes with a higher fanout, by partitioning the distance values between the vantage point and the data objects into m groups of (almost) equal cardinality. Then, the distance values $\mu_1, \ldots, \mu_{m-1}$ used to partition the set are stored within each node, replacing the median value μ. Such values are referred to as *cutoff* values. Figure 3.4 shows the root node of a 3-way vp-tree and the corresponding space partitioning.

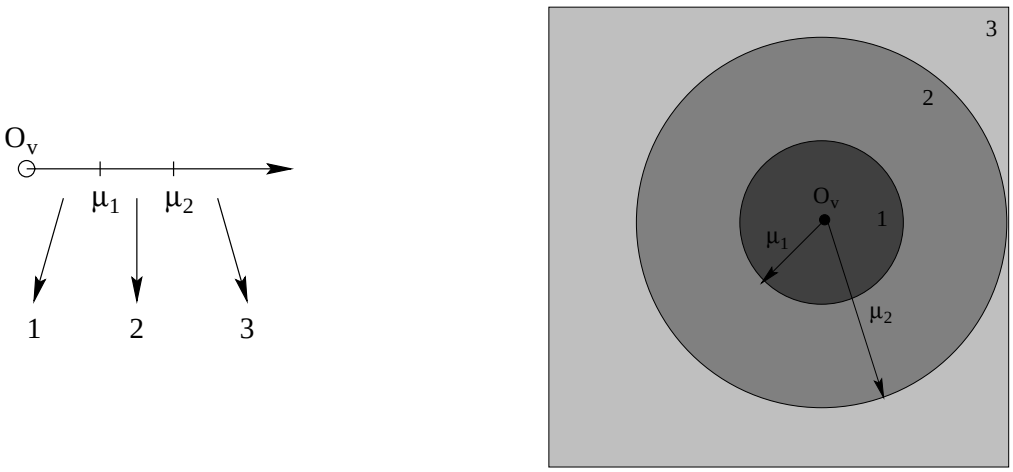

Figure 3.4: A node of a 3-way vp-tree and the relative space partitioning.

3.2.2 The mvp-tree

The *multi-vantage-point tree* [BÖ97] is a generalization of the vp-tree. Unlike the vp-tree, however, the space is partitioned using more than one vantage point at each level, and extra information for data objects is kept in the leaves in order to effectively prune the search space. An mvp-tree is characterized by 4 parameters:

1. the number of vantage points in every node (in [BÖ97] only 2 vantage points are considered),

2. the number of partitions created by each vantage point (v),

3. the maximum capacity of leaf nodes (f), and

4. the number of distances to be stored for the data objects at leaves' level (p).

In each node of the mvp-tree, the first vantage point divides the space into v parts using $v-1$ cutoff values, while the second vantage point divides each of these parts in v partitions, using $v-1$ cutoff values for each partition. In Figure 3.5 it is shown how a spherical shell partition can be split using a different vantage point. To partition the space in v spherical cuts, the data objects are ordered with respect to their distances from the vantage point, and then divided in v groups of (almost) equal cardinality. The $v-1$ distance values used to partition the data space (the cutoff values) are stored in each internal node of the tree. The v^2 groups of data objects are, then, recursively indexed by the v^2 children of the root node. The fanout of each node, thus, is v^2 (in general, it is v to the power of the number of vantage points).

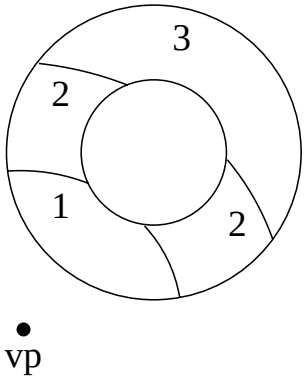

Figure 3.5: How a spherical shell partition can be split using a different vantage point.

The leaf nodes of the tree store the exact distances between the f data objects and the 2 vantage points of that leaf, as well as the $f \cdot p$ distances between each data object x and the first p vantage points along the path from the root to the leaf node containing x.

During the construction phase, at each level, the first vantage point is chosen randomly, while the second vantage point is the farthest object from the first vantage point. This, as stated in [Sha77], increases the effectiveness of the data space partitioning during the search phase.

The search algorithm for the mvp-tree is similar to that of the vp-tree, but the cutoff values for both vantage points in every node are used to prune the search and to avoid distance computations.

3.2.3 The gh-tree

The *generalized hyperplane tree* is based on the GH decomposition proposed in [Uhl91]. For each node of the tree, two objects are chosen. Then, the remaining objects are partitioned, based on which of the two chosen objects they are closer to. Again, the same principle is recursively applied to lower levels of the tree.

The major limitations of this structure is the low fanout of each node, which is limited to two, and the fact that the structure tends to be unbalanced.

3.2.4 The GNAT

To overcome the low fanout problem of gh-trees, in [Bri95] the *Geometric Near-neighbor Access Tree* (GNAT) was proposed, which is based on the concept of *Dirichlet domains*.[5]

At each level of the tree, k *split points* $\{x_1, \ldots, x_k\}$ from the dataset are chosen. The remaining objects in the dataset are then divided into the k Dirichlet domains D_{x_i} $(i = 1, \ldots, k)$ of the split points. For each pair of split points (x_i, x_j) the interval $range(x_i, D_{x_j}) = [\min_d(x_i, D_{x_j}), \max_d(x_i, D_{x_j})]$ is computed, representing the minimum and the maximum of $d(x_i, x)$, $\forall x \in D_{x_j} \cup \{x_j\}$. The same approach is then recursively applied to each D_{x_i}, possibly using a different value for k, the node degree, in order to obtain a height-balanced tree. Figure 3.6 shows a sample GNAT.

For a range query $\texttt{range}(Q, r_Q, \mathcal{C})$, the GNAT is recursively searched in the following way:

1. Let P represent the set of split points in the current node.
2. Choose a point x_i from P (never the same one twice); if $d(Q, x_i) \leq r_Q$, add x_i to the result.
3. $\forall x_j \in P$, if $[d(Q, x_i) - r, d(Q, x_i) + r,] \cap\ range(x_i, D_{x_j}) = \emptyset$, remove x_j from P.
4. Repeat steps 2. and 3. until all the objects in P have been tried.
5. $\forall x_j \in P$, recursively search D_{x_j}.

[5] Given a set of points $\{x_1, \ldots, x_k\}$, the Dirichlet domain of x_i consists of all possible objects of the space wich are closer to x_i than to any other point $x_j (j \neq i)$.

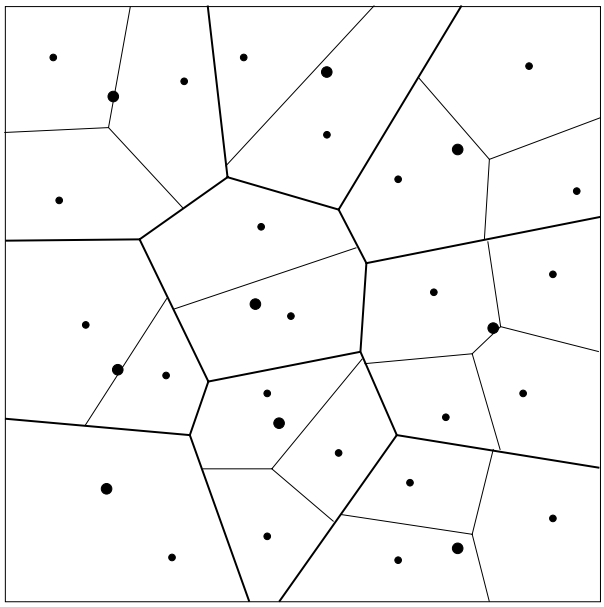

Figure 3.6: A simple GNAT in the real plane with the Euclidean distance.

Chapter 4

The M-tree

In the previous Chapter, we pointed out the required features for an access structure that would have to deal with similarity queries in a MMDBMS, i.e. dinamicity, scalability, efficiency, independence of the data, and use of secondary storage. All the access structure that we reviewed in the previous Chapter, however, fail the test:

- SAMs have good properties of dinamicity and scalability, and efficiently exploit secondary storage devices, but are restricted to vector spaces.
- Some metric trees, like vp- and mvp-trees, are balanced, hence providing a good scalability, but are static, since they are built in a top-down manner.
- Other metric indices, like GNAT, are, at least in principle, dynamic but not balanced.
- Moreover, all known metric trees are memory-resident and do not use secondary storage.

To overcome these problems, in [CPZ97] we presented the M-tree, a dynamic, paged, and height-balanced metric tree.

4.1 Basic Principles

The M-tree organizes the objects into fixed-size nodes.[1] Each node can store up to M entries — this is the *capacity* of M-tree nodes. (The features of) DB objects are stored into leaf nodes, whereas internal nodes store the so-called *routing objects*. A routing object is a database object to which a routing role is assigned by a specific, called *promotion*,

[1] Nothing would prevent using variable-size nodes, à la X-tree [BKK96]. For simplicity, however, we do not consider this possibility here.

algorithm (see Section 4.4). An entry for a routing object O_r also include a pointer, denoted $ptr(T(O_r))$, which references the root of a sub-tree, $T(O_r)$, called the *covering tree* of O_r, a *covering radius* $r(O_r) > 0$, and $d(O_r, P(O_r))$, the distance to the parent object $P(O_r)$, i.e. the routing object which references the node where the O_r entry is stored.[2]

$$entry(O_r) = [O_r, ptr(T(O_r)), r(O_r), d(O_r, P(O_r))]$$

The semantics of the covering radius is the following: All the objects stored in the covering tree of O_r are within the distance $r(O_r)$ from O_r, i.e. $\forall O_i \in T(O_r)$, $d(O_r, O_i) \leq r(O_r)$. A routing object O_r, hence, defines a region in the metric space $\mathcal{M}$, centered on O_r and with radius $r(O_r)$ (see Figure 4.1).

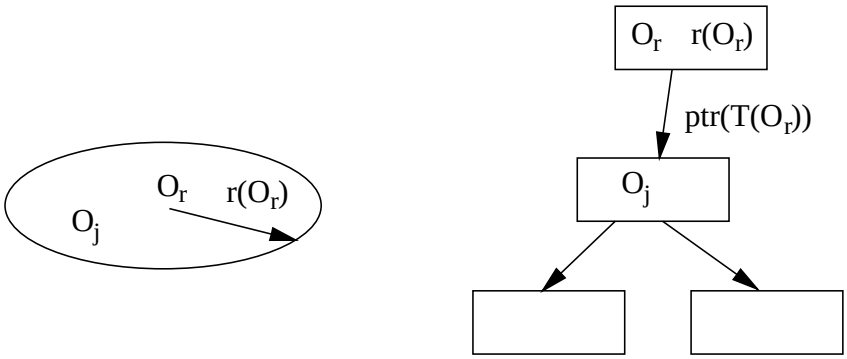

Figure 4.1: A routing object O_r has a covering radius $r(O_r)$ and references a covering tree $T(O_r)$.

For each (*ground*) DB object, one entry having the format

$$entry(O_j) = [O_j, oid(O_j), d(O_j, P(O_j))]$$

is stored in a leaf node, where $oid(O_j)$ is the identifier of the object, which is used to provide access to the whole object resident on a separate data file.[3]

The M-tree, therefore, organizes the space into a set of (possibly overlapping) regions, to which the same principle is recursively applied. The covering radius, $r(O_r)$, and the distance between the object and its parent object, $d(O_r, P(O_r))$, both stored in each entry of the tree, are used to "prune" the search space during the search phase (see Section 4.2).

Figures 4.2, 4.3, and 4.4 show three sample M-trees, built on the same 2-D synthetic dataset, but with different metrics: In Figure 4.2 we used the Manhattan distance (L_1),

[2] Obviously, this distance is not defined for entries in the root of the M-tree.

[3] Of course, the M-tree can also be used as a primary data organization, where the whole objects are stored in the leaves of the tree.

for Figure 4.3 we used the Euclidean distance (L_2), while in Figure 4.4 we used the L_∞ metric. Green regions correspond to leaf nodes whereas level 1 nodes are shown in red.

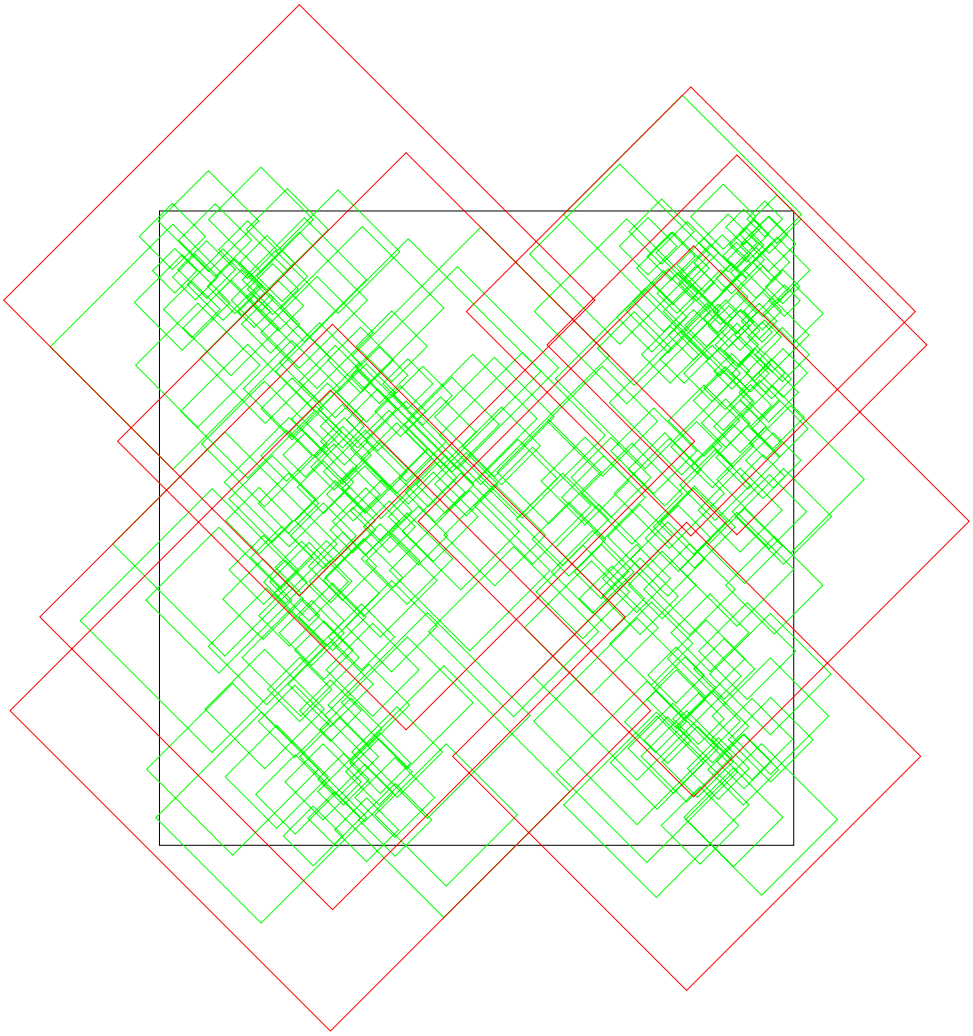

Figure 4.2: A sample M-tree on the $[0, 1]^2$ domain with the L_1 distance.

4.2 Searching the M-tree

Before presenting specific algorithms for building the M-tree, we show how the information stored in nodes is used for processing similarity queries. Clearly, the performance of search algorithms is largely influenced by the actual construction of the M-tree, even though the *correctness* and the logic of search are independent of such aspects.

In order to minimize both the number of accessed nodes and computed distances, all the information concerning (pre-computed) distances which are stored in the M-tree

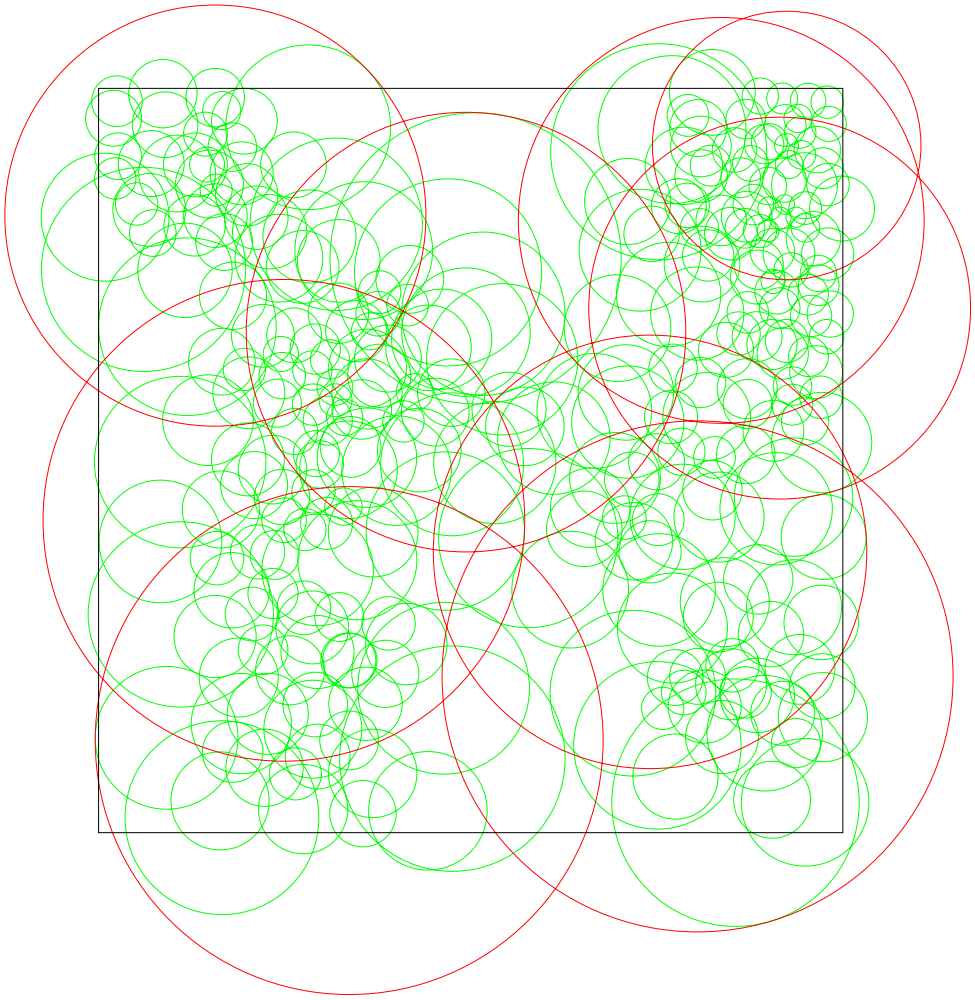

Figure 4.3: A sample M-tree on the $[0, 1]^2$ domain with the L_2 distance.

nodes, i.e. $d(O_i, P(O_i))$ and $r(O_i)$, is used to efficiently apply the triangle inequality property.

4.2.1 Range Queries

According to Definition 2.4, the query `range`$(Q, r_Q, \mathcal{C})$ requests for all the database objects O_j, such that $d(O_j, Q) \leq r_Q$. Therefore, the algorithm `RS` (Range Search) has to follow all such paths in the M-tree which cannot be excluded from leading to objects satisfying the above inequality. Since the query threshold, r_Q, does not change during the search process, and provided the response set is required as a unit, the order with which nodes are visited has no effect on the performance of `RS` algorithm. The `RS` algorithm is given in Figure 4.5.

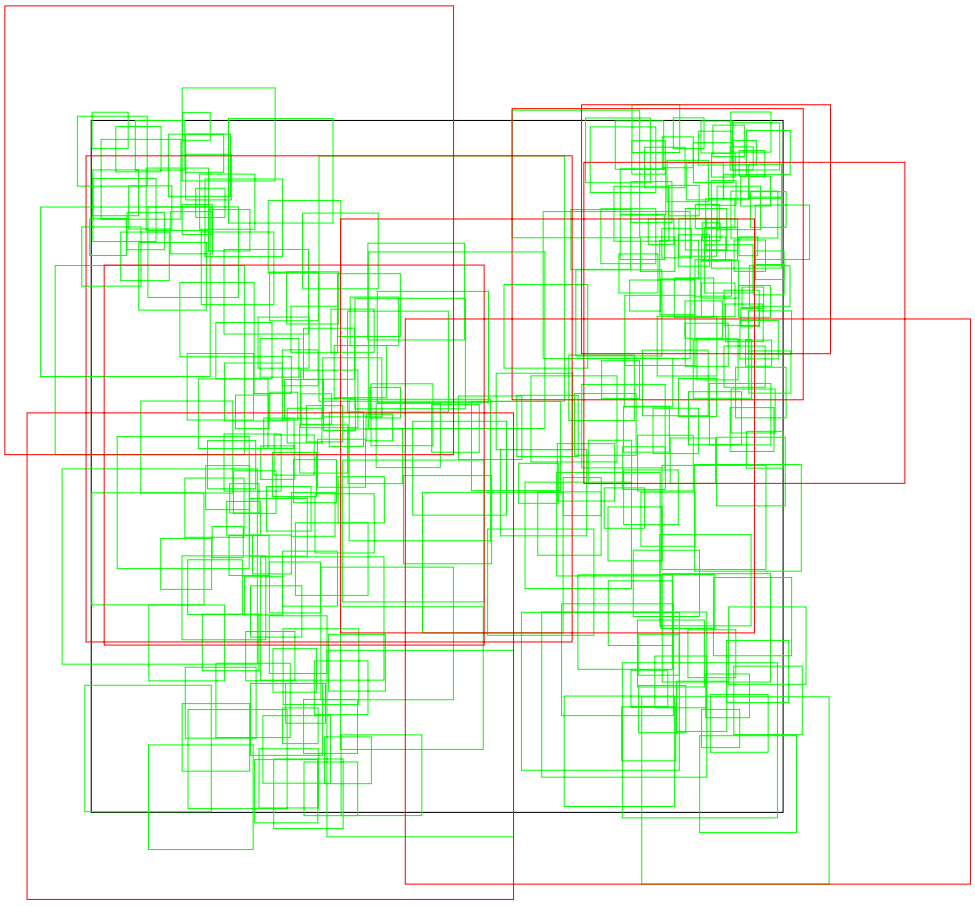

Figure 4.4: A sample M-tree on the $[0,1]^2$ domain with the L_∞ distance.

Since, when accessing node N, the distance between Q and O_p, the parent object of N, has already been computed, it is possible, by applying the triangle inequality, to prune a whole sub-tree without computing any new distance at all. The condition for pruning is as follows.

Lemma 4.1
If $d(O_r, Q) > r_Q + r(O_r)$, then, for each object O_j in $T(O_r)$, it is $d(O_j, Q) > r_Q$. Thus, $T(O_r)$ can be safely pruned from the search.

Proof: Since $d(O_j, O_r) \leq r(O_r)$ holds for any object O_j in $T(O_r)$, it is

$$\begin{aligned} d(O_j, Q) &\geq d(O_r, Q) - d(O_j, O_r) && \text{(triangle inequality)} \\ &\geq d(O_r, Q) - r(O_r) && \text{(def. of covering radius)} \\ &> r_Q && \text{(by hypothesis)} \end{aligned} \tag{4.1}$$

□

```
RS(N: node, range(Q, r_Q): query)
{ let O_p be the parent object of node N;
  if N is not a leaf
  { ∀O_r in N do:
    if |d(O_p, Q) − d(O_r, O_p)| ≤ r_Q + r(O_r)
    { Compute d(O_r, Q);
      if d(O_r, Q) ≤ r_Q + r(O_r)
        RS(*ptr(T(O_r)), range(Q, r_Q)); } }
  else
  { ∀O_j in N do:
    if |d(O_p, Q) − d(O_j, O_p)| ≤ r_Q
    { Compute d(O_j, Q);
      if d(O_j, Q) ≤ r_Q
        add oid(O_j) to the result; } } }
```

Figure 4.5: The RS algorithm for range queries.

In order to apply Lemma 4.1, the distance $d(O_r, Q)$ has to be computed. This can be avoided by taking advantage of the following result.

Lemma 4.2
If $|d(O_p, Q) - d(O_r, O_p)| > r_Q + r(O_r)$, *then* $d(O_r, Q) > r_Q + r(O_r)$.

Proof: This is a direct consequence of the triangle inequality, which guarantees that both $d(O_r, Q) \geq d(O_p, Q) - d(O_r, O_p)$ and $d(O_r, Q) \geq d(O_r, O_p) - d(O_p, Q)$ hold (see Figure 4.6). □

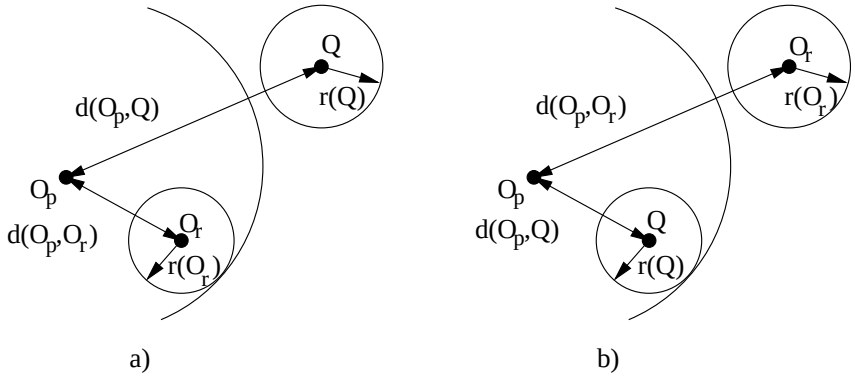

Figure 4.6: How Lemma 4.2 is used to avoid computing distances. Case a): $d(O_r, Q) \geq d(O_p, Q) - d(O_r, O_p) > r(Q) + r(O_r)$; Case b): $d(O_r, Q) \geq d(O_r, O_p) - d(O_p, Q) > r(Q) + r(O_r)$. In both cases computing $d(O_r, Q)$ is not needed.

Experimental results (see Section 4.7.7) show that this technique can save up to 40% distance computations. The only case where distance are necessarily computed is when dealing with the root node of the M-tree, for which O_p is undefined.

4.2.2 Nearest Neighbor Queries

Given a k-nearest neighbors query $\texttt{NN}(Q, k, \mathcal{C})$, the `k-NN_Search` algorithm retrieves the k nearest neighbors of the query object Q — it is assumed that at least k objects are indexed by the M-tree. The steps of the `k-NN_Search` algorithm closely resemble those of the `RS` algorithm. However, since the pruning criterion of `k-NN_Search` is *dynamic* (i.e. the current search radius is determined by the distance between Q and the k-th nearest neighbor at a given moment), specific attention should be paid to the order in which the nodes are visited. Intuitively, if k objects "very close" to Q are found in the first stages of the search, performance improves since the likelihood that more sub-trees can be pruned increases significantly. As we saw before, the conditions which allow to avoid computing a distance and accessing a node both require the search radius to be as small as possible.

We use a branch-and-bound technique, quite similar to the one designed for R-trees [RKV95], which utilizes two global structures: A priority queue, `PR`, of pending requests, and a k-elements array, `NN`, which, at the end of execution, contains the result.

Each entry in the `PR` queue is a pair $(ptr(T(O_r)), d_{min}(T(O_r)))$. The first field is, as in algorithm `RS`, the pointer to (the root of) sub-tree $T(O_r)$, whereas the second field is a lower bound on the distance between Q and any object O_j in $T(O_r)$, that is:

$$d_{min}(T(O_r)) \leq d(O_j, Q) \qquad \forall O_j \in T(O_r)$$

Clearly, the $d_{min}(T(O_r))$ lower bound is given by:

$$d_{min}(T(O_r)) = \max\{d(O_r, Q) - r(O_r), 0\}$$

since no object in $T(O_r)$ can have a distance from Q less than $d(O_r, Q) - r(O_r)$. These bounds are used by the `ChooseNode` function to extract the next node to be examined from the `PR` queue. The heuristic criterion implemented by the `ChooseNode` function is to select the node for which the d_{min} lower bound is minimum.

At the end of execution, the i-th entry of the `NN` vector contains the pair $(oid(O_j), d(O_j, Q))$, where O_j is the i-th nearest neighbor of Q. The distance value in the i-th entry is also denoted as d_i (thus d_k is the largest distance value in `NN`). Clearly, d_k can be seen as a *dynamic search radius*, since any sub-tree for which $d_{min}(T(O_r)) \geq d_k$ can be safely pruned.

```
node ChooseNode(PR: priority_queue)
{ let dmin(T(Or*)) = min{dmin(T(Or))}, considering all the entries in PR;
  Remove entry [ptr(T(Or*)), dmin(T(Or*))] from PR;
  return *ptr(T(Or*)); }
```

Figure 4.7: The `ChooseNode` function.

Entries of the `NN` array are initially set to `NN[i] = [_, ∞]` (`i` $= 1, \ldots, k$), i.e. oid's are undefined and $d_i = \infty$. As the search starts and nodes are accessed, the basic idea is to compute, for each sub-tree $T(O_r)$, an upper bound, $d_{max}(T(O_r))$, on the distance of any object stored in $T(O_r)$ from Q. The upper bound is easily computed as:

$$d_{max}(T(O_r)) = d(O_r, Q) + r(O_r)$$

This upper bound can be used to prune nodes from the priority queue. Consider the simplest case where $k = 1$, two sub-trees, $T(O_{r_1})$ and $T(O_{r_2})$, and assume that $d_{max}(T(O_{r_1})) = 0.3$ and $d_{min}(T(O_{r_2})) = 0.5$. Since $d_{max}(T(O_{r_1}))$ guarantees that an object whose distance from Q is at most 0.3 exists in $T(O_{r_1})$, $T(O_{r_2})$ can be pruned from the search. The d_{max} bounds are inserted in appropriate positions in the `NN` array, such that the array is ordered for growing distance values, just leaving the *oid* field undefined. The `k-NN_Search` algorithm is given in Figure 4.8.

```
k-NN_Search(T: root_node, NN(Q,k): query)
{ PR = [ptr(T), _];
  for i=1 to k
    NN[i] = [_, ∞];
  while PR ≠ ∅ do
  { Next_Node = ChooseNode(PR);
    k-NN_NodeSearch(Next_Node, NN(Q,k)); } }
```

Figure 4.8: The `k-NN_Search` algorithm.

Most of the search logic is implemented in the `k-NN_NodeSearch` function. On an internal node, it first determines active sub-trees and inserts them into the `PR` queue. Then, if needed, it calls the `NN_Update` function (not specified here) to perform an ordered insertion in the `NN` array, receiving back a (possibly new) value of d_k. This value is then used to remove from `PR` all sub-trees for which the d_{min} lower bound exceed d_k. Similar actions are performed in leaf nodes. In both cases, the optimization of Lemma 4.2 to

reduce the number of distance computations by means of the pre-computed distances from the parent object is also applied. Finally, note that a sub-tree can either be pruned when testing the corresponding routing object in an internal node, or if the sub-tree was previously inserted in the PR queue but the d_k value has changed since then.

```
k-NN_NodeSearch(N: node, NN(Q,k): query)
{ let O_p be the parent object of node N;
  if N is an internal node
  { ∀O_r in N do
    if |d(O_p,Q) − d(O_r,O_p)| ≤ d_k + r(O_r)
    { Compute d(O_r,Q);
      if d_min(T(O_r)) ≤ d_k
      { add [ptr(T(O_r)), d_min(T(O_r))] to PR;
        if d_max(T(O_r)) < d_k
        { d_k = NN_Update([_, d_max(T(O_r))];
          Remove from PR all entries for which d_min(T(O_r)) > d_k; } } } }
  else /* N is a leaf */
  { ∀O_j in N do
    if |d(O_p,Q) − d(O_j,O_p)| ≤ d_k
    { Compute d(O_j,Q);
      if d(O_j,Q) ≤ d_k
      { d_k = NN_Update([oid(O_j), d(O_j,Q)];
        Remove from PR all entries for which d_min(T(O_r)) > d_k; } } } }
```

Figure 4.9: The `k-NN_NodeSearch` function.

The algorithm `k-NN_Search` is *optimal*, in the sense of [BBKK97], as it follows from the following theorem.

Theorem 4.1
The algorithm `k-NN_Search` is optimal since it only accesses those nodes whose region intersects the $\texttt{NN}(Q,k)$ *ball, that is, the ball centered in* Q *with radius given by the distance between* Q *and its* k*-th nearest neighbor.*

Proof: Without loss of generality, let us assume that $k = 1$ and suppose that the algorithm `k-NN_Search` accesses a node N, with routing object O_r, whose region does not intersect the $\texttt{NN}(Q,k)$ ball, i.e. $d_{min}(T(O_r)) > d_k$. Let N_0 be the leaf node containing the nearest neighbor of Q (with routing object O_{r_0}), N_1 the parent node of N_0 (with routing object O_{r_1}), ... , and N_h the root of the tree. From the definition of d_{min} and of covering

radius, it follows that

$$d_k \geq d_{min}(T(O_{r_0})) \geq \ldots \geq d_{min}(T(O_{r_{h-1}}))$$

Thus, it is

$$d_{min}(T(O_r)) > d_k \geq d_{min}(T(O_{r_0})) \geq \ldots \geq d_{min}(T(O_{r_{h-1}}))$$

During the search process, the root node N_h is replaced in the `PR` queue by its children N_{h-1}, and so on, until the leaf node N_0 is loaded. Since $d_{min}(T(O_r)) > d_{min}(T(O_{r_0}))$, N cannot be accessed until N_0 has been loaded. If N_0 is loaded, however, all the nodes having d_{min} greater than d_k are removed form the `PR` queue. Hence, N is not accessed and this contradicts the assumption. □

4.3 How M-tree Grows

In general, algorithms for building the M-tree have to specify the way how objects are inserted and deleted, and how node overflows and underflows are managed.

The `Insert` algorithm recursively descends the M-tree to locate the most suitable leaf node for accommodating the new object, O_n. If insertion into the chosen node causes overflow, a split is triggered and updates are propagated up to higher level(s) of the tree.

The basic rationale used to find the "most suitable" leaf node is to follow a path which would avoid any enlargement of the covering radius, i.e. at each level of the tree, a sub-tree $T(O_r)$ is chosen, for which it is $d(O_r, O_n) \leq r(O_r)$. If multiple paths with this property exist, the one for which object O_n is closest to the routing object, that is, $d(O_r, O_n)$ is minimum, is chosen. Intuitively, this heuristics tries to obtain well-clustered sub-trees, which has a beneficial effect on performance.

If no routing object for which $d(O_r, O_n) \leq r(O_r)$ exists, enlargement of a covering radius is indispensable. In this case, the choice is to minimize the *increase* of the covering radius, that is the quantity $d(O_r, O_n) - r(O_r)$. This choice is tightly related to the heuristic criterion that suggests to minimize the overall "volume" covered by routing objects in the current node. The `Insert` algorithm is given in Figure 4.10.

The pruning technique of Lemma 4.2 can be applied in the `Insert` algorithm to reduce the number of computed distance by using stored and precomputed distances. Let O_i^* be the optimal choice obtained so far: In each entry `entry(`O_i`)` of $\mathcal{N}$ we have stored the distance $d(O_p, O_i)$, and, at the previous stage of the `Insert` algorithm, we have computed the distance $d(O_n, O_p)$, where O_p is the parent object of O_i. The value $|d(O_n, O_p) - d(O_p, O_i)|$ is, therefore, a lower bound on $d(O_n, O_i)$, as follows from triangle inequality. If

```
Insert(N: node, entry(O_n): M-tree_entry)
{ let 𝒩 be the set of entries in node N;
  if N is an internal node
  { let 𝒩_in the set of entries for which d(O_r, O_n) ≤ r(O_r);
    if 𝒩_in ≠ ∅
      let entry(O*_r) ∈ 𝒩_in: d(O*_r, O_n) is minimum;
    else
    { let entry(O*_r) ∈ 𝒩: d(O*_r, O_n) − r(O*_r) is minimum;
      let r(O*_r) = d(O*_r, O_n); }
    Insert(*ptr(T(O*_r)), entry(O_n)); }
  else /* N is a leaf */
  { if N is not full
    store entry(O_n) in N
    else Split(N, entry(O_n)); } }
```

Figure 4.10: The `Insert` algorithm.

$d(O_n, O_i^*) \leq |d(O_n, O_p) - d(O_p, O_i)|$, we can safely avoid to compute $d(O_n, O_i)$, since this would be surely greater than $d(O_n, O_i^*)$. Now, let us suppose that $d(O_n, O_i^*) \leq r(O_i^*)$, i.e. we have found a sub-tree, $T(O_i^*)$, for which no enlargement of covering radius is needed: If $|d(O_n, O_p) - d(O_p, O_i)| > r(O_i)$, we can safely avoid to compute $d(O_n, O_i)$, since this would be greater than $r(O_i)$ and would produce an enlargement of the covering radius of $T(O_i)$. Note that these optimizations cannot be applied to the root node, which has no routing object.

The algorithm that manages deletion of objects has to mantain the tree balanced, avoiding node underflows. If, after deletion of an object from a leaf node N, the number of entries in N is lower than the minimum capacity m, the node is deleted and its entries are re-inserted in the sibling nodes of the underflown node. The node deletion is, then, propagated upwards as necessary, adjusting the covering radius of involved nodes.

4.4 Split Management

As any other balanced tree, M-tree grows in a bottom-up fashion. The overflow of a node N is managed by allocating a new node N', at the same level of N, partitioning the entries among these two nodes, and posting (*promoting*) to the parent node, N_p, two routing objects to reference the two nodes. When the root splits, a new root is also created and the M-tree grows by one level up. The `Split` algorithm is given in Figure 4.11.

The `Promote` method chooses, according to some specific criterion, two routing objects,

```
Split(N: node, E: M-tree_entry)
{ let 𝒩 be the set of entries in node N∪{E};
  if N is not the root
    let O_p be the the parent of N, stored in node N_p;
  allocate a new node N';
  Promote(𝒩, O_p1, O_p2);
  Partition(𝒩, O_p1, O_p2, 𝒩_1, 𝒩_2);
  store 𝒩_1's entries in N and 𝒩_2's entries in N';
  if N is the current root
  { allocate a new root node, N_p;
    store entry(O_p1) and entry(O_p2) in N_p; }
  else
  { replace entry(O_p) with entry(O_p1) in N_p;
    if N_p is full
      Split(N_p, entry(O_p2));
    else store entry(O_p2) in N_p; } }
```

Figure 4.11: The `Split` algorithm.

O_{p_1} and O_{p_2}, to be inserted in the parent node, N_p. The `Partition` method divides entries of the overflown node (the $\mathcal{N}$ set) into two disjoint subsets, $\mathcal{N}_1$ and $\mathcal{N}_2$, which are then stored in nodes N and N', respectively. A specific implementation of the `Promote` and `Partition` methods defines what we call a *split policy*. Unlike other (static) metric trees designs, each relying on a specific criterion to organize objects, M-tree offers a possibility of implementing alternative split policies, in order to tune performance depending on specific application needs (see Section 4.5).

Regardless of the specific split policy, the semantics of covering radii has to be preserved. If the split node is a leaf, then the covering radius of a promoted object, say O_{p_1}, is set to

$$r(O_{p_1}) = \max\{d(O_j, O_{p_1}) : O_j \in \mathcal{N}_1\}$$

whereas if overflow occurs in an internal node

$$r(O_{p_1}) = \max\{d(O_r, O_{p_1}) + r(O_r) : O_r \in \mathcal{N}_1\}$$

which guarantees that $d(O_j, O_{p_1}) \leq r(O_{p_1})$ holds for any object O_j in $T(O_{p_1})$.

As a final observation, it has to be emphasized that, since reference objects are chosen from the set of entries in the split node and then promoted and inserted into the parent node, multiple copies of routing objects occur.

4.5 Split Policies

Effective implementation of M-tree requires a careful choice of specific algorithms for managing the tree evolution. In particular, split operations should try to satisfy a set of somewhat contrasting requirements, which can be summarized as follows:

Minimum "volume". Since pruning of the search space is tightly related to the "volumes" covered by routing objects, and these are directly related to the values of the covering radii, it is advisable to keep such values as small as possible.

Minimum "overlap". In order to reduce the number of paths that have to be traversed for answering a query, it would be convenient to have a tree organization such that the regions covered by the routing objects are well-separated. It has to be remarked that, in a generic metric space, minimization of overlap has no precise mathematical formulation. In other terms, given two non-disjoint regions, it is not possible, without a detailed knowledge of the distance function, to *quantify* the amount of overlap. However, when applying this heuristics to the split algorithm, from a qualitative point of view, it can be said that, for fixed values of the covering radii, the distance between the two chosen reference objects should be maximized.

Balanced split. This is a classical requirement for height-balanced access methods, which also aims to keep the height of the tree as small as possible.

Although the above requirements can be considered quite "standard" also for SAMs [BKSS90], in the "metric space" scenario they have to be considered from a rather different perspective. Besides the already done observations related to the overlap definition, at least two additional facts are still to be noticed:

1. The possible high CPU cost of computing distances suggests for choosing reference objects also algorithms which would otherwise be considered naïve (e.g. a random choice) — a quadratic cost split algorithm may turn to be unacceptable in many cases.

2. Balanced distribution of entries (possibly specified by a minimum threshold value) does not appear to be a really pressing requirement, compared to the other two. While satisfying this criterion with multi-dimensional access methods can usually be accomplished by enlarging regions along only the necessary dimensions, in a metric space the consequent increase of the covering radius would propagate to *all* the "dimensions".

Since it seems quite difficult to rely on well-founded arguments to *a priori* rule out some partitioning heuristic criteria, we decided to start with a moderately large set of alternative solutions, and to experimentally evaluate all of them (see Section 4.7).

4.5.1 Choosing the Routing Objects

The `Promote` method determines, given a set of entries, $\mathcal{N}$, two objects to be promoted and stored into the parent node. The specific algorithms we consider can first be classified according to whether or not they "confirm" the original routing object in its role.

Definition 4.1 (Confirmed split policy)
A *confirmed* split policy chooses as one of the promoted objects, say O_{p_1}, the object O_p, i.e. the routing object of the split node.

In other terms, a confirmed split policy just "extracts" a region, centered on the second routing object, O_{p_2}, from the region which will still remain centered on O_p. In general, this simplifies split execution and reduces the number of distance computations.

We implemented and experimentally evaluated (see Section 4.7) all of the following alternatives, both in the confirmed and in the non-confirmed version.

`RANDOM` This variant simply selects in a random way the reference objects. Although it is not a "smart" strategy, it is fast and its performance can be used as a reference for other policies.

`SAMPLING` This is the `RANDOM` policy, but iterated over a sample of objects of size $s > 1$. For each of the $s(s-1)/2$ pairs of objects in the sample, entries are distributed and potential covering radii established. The pair for which the resulting maximum of covering radii is minimum is then selected. In case of confirmed promotion, only s different distributions are tried. The sample size in our experiments was 1/10-th of the node capacity, unless otherwise stated.

`M_LB_DIST` The acronym stands for "Maximum Lower Bound on DISTance". This policy differs from previous ones in that it only uses precomputed stored distances. In the confirmed version, where $O_{p_1} \equiv O_p$, the algorithm determines O_{p_2} as the farthest object from O_p, that is

$$d(O_{p_2}, O_p) = \max_j \{d(O_j, O_p)\}$$

`M_UB_DIST` The acronym stands for "Maximum Upper Bound on DISTance". This variant is the pessimistic version of `M_LB_DIST`, and has the purpose of maximizing the upper

bound of the distance of the objects to be promoted. This is achieved by selecting the two objects which are farthest from O_p, that is

$$\begin{aligned} d(O_{p_1}, O_p) &= \max_j\{d(O_j, O_p)\} \\ d(O_{p_2}, O_p) &= \max_j\{d(O_j, O_p), O_j \neq O_{p_1}\} \end{aligned}$$

`mM_LB_RAD` This variant is basically conceived for confirmed promotion, and can be concisely explained as follows. Consider the pair-wise lower bounds on distances among all the entries in the node (no *new* actual distance has to be computed for this purpose). For each object O_i compute $\max_j\{|d(O_i, O_p) - d(O_j, O_p)|\}$ and promote the object for which the maximum is minimized. The acronym, hence, stands for "minimum Maximum Lower Bound on RADius". This criterion selects for promotion object O_{p_2} which has an "intermediate" distance from O_p.

`mM_UB_RAD` This variant is the "pessimistic" version of `mM_LB_RAD`, in that it uses upper bounds $d(O_i, O_p) + d(O_j, O_p)$. The net effect is to promote an object which is the closest to O_{p_1}.

`mM_AVG_RAD` This is a variant which tries to be "neutral" with respect to lower and upper bound information, taking their average and then applying the min-Max selection criterion.

`m_RAD` The "minimum (sum of) RADii" algorithm is the most complex in terms of distance computations. It considers all possible pairs of objects and, after partitioning the set of entries, promotes the pair of objects for which the sum of covering radii, $r(O_{p_1}) + r(O_{p_2})$, is minimum.

`mM_RAD` This is similar to `m_RAD`, but it minimizes the maximum of the two radii.

Figure 4.12 provides a graphical intuition on the behavior of some of the split variants.

4.5.2 Distribution of the Entries

Given a set of entries $\mathcal{N}$ and two routing objects O_{p_1} and O_{p_2}, the problem is how to efficiently partition $\mathcal{N}$ into two subsets, $\mathcal{N}_1$ and $\mathcal{N}_2$. For this purpose we consider two basic strategies. The first one is based on the idea of the *generalized hyperplane decomposition* [Uhl91] and leads to unbalanced splits, whereas the second obtains a balanced distribution. They can be shortly described as follows.

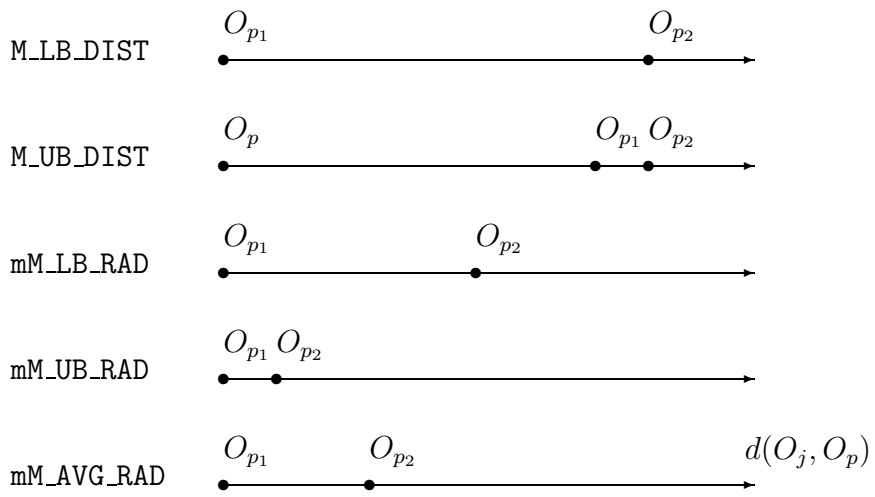

Figure 4.12: A graphical representation of how some split variants work. All variants except `M_UB_DIST` are shown for the case of confirmed promotion ($O_{p_1} \equiv O_p$).

`Generalized Hyperplane` **Distribution.** Assign each object $O_j \in \mathcal{N}$ to the nearest routing object, that is, if $d(O_j, O_{p_1}) \leq d(O_j, O_{p_2})$ then assign O_j to $\mathcal{N}_1$, else assign O_j to $\mathcal{N}_2$.

`Balanced` **Distribution.** Compute $d(O_j, O_{p_1})$ and $d(O_j, O_{p_2})$ for all $O_j \in \mathcal{N}$. Repeat until $\mathcal{N}$ is empty:

- Assign to $\mathcal{N}_1$ the nearest neighbor of O_{p_1} in $\mathcal{N}$ and remove it from $\mathcal{N}$;
- Assign to $\mathcal{N}_2$ the nearest neighbor of O_{p_2} in $\mathcal{N}$ and remove it from $\mathcal{N}$.

Depending on data distribution and on the way how routing objects are chosen, an unbalanced split policy can lead to a better objects' partitioning, due to the additional degree of freedom it obtains. This intuition, however, has to be verified through experimental evaluation.

An intermediate behavior can be obtained by combining the two above algorithms considering a minimum threshold on node utilization. If at least $m \leq M/2$ entries per node are required, the `Balanced` distribution can be applied to the first $2m$ objects, after which the `Generalized Hyperplane` is used. The effect of the minimum node utilization is investigated in Section 4.7.1.

4.6 Implementation Issues

Our M-tree implementation is based on the Generalized Search Tree (GiST) C++ package, a structure extendible both in the data types and in the queries it can support [HNP95].[4]

A GiST is a balanced tree with variable fanout k, where $m < k < M$ (m and M being the *minimum* and the *maximum node capacity*, respectively). Leaf nodes store entries having the form $E = (p, \texttt{ptr})$, where p is a predicate used as a search key and `ptr` is the object identifier. Internal nodes store entries having the form $E = (p, \texttt{ptr})$, where p is a predicate used as a search key and `ptr` is the pointer to another tree node. By using "key compression" techniques, a given predicate p may take as little as zero bytes of storage, as for B-trees. In this framework, a specific access method is specified by defining the predicate p for each entry and by providing the code for a limited set of required methods:

`Consistent`(E, q)**.** Given an entry $E = (p, \texttt{ptr})$, and a query q, returns false iff $p \wedge q$ can be guaranteed unsatisfiable, and true otherwise.

`Union`(P)**.** Given a set P of entries $\{(p_1, \texttt{ptr}_1), \ldots, (p_n, \texttt{ptr}_n)\}$, returns some predicate r that holds for all objects stored below $\texttt{ptr}_1$ through $\texttt{ptr}_n$.

`Penalty`(E_1, E_2)**.** Given two entries $E_1 = (p_1, \texttt{ptr}_1)$ and $E_2 = (p_2, \texttt{ptr}_2)$, returns a domain-specific penalty for inserting E_2 into the sub-tree rooted at E_1.

`PickSplit`(P)**.** Given a set P of $M + 1$ entries, splits P into two sets of entries P_1 and P_2, each of size at least m.

For the M-tree, the predicate associated to each entry of the tree consists of the entry region, that is the pair $(O_r, r(O_r))$, where $r(O_r) = 0$ for ground entries, i.e. for entries in leaf nodes. The basic M-tree version of `Consistent`, thus, returns false iff the region associated with the entry $E = ((O_j, r(O_j)), \texttt{ptr}_j)$ is guaranteed to be outside of the query region, i.e. iff $d(O_j, Q) > r(O_j) + r_Q$. The search algorithm `RS`, then, uses this information to descend all paths in the tree whose entries are consistent with the query. `Consistent` can also be used for k-nearest neighbor query, by assigning to the query radius r_Q the actual distance to the k-th nearest neighbor obtained so far, i.e. d_k.

The `Union` method is used in the insertion phase to compute the covering radius for a node N, given the set P of entries stored within N. Of course, this can be computed as:

$$r(O_r) = \max\{d(O_r, O_j) + r(O_j) : E = ((O_j, r(O_j)), \texttt{ptr}_j) \in P\}$$

[4]The GiST source code is freely available at URL `http://gist.cs.berkeley.edu:8000/gist/`.

The `Penalty` method is used by the insertion algorithm to find the most suitable leaf node to store a new entry E. In our case, the penalty for inserting $E_2 = ((O_n, 0), \texttt{ptr}_n)$ in the sub-tree rooted at $E_1 = ((O_j, r(O_j)), \texttt{ptr}_j)$ is given by the distance between O_j and O_n, $d(O_j, O_n)$, if no radius enlargement is needed, i.e. if $d(O_j, O_n) \leq r(O_j)$, and by the necessary radius increase, i.e. $d(O_j, O_n) - r(O_j)$, otherwise.

The M-tree implementation of the `PickSplit` method depends on the chosen split policy, and is given by the `Split` algorithm proposed in Section 4.4.

A more detailed description of M-tree implementation can be found in Appendix A.

4.7 Experimental Results

In this Section we provide experimental results on the performance of the M-tree in processing similarity queries. We tested all the split policies described in Section 4.5, and evaluated them under a variety of experimental settings. To gain the flexibility needed for comparative analysis, most experiments were based on synthetic data sets, and only a relatively small fraction were conducted on real data sets. Synthetic data sets were obtained by using the procedure described in [JD88] which generates normally-distributed clusters in a D-dimensional vector space. Unless otherwise stated, in all the experiments we set the number of clusters to 10, with centers uniformly distributed and an intra-cluster variance of 0.01, and used 10^4 data objects. Figure 4.13 shows a 2D data set sample. The results we show are obtained by using as distance function the L_∞ metric, which leads to hyper-cubic search (and covering) regions. Graphs concerning construction costs are obtained by averaging the costs of building 10 M-trees, and results about performance on query processing are averaged over 100 queries. In all experiments, we used a constant node size of 4 Kbytes. This, of course, influences M-tree performance, since node capacity is inversely related to the dimensionality of the data sets. The effect of changing the node size is investigated in Section 4.7.6.

4.7.1 Storage Utilization

In Section 4.5, we stated that a "good" clustering of the data during the split phase is more important that a balanced entry distribution. In the following, we will consider the effect of a minimum storage utilization threshold on the index performance during both the construction and the search phases.

Figures 4.14 and 4.15 show the I/O and CPU costs, respectively, for tree construction, as a function of the space dimensionality and of the minimum utilization threshold; the split policy used is the non-confirmed `mM_RAD`. The threshold is expressed as a percentage of

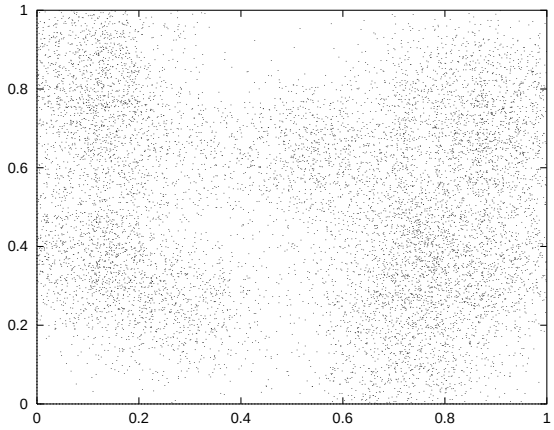

Figure 4.13: A sample data set used in the experiments.

the total node capacity; thus, 0 represents the original `Generalized Hyperplane` strategy, while 0.5 is the `Balanced` strategy. Construction costs for more balanced strategies are, of course, lower than those of unbalanced ones, since a balanced strategy leads to smaller trees and to a lower number of splits during construction phase. Moreover, the gap is increasing for lower thresholds, growing from a 2% overhead between 0.3 and 0.4, up to 27% between 0 and 0.1 for 50-D data.

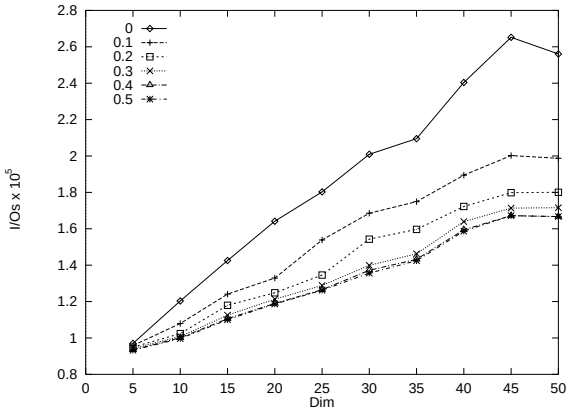

Figure 4.14: I/O costs during construction phase for different storage utilization thresholds.

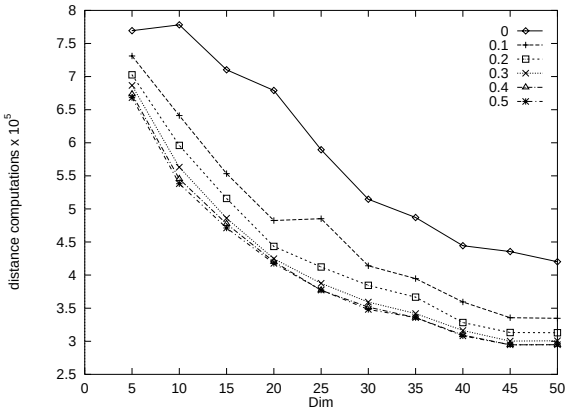

Figure 4.15: CPU costs during construction phase for different storage utilization thresholds.

As to search costs, however, Figures 4.16 and 4.17 show that the best performance is achieved by intermediate strategies (i.e. 0.2 and 0.3), attaining the lower values for both I/O and CPU costs for range queries (unless otherwise stated, here and in the following, range queries ask for objects standing in a region with a volume equal to 1/100-th of the total space volume, thus having a query radius of $\sqrt[D]{0.01}/2$).

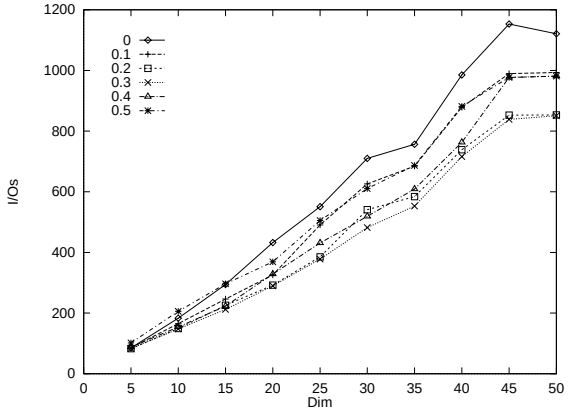

Figure 4.16: I/O costs for range queries for different storage utilization thresholds.

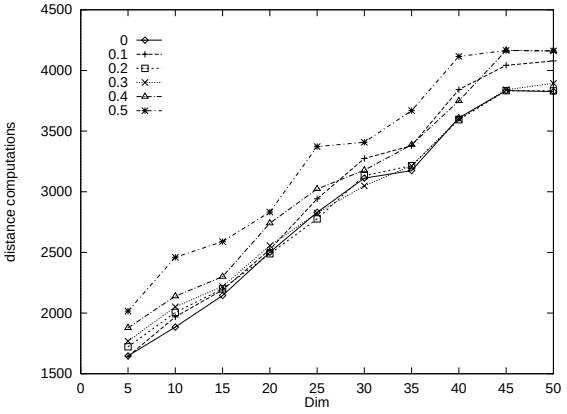

Figure 4.17: CPU costs for range queries for different storage utilization thresholds.

The observed behavior is due to the better average volume per page obtained from trees created using lower utilization thresholds, as shown by Figure 4.18. For 10-NN queries, though, the trend is decreasing for decreasing thresholds, as can be seen in Figures 4.19 and 4.20; in other words, more unbalanced strategies obtain best results. This, again, is due to the better objects' distribution attained by unbalanced strategies.

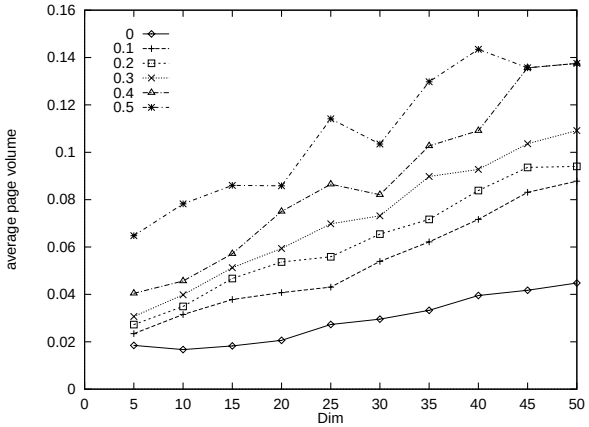

Figure 4.18: Average volume per page for different storage utilization thresholds.

Looking at the results, it appears that the best strategy would be to consider a minimum utilization threshold between 20% and 30% of the total node capacity; in fact, these strategies attain both construction and search costs similar to the best ones, while other strategies, even if they obtain the best results for either construction or search phase, are far worse during the other phase. If, however, the application is very search-intensive, one should consider the totally unbalanced strategy, thus obtaining query costs lower than any other strategy. Because of these considerations, in the following all the split policies are

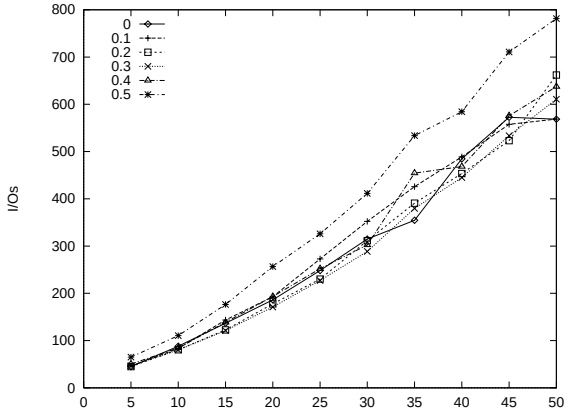

Figure 4.19: I/O costs for 10-NN queries for different storage utilization thresholds.

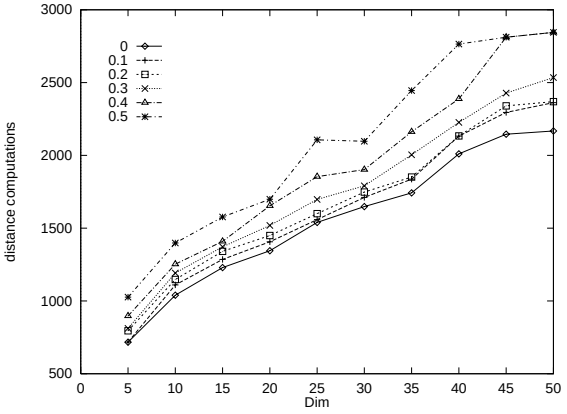

Figure 4.20: CPU costs for 10-NN queries for different storage utilization thresholds.

based on the `Generalized Hyperplane` distribution. Other results, not shown here, also suggested to discard the "pessimistic" split variants, namely `M_UB_DIST` and `mM_UB_RAD`, whose performance was clearly worse than others regardless of balancing issues.

4.7.2 The Effect of Dimensionality

We now consider how increasing the dimensionality of the data set influences the performance of M-tree. Here and in the following, a "confirmed" split policy is identified by the suffix `1`, whereas `2` designates a "non-confirmed" policy (see Definition 4.1). Figure 4.22 shows that all the split policies but `m_RAD_2` and `mM_RAD_2` compute almost the same number of distances for building the tree, and that this decreases when D grows. The explanation is that, with a fixed node size, increasing D reduces the node capacity, which has a beneficial effect on the numbers of distances computed by the insertion and split algorithms. The reduction is particularly evident for `m_RAD_2` and `mM_RAD_2`, whose CPU split costs vary with the square of node capacity. I/O costs, shown in Figure 4.21, have an inverse trend, thus growing with space dimensionality. This can again be explained by the reduction of node capacity. The fastest split policy is `RANDOM_2`, and the slowest one is, not surprisingly, `m_RAD_2`.

Figure 4.23 shows that the "quality" of tree construction, measured by the average covered volume per page, depends on split policy, and that the heuristic criterion of the cheap `M_LB_DIST_1` policy is indeed effective enough.

Performance on range and 10-NN query processing, considering both I/O's and distance selectivities, is shown in Figures 4.24, 4.25, 4.26, and 4.27 — distance selectivity is the ratio of computed distances to the total number of objects.

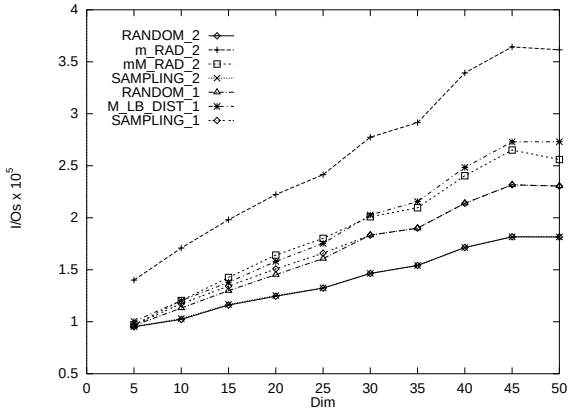

Figure 4.21: I/O costs for building M-tree.

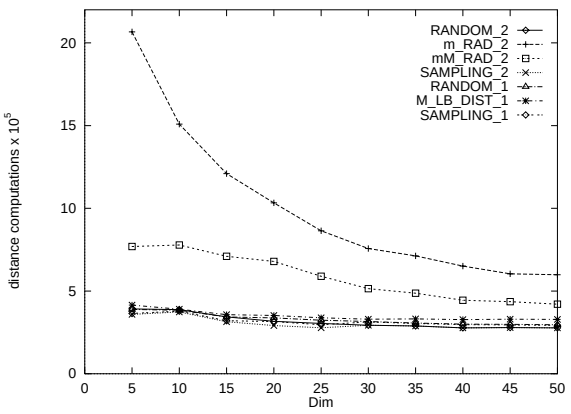

Figure 4.22: CPU costs for building M-tree.

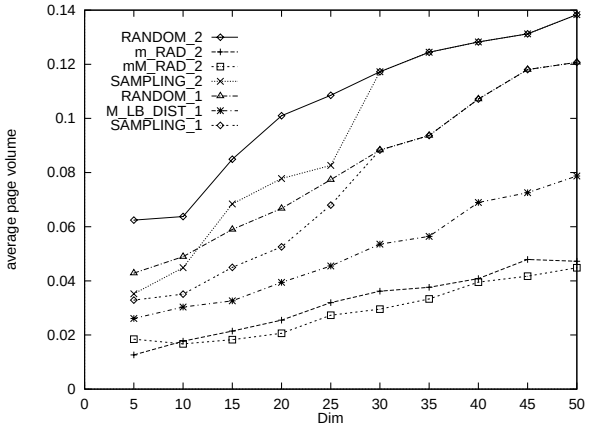

Figure 4.23: Average covered volume per page.

Some interesting observations can be done about these results. First, policies based on "not-confirmed" promotion, such as `m_RAD_2` and `RANDOM_2`, perform better that "confirmed" policies as to I/O costs, especially on high dimensions where they save up to 25% I/O's. This can be attributed to the better objects' clustering that such policies can obtain. I/O costs increase with the dimensionality mainly because of the reduced page capacity, which leads to larger trees. For the considered range of D values, node capacity varies with a factor of 10, which almost coincides with the ratio of I/O costs at $D = 50$ to the costs at $D = 5$.

As to distance selectivity, differences emerge only with high values of D, and favor `mM_RAD_2` and `m_RAD_2`, which exhibit only a moderate performance degradation. Since these two policies have the same complexity, and because of results given by Figures 4.25 and 4.27, `m_RAD_2` is discarded in subsequent analyses.

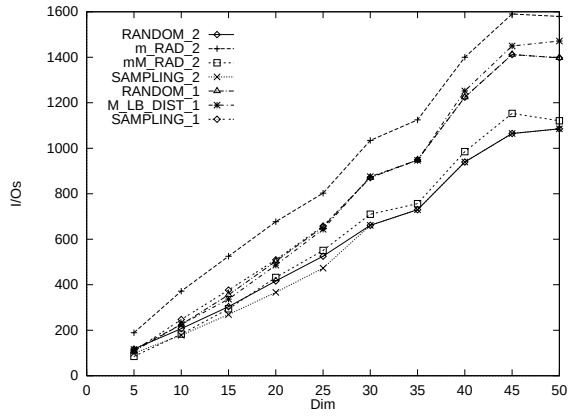

Figure 4.24: I/O costs for processing range queries.

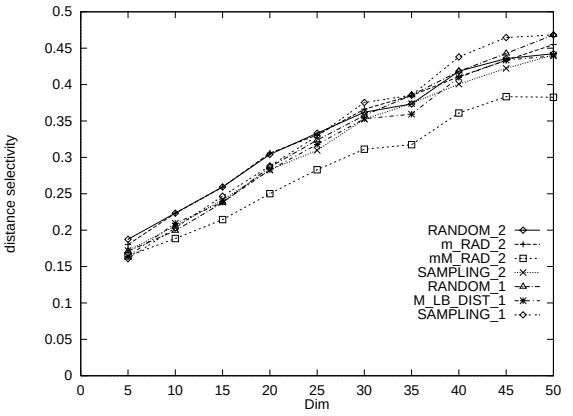

Figure 4.25: Distance selectivity for range queries.

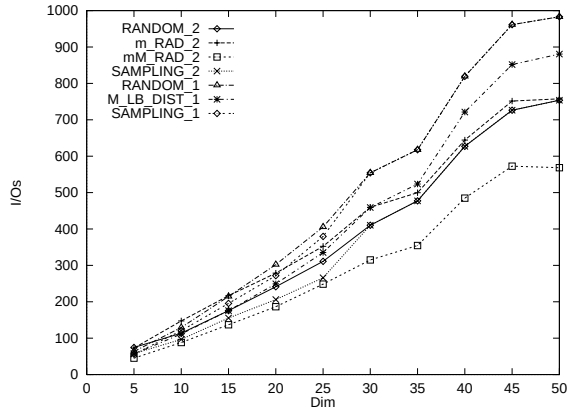

Figure 4.26: I/O costs for processing 10-NN queries.

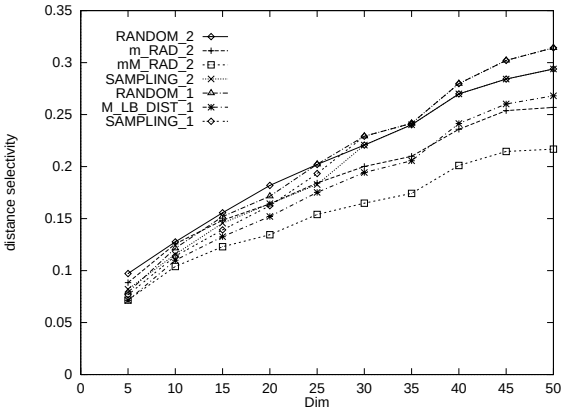

Figure 4.27: Distance selectivity for 10-NN queries.

4.7.3 Scalability

Another major challenge in the design of M-tree was to ensure scalability of performance with respect to the size of the indexed data set. This addresses both aspects of efficiently building the tree and of performing well on similarity queries.

Table 4.1 shows the average number of distance computations and I/O operations per inserted object for building the M-tree, for 2D datasets whose size varies in the range $10^4 \div 10^5$. Results refer to the `RANDOM_2` policy, but similar trends were observed also for the other policies. The moderate increase of the average number of distance computations depends both on the growing height of the tree and on the higher density of indexed objects within clusters. This is because the number of clusters was kept fixed at 10, regardless of the data set size.

n. of objects ($\times 10^4$)	1	2	3	4	5	6	7	8	9	10
avg. n. dist. comp.	45.0	49.6	53.6	57.5	61.4	65.0	68.7	72.2	73.6	74.7
avg. n. I/O's	8.9	9.3	9.4	9.5	9.6	9.6	9.6	9.6	9.7	9.8

Table 4.1: Average number of distance computations and I/O's for building the M-tree, as a function of the number of indexed objects.

Figures 4.28 and 4.29 show that both I/O and CPU (distance computations) 10-NN search costs grow logarithmically with the number of objects, which demonstrates that M-tree scales well in the data set size, and that the dynamic management algorithms do not deteriorate the quality of the search. It has to be emphasized that this behavior is peculiar to the M-tree, since other known metric trees are intrinsically static.

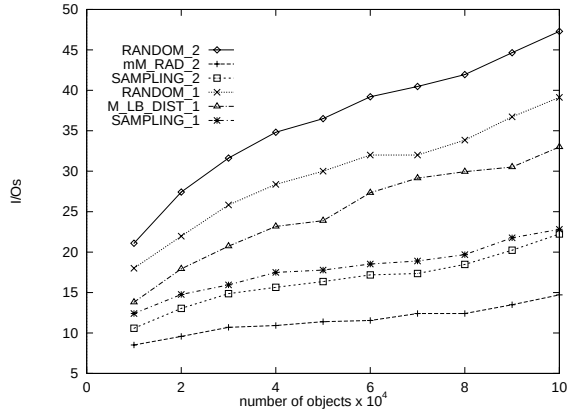

Figure 4.28: I/O costs for processing 10-NN queries.

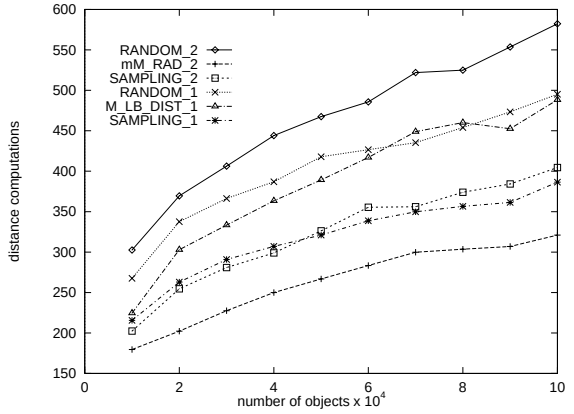

Figure 4.29: Distance computations for 10-NN queries.

As to the relative behaviors of split policies, figures show that "cheap" policies (e.g. `RANDOM_2` and `M_LB_DIST_1`) are penalized by the high node capacity ($M = 60$), arising when indexing 2D points. Indeed, the higher M is, the more effective "complex" split policies are. This is because the number of alternatives for objects' promotion grows as M^2, thus, for high values of M, the probability that cheap policies perform a good choice considerably decreases.

4.7.4 Saving Distance Computations during Insertion

As we saw in Section 4.3, the pruning technique used for search algorithm can be used to reduce the number of computed distances during construction of the tree. In this Section we show the efficiency of such optimization.

Figures 4.30 and 4.31 show, respectively, the distance computation saving and the total number of computed distances during the construction phase of the M-tree when using the optimization, as a function of the space dimensionality and for different split policies. It can be easily seen that the effect of the optimization technique on the `mM_RAD_2` policy is quite poor: This is due to the fact that this policy computes most distances in the split phase, and not during insertion; as dimensionality increases, though, the number of distance computed during the split phase slowly decreases (as we also saw in Figure 4.22), leading to an increasing trend for the distance computations saving. Vice versa, for other methods the trend is decreasing with increasing dimensionality: The cause for this is the lower number of entries in each node that leads to a lower chance to prune away some distance computations.

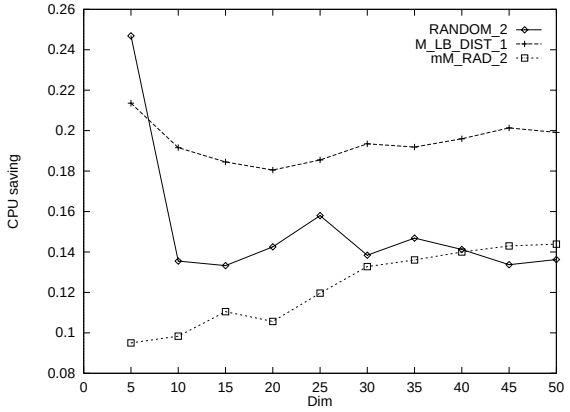

Figure 4.30: CPU costs savings for different policies.

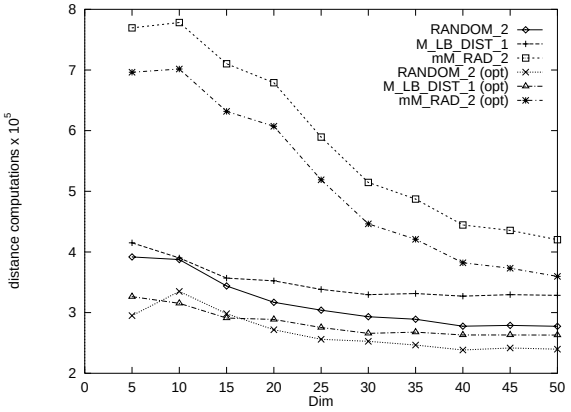

Figure 4.31: Comparison of CPU costs for basic and optimized split strategies.

4.7.5 Choosing the Right Sample Size

In previous experiments, we assumed that the sample size for the `SAMPLING` split strategy is 1/10-th of the total node capacity. In this Section, we will investigate in detail the effect of the sample size on the performance of the above strategy.

As we saw before, `mM_RAD_2` is the best split policy regarding query performance; this policy, however, is the slowest in the construction phase, since its CPU costs during split grow with the square of node capacity. On the other hand, the complexity of node split using the `SAMPLING_2` policy is proportional to the square of the sample size and, therefore, it is possible to exert some control over the performance of the latter algorithm.

Figures 4.32 and 4.33 show I/O and CPU costs for building the M-tree as a function of the space dimensionality and of the sample size, the latter expressed as a percentage of

the total node capacity, so that 0.2 means that the number of samples is the 20% of the total number of entries in a node, while 1 represents the `mM_RAD_2` strategy. The results in Figure 4.32 show that I/O costs are almost independent on the sample size, with the exception of `mM_RAD_2`, which leads to more unbalanced indices, thus having higher I/O costs.

Results in Figure 4.33 need a detailed discussion. Since, as stated before, the number of distances computed during the split of a node grows with the square of the sample size, we expected that CPU costs would decrease as dimensionality increases and the sample size decreases. The effect of dimensionality is confirmed by our experiments, whereas the impact of sample size is neglected by the behavior of `mM_RAD_2` policy. This strategy leads to a lower number of distance computations than expected, since it can obtain a far better objects' partitioning, thus leading to a lower number of splits with respect to other `SAMPLING` policies. The better distribution for `mM_RAD_2` strategy can be observed by looking at Figure 4.34, showing the average volume per page.

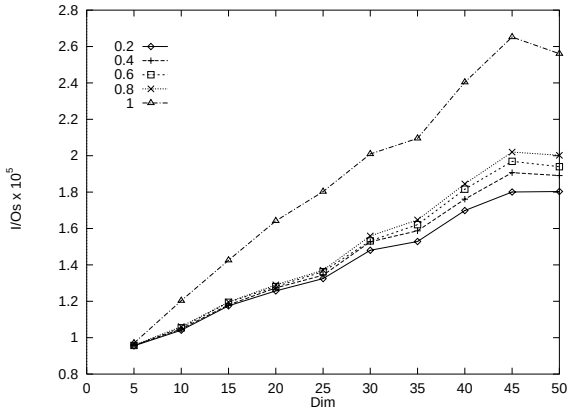

Figure 4.32: I/O costs for building M-tree for different sample sizes.

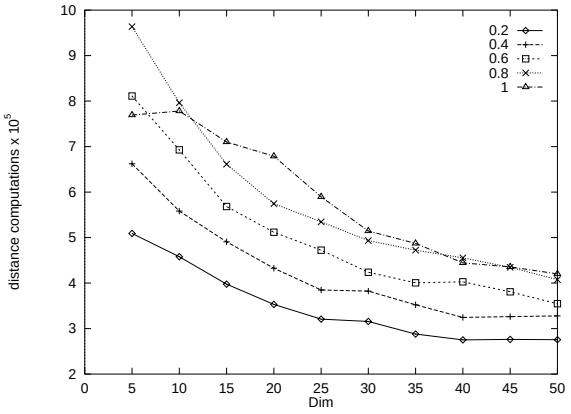

Figure 4.33: CPU costs for building M-tree for different sample sizes.

As to the query performance, Figures 4.35 and 4.36 show I/O and CPU costs for processing range queries. CPU costs show what we expected: The greater the sample size, the better the search costs. I/O costs show a similar trend, with the exception of `mM_RAD_2`, whose I/O performance is not the best one, due to the larger size of generated trees.

From these experiments we can observe that:

- Lower sample sizes (e.g. 0.2 – 0.4) are penalized for search-intensive domains, since their lower construction costs do not balance higher search costs.

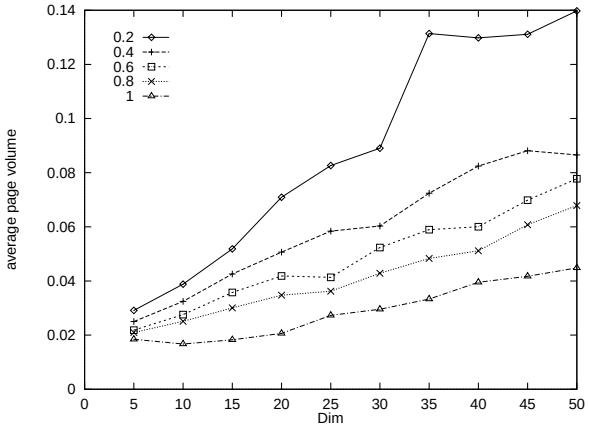

Figure 4.34: Average volume per page for different sample sizes.

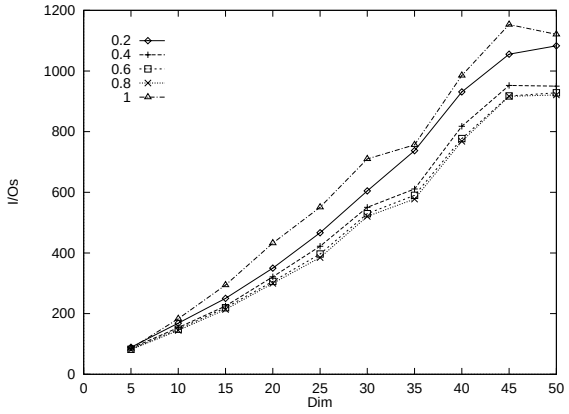

Figure 4.35: I/O costs for range queries for different sample sizes.

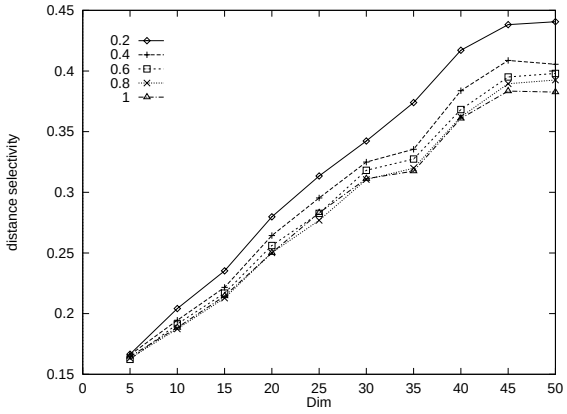

Figure 4.36: CPU costs for range queries for different sample sizes.

- Higher sample sizes (e.g. 0.6 – 1) show similar search CPU costs, as well as for the construction phase.
- The `mM_RAD_2` policy leads to higher I/O costs, during both construction and querying phases.

These considerations led us to the following conclusions:

- For non search-intensive domains, the sample size should be low (i.e. 0.3 – 0.4), in order to obtain lower construction costs.
- For search-intensive domains, the sample size should be a high one (i.e. 0.6 – 0.9), in order to obtain lower search costs, but not the highest (i.e. `mM_RAD_2`), whose I/O costs are too high.

4.7.6 The Fanout Problem

As we said before, the fanout of the tree, i.e. the maximum number of branches in a node, decreases for growing dimensionalities of the space, since we are using fixed-size nodes and the size of each entry increases as well. It is, therefore, difficult to understand if the deterioration of index' performance during search for increasing dimensionalities of the space is due to the reduced fanout of the tree or to the intrinsic "complexity" of high-dimensional spaces. To overcome this problem, we conducted a series of experiments with fixed fanout $M = 20$ for different dimensionalities using the unbalanced `mM_RAD_2` split policy. Figures 4.37 and 4.38 show CPU construction costs and the total number of pages for M-tree, respectively. Both graphs show a similar behavior: An increasing trend, a maximum for $D = 20$, and a stable behavior for higher D's. This trend is due to different factors:

- The used distance, i.e. L_∞, is such that, for increasing dimensionalities of the space, the variance of distribution of distances between objects steeply decreases, while the mean value increases (this effect is shown in Figure 4.39). In high-dimensional spaces, hence, the distance between two random objects is almost always the same.
- When we reach $D = 20$, this effect shows a stabilization, as indicated in Figure 4.37.

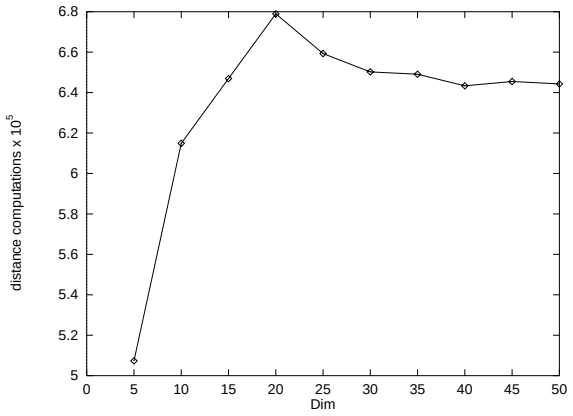

Figure 4.37: CPU costs for building M-tree with fixed fanout.

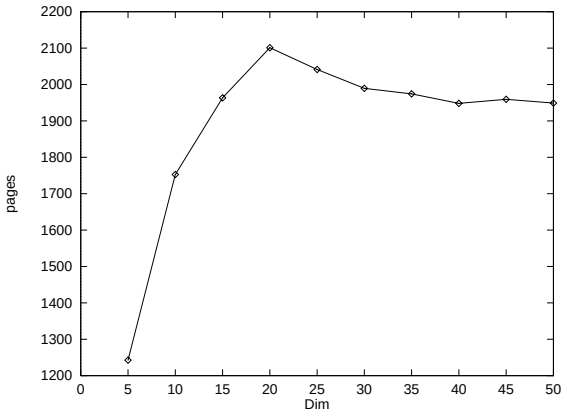

Figure 4.38: Number of pages of the index with fixed fanout.

On the other hand, search costs have an increasing trend, stabilizing themselves at higher dimensionalities, as shown in Figures 4.40 and 4.41.

All these graphs show that also the M-tree suffers from the "dimensionality curse", but that the performance degradation is not directly proportional to the space dimensionality. Indeed, what is observed is that M-tree performance highly depends on the distribution

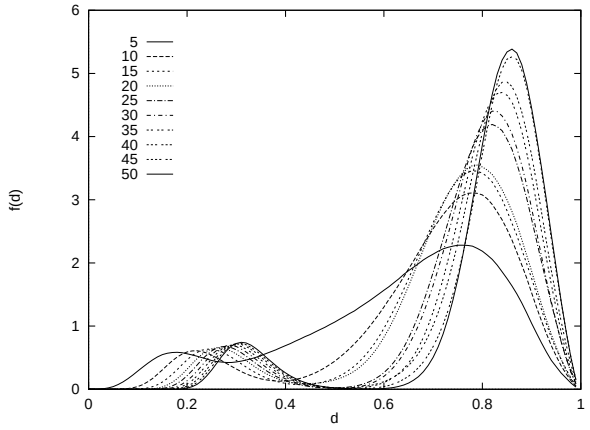

Figure 4.39: Distance distribution for clustered datasets of different dimensionalities.

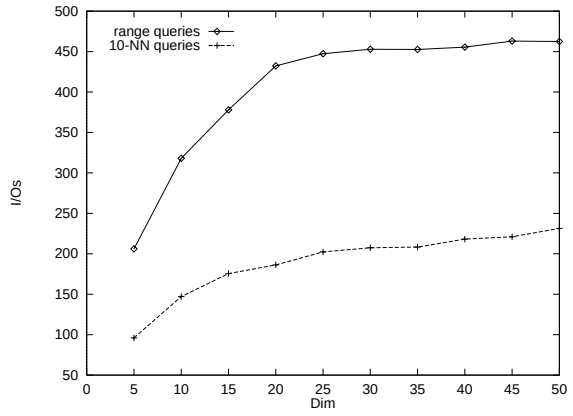

Figure 4.40: I/O costs for range and 10-NN queries with fixed fanout.

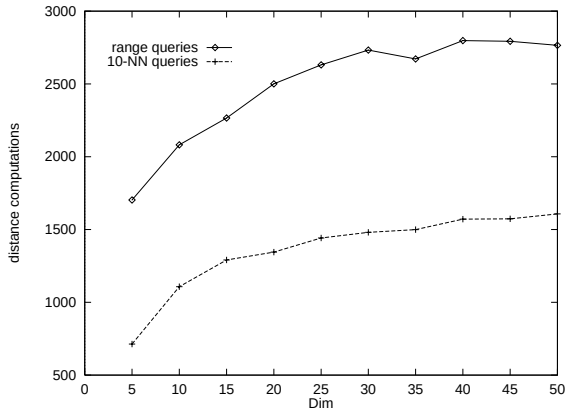

Figure 4.41: CPU costs for range and 10-NN queries with fixed fanout.

of distances between objects. We will clarify this observation in Chapter 6, where a cost model for M-tree will be presented, exploiting the concept of *distance distribution*.

4.7.7 Comparing M-tree and R*-tree

The final set of experiments we present compares M-tree with R*-tree. The R*-tree implementation we use is the one available with the GiST package. We definitely do not deeply investigate merits and drawbacks of the two structures, rather we provide some reference results obtained from an access method which is well-known and largely used in both commercial and experimental database systems. Furthermore, although M-tree has an intrinsic wider applicability range, we consider important to evaluate its relative performance on "traditional" domains where other access methods could be used as well.

Results in Figures 4.42 and 4.43 compare I/O and CPU costs, respectively, to build

R*-tree and M-tree, the latter only for `RANDOM_2`, `M_LB_DIST_1`, and `mM_RAD_2` policies. The trend of the graphs for R*-tree confirms what already observed about the influence of the node capacity (see Figures 4.21 and 4.22). Graphs emphasize different performance of M-trees and R*-trees in terms of CPU costs, whereas both structures have similar I/O building costs.

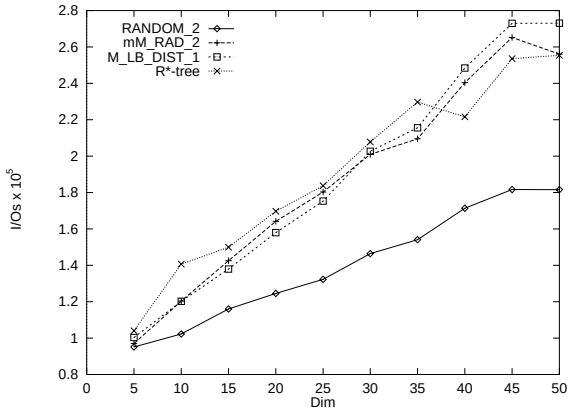

Figure 4.42: I/O costs for building M-tree and R*-tree.

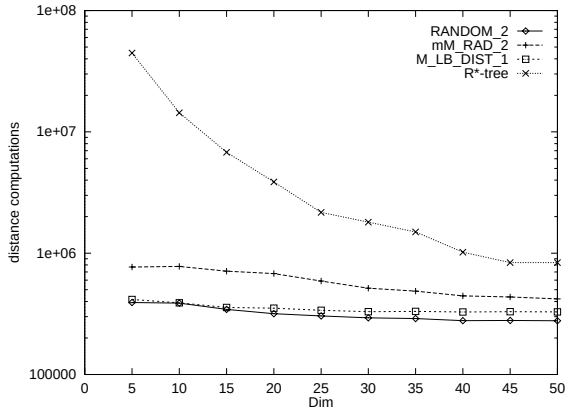

Figure 4.43: CPU costs for building M-tree and R*-tree.

Figures 4.44 and 4.45 show search costs for square range queries. It can be observed that I/O costs for R*-tree are higher than those of all M-tree variants. In order to present a fair comparison of CPU costs, Figure 4.45 also shows, for each M-tree split policy, a graph (labelled `(non opt)`) where the optimization for reducing the number of distance computations (see Lemma 4.2) is not applied. Graphs show that this optimization is highly effective, saving up to 40% distance computations (similar results were also obtained for NN-queries). Note that, even without such an optimization, M-tree is almost always more efficient than R*-tree.

Figures 4.46 and 4.47 show, respectively, normalized I/O and CPU costs per retrieved object for processing range queries when the query volume varies in the range $10^{-10} \div 10^{-1}$ on the 20D vector space. In order to fairly compare the access methods, we did not use any optimization in the M-tree search algorithm for reducing the number of distances to be computed. Both figures show that the overall behavior of M-tree is better than that of R*-tree, regardless of the query volume and of the considered split policy.

From these results, which we remind are far from providing a detailed comparison of M-trees and R*-trees, we can anyway see that M-tree is a competitive access method even for indexing data from vector spaces.

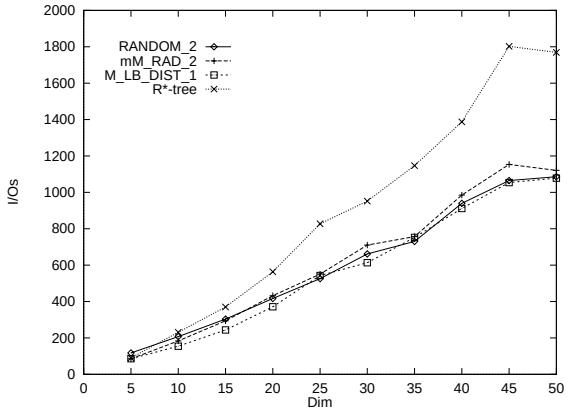

Figure 4.44: I/O costs for processing range queries.

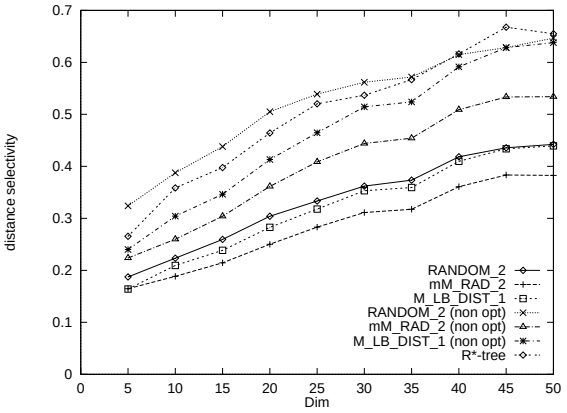

Figure 4.45: Distance selectivity for range queries.

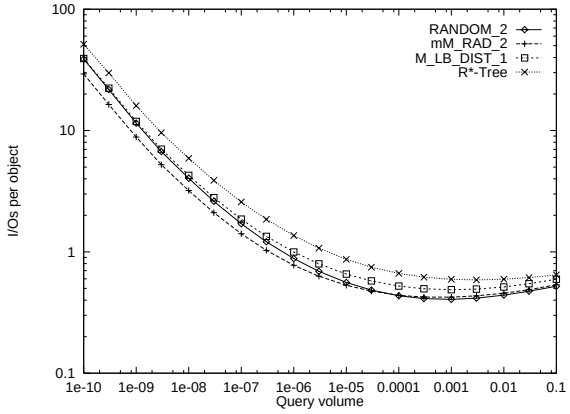

Figure 4.46: I/O costs per retrieved object, as a function of the query volume.

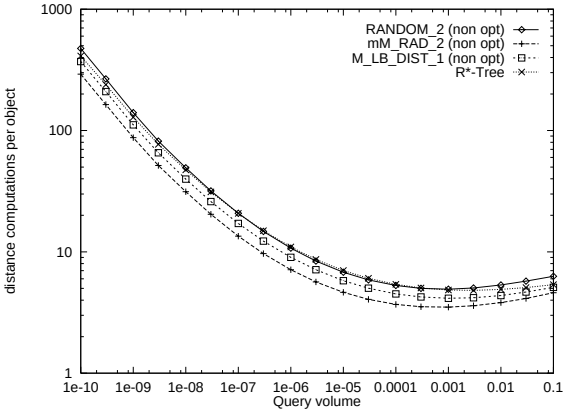

Figure 4.47: Distance computations per retrieved object, as a function of the query volume.

Chapter 5

Bulk Loading the M-tree

The incremental construction of an M-tree could lead, depending on the order of insertion of the objects, to very different performances during the querying phase, as shown in Section 4.7. In [CP98] we presented an algorithm to optimize the building of an M-tree given a set of data objects. This "loading" of the tree can be done to speed-up the index creation on a static database, or to reorganize the tree on a dynamic database, when allowed by time constraints.

5.1 Bulk Loading Techniques

Typical spatial (multidimensional) index structures support random insertion, deletions and updates, but, recently, there has been an increasing interest in *bulk operations* (i.e. a series of operations executed atomically, without interruption by other actions). The most common of such operations is the creation of an index from a given set of record (bulk loading). A remarkable example is index creation to support index-based *spatial joins* [LR94].

A great variety of bulk loading techniques have been proposed for R-trees. Most of them [RL85, KF93, LLE97] sort the dataset using one-dimensional criteria, usually based on the clustering properties of space-filling (e.g. Hilbert) curves. Only a few methods [LL91, Gav94] exploit the "metric" properties of the dataset (i.e. relative distances between objects), and try to achieve a good clustering of the objects by iteratively improving on the choice of clusters' "centers".

A generic algorithm to bulk loading multidimensional index structures (but the method could be easily extended to metric indices) has been proposed in [vdBSW97]. The index is built bottom-up by using *buffer-trees*. The major drawbacks of this technique are that its performance still depends on the order in which data are inserted and its goal is to reduce only I/O costs, thus ignoring CPU costs.

Another choice for indexing objects in a metric space could be to use a mapping technique like *FastMap* [FL95]. This technique maps objects into points of a D-dimensional space (where D is user-defined), such that the distances between objects are preserved as much as possible. The benefits of this approach are:

1. the D-dimensional points can be indexed using a SAM like R-tree, and
2. if objects are plotted as points in $D = 2$ or 3 dimensions, the user can visualize the data space, in order to reveal the inner structure of the dataset.

However, the method suffers from using approximated distances instead of the *real* ones and from being intrinsically static.

5.2 The `BulkLoading` Algorithm (Base Version)

We propose here a batch bulk loading algorithm that builds the M-tree bottom-up in a recursive way. The algorithm performs a clustering of a set of n *data objects* $\mathcal{S} = \{O_1, \ldots, O_n\}$, with constraints on minimum, u_{min}, and maximum, u_{max}, node utilization, and returns an M-tree $\mathcal{T}$. We set the value of parameter u_{max} to 1, although using a lower value would more easily allow subsequent insertions.

The basic `BulkLoading` algorithm can be described as follows: Given the set of objects $\mathcal{S}$, we first perform an initial clustering by producing k sets of objects $\mathcal{F}_1, \ldots, \mathcal{F}_k$. The k-way clustering is achieved by sampling k objects $O_{f_1}, \ldots, O_{f_k}$ from the $\mathcal{S}$ set, inserting them in the sample set $\mathcal{F}$, and then assigning each object in $\mathcal{S}$ to its nearest sample, thus computing a $k \cdot n$ distance matrix. In this way, we obtain k sets of relatively "close" objects. Now, we invoke the bulk loading algorithm on each of these k sets, obtaining k sub-trees $\mathcal{T}_1, \ldots, \mathcal{T}_k$.[1] The effect of these recursive calls is that, in the leaves of each sub-tree, we obtain a partition of the dataset up to the desired level of granularity. Then, we have to invoke the bulk loading algorithm one more time on the set $\mathcal{F}$, obtaining a super-tree $\mathcal{T}_{sup}$. Finally, we append each sub-tree $\mathcal{T}_i$ to the leaf of $\mathcal{T}_{sup}$ corresponding to the sample object O_{f_i}, and obtain the final tree $\mathcal{T}$.

Of course, the partitioning of the dataset highly depends on the choice of the sample objects: Taking samples in a sparse region would produce very low sub-trees, since the corresponding sets will have a very low cardinality, while a sample in a dense region would produce a higher sub-tree.

Figure 5.1 shows a 2D example and the resulting tree with node capacity $M = 3$: At the first step, the algorithm selects the objects A, B, and C as samples for the sub-trees.

[1] This is similar to the generation of *seeded trees* presented in [LR95].

Other named objects are samples for other sub-trees (note that, in order to simplify the drawing, in the example we assumed that a sample at a higher level is also a sample for lower levels, e.g. C=C'=C").

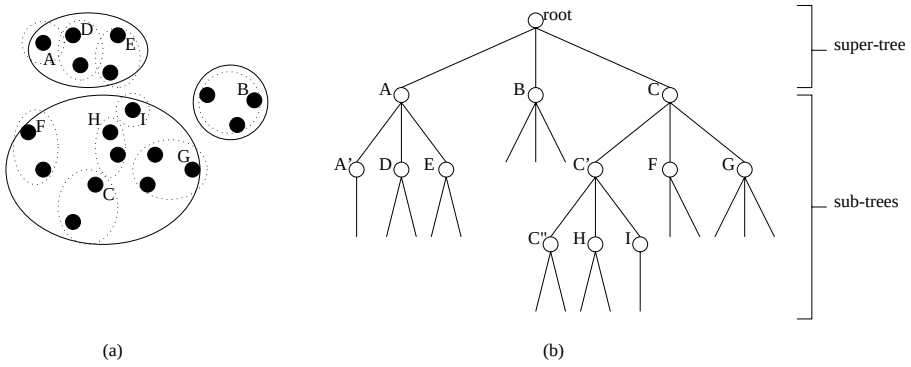

Figure 5.1: A 2D example (a) and the resulting tree (b).

5.3 The Refinement Step

The algorithm, as presented, would eventually produce a non-balanced tree, if the sub-trees have different heights, or underfilled nodes, if a set $\mathcal{F}_i$ has less than $m \stackrel{\text{def}}{=} u_{min} \cdot M$ objects (both cases are included in the example of Figure 5.1). To resolve these problems we use two different techniques:

1. reassign the objects in underfilled sets to other sets, and delete the corresponding sample object from $\mathcal{F}$, and

2. split the "taller" sub-trees, obtaining a number of "shorter" sub-trees; the roots of the obtained sub-trees will be inserted in the sample set $\mathcal{F}$, replacing the original sample object.

The first heuristics ensures that each node of the sub-trees has a minimum storage utilization, deleting those sets having a number of objects lower than the minimum threshold and redistributing their objects between other sets, thus leading to a lower number of samples, while the latter technique increases this number by splitting the taller sub-trees. At the end of the redistribution phase, the algorithm builds the sub-trees on a sample set $\mathcal{F}$ whose cardinality could be very different from the original k. If, however, the redistribution phase leads to a single set of objects, we repeat the overall process, starting from a completely new sampling stage.

In the example of Figure 5.1, supposing $u_{min} = 1/2$, nodes A' and I are deleted and their object reassigned to nodes D and H, respectively. Then, since the sub-tree with minimum height is that having root in B, the sub-trees rooted in A and in C are split, generating the sub-trees rooted in D, E, C", H, F, and G. Finally, the algorithm builds the super-tree on all these 1-level sub-trees (see Figure 5.2, supposing that the samples for the super-tree would be objects D, B, and C).

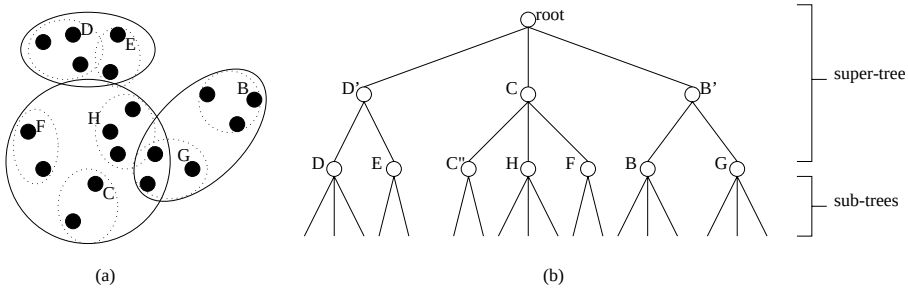

Figure 5.2: The example of Figure 5.1 after the refinement step of the algorithm.

The algorithm proposed so far, though, cannot guarantee that the root node of each sub- or super-tree would have a storage utilization higher than the minimum threshold u_{min}, since this check is evaluated only on low level nodes. This is not a problem for the root node of the whole M-tree that, by hypothesis, can have a minimum of 2 children, but could lead to low storage utilizations for internal nodes. To avoid this problem, we check if the root of the sub-tree just created is underfilled and, if this is the case, split the sub-tree at root level. The complete `BulkLoading` algorithm is given in Figure 5.3.

Examining the behavior of the algorithm during our experiments, we noted that the initial sampling phase often produces at least one sub-tree having height 1, that is, an M-tree with only the root node. So, all other sub-trees having a height greater than 1 have to be split, eventually producing a number of sub-trees of height 1, i.e. nodes representing the leaves of the final M-tree.[2] The super-tree will be built on the root objects of these sub-trees, thus, even if this fact is not coded in the algorithm, the global index is built in a bottom-up fashion, leading to a very good objects' distribution, as shown by experimental results presented in Section 5.5.

5.4 Optimization Techniques

The proposed algorithm, as presented above, has proven itself to be very effective with respect to search costs (as we will see in Section 5.5), but its major drawback is the high

[2]Of course, since we always know the height of the actual lower sub-tree, we do not need to build the upper part of the tree for the taller sub-trees.

```
BulkLoading(S: objects_set, M: integer, m: integer)
{ if ||S|| ≤ M, create a new M-tree T, insert all O_i ∈ S in T and return T;
  else
  { sample k objects O_f1,...,O_fk from S and insert them in F;
      // build the sampling set
    for each O_i ∈ S, insert O_i in F_j, where d(O_i,O_fj) ≤ d(O_i,O_fp),∀O_fp ∈ F;
      // assign each object to its nearest sample
    for each F_j, if ||F_j|| < m // redistribution phase
    { delete O_fj from F;
      for each O_i ∈ F_j, insert O_i in F_l, where d(O_i,O_fl) ≤ d(O_i,O_fp),∀O_fp ∈ F; }
    if ||F|| = 1, restart from the sampling phase;
    for each F_j // build the sub-trees
    { let T_j =BulkLoading(F_j, M, m);
      if root(T_j) is underfilled, split T_j into p sub-trees T_j,...,T_j+p−1; }
    let h_min be the minimum height of the sub-trees T_j;
    let T' = ∅ be the sub-trees set;
    for each T_j, if height(T_j)> h_min // split the higher trees
    { delete O_fj from F;
      split T_j into p sub-trees T'_1,...,T'_p of height h_min;
      insert T'_1,...,T'_p in T'; // build the set of sub-trees
      insert the root objects of T'_1,...,T'_p, O'_f1,...,O'_fp, in F; }
    else insert T_j in T';
    let T_sup =BulkLoading(F, M, m); // build the super-tree
    append each T_j ∈ T' to the leaf of T_sup corresponding to O_fj ∈ F,
      obtaining a new M-tree T;
      // append each sub-tree to the corresponding leaf of the super-tree
    update the radius of the upper regions of T;
    return T; } }
```

Figure 5.3: The `BulkLoading` algorithm

number of computed distances during the building phase, as compared with other M-tree insertion strategies (its CPU costs are similar to those of the very costly `mM_RAD_2` split policy) and with other metric indexing structures. This led us to investigate how to use Lemma 4.2 to reduce the number of distance computations during the construction phase.

5.4.1 Saving Some Distance Computations

At each call after the initial one, we have to build a tree $\mathcal{T}_r$ rooted in O_r on a subset $\mathcal{S}_r$ of $\mathcal{S}$. By construction, observe that, for each $O_j \in \mathcal{S}_r$, we have already computed, in the previous step, the distance $d(O_r, O_j)$. The sampling phase applied to $\mathcal{S}_r$ yields a set of k sample objects $O_{f_1}, \ldots, O_{f_k}$ and we have to find, for each $O_j \in \mathcal{S}_r$, its nearest sample

object. Suppose O_f^* is the nearest sample for object O_j obtained so far, and the distance between O_j and a sample O_{f_p} has to be computed: Since the value $\mid d(O_j, O_r) - d(O_r, O_{f_p}) \mid$ is a lower bound on $d(O_j, O_{f_p})$, if $d(O_j, O_f^*) \leq \mid d(O_j, O_r) - d(O_r, O_{f_p}) \mid$, we can safely avoid to compute $d(O_j, O_{f_p})$, because this would surely be greater than $d(O_j, O_f^*)$. The root object, thus, acts as a *vantage point* for the computation of the distance matrix [Sha77].

This technique has two major limitations:

1. its application is possible only during the construction of sub-trees, whereas a lot of distance computations are performed after the initial sampling phase (where no distance has been computed yet) and during the construction of the super-tree, and

2. the use of the root object as a vantage point is not very effective, since it is likely that it lies in the "center" of the cluster constituted by the set $\mathcal{S}_r$, while it is suggested [Sha77] that vantage points should be multiple and far from the center of the cluster.

These considerations led us to consider a further optimization technique.

5.4.2 Saving More Distance Computations

In the base version of `BulkLoading`, we do not compute the relative distances between sample objects, since it is clear that the nearest sample of such objects will be the sample itself. If, though, we compute such distances, the sample objects can play the role of *multiple vantage points*, like the root object in Section 5.4.1. In this case, however, the sample objects are not crowded near the center of the cluster, thus leading to a more efficient distance pruning. Experimental results will show if the overhead introduced by the computation of the relative distances between the sample objects can result in a lower number of computed distances. The global algorithm for the distance matrix computation is shown in Figure 5.4.

Figures 5.5 and 5.6 show the results for both optimization techniques in terms of percentage of distance computations saving and of total computed distances, respectively, as a function of the space dimensionality (in the Figures `BulkLoading0` refers to the original algorithm, `BulkLoading1` to the first optimization technique, while `BulkLoading2` uses both optimization techniques). Here and in the experiments of Section 5.5, we will use the same datasets and values used in Section 4.7.

The second optimization achieves far better results than the first one, reaching a 70% saving for $D = 5$. The decreasing trend of distance computations saving is essentially due to two factors:

```
DistanceMatrix(S: objects_set, F: sample_set, O_r: root_object, D: distance_matrix)
{ for each O_i ∈ S
  { if O_i = O_{f_k} ∈ F, then let D_{j,i} = ∞, ∀j ≠ k; let D_{k,i} = 0;
      // assign each sample object to itself
    else
    { D_{1,i} = d(O_{f_1}, O_i) ; // compute the first distance
      j* = 1;
      for each O_{f_j} ∈ F, j > 1;
      { if (| d(O_r, O_{f_j}) − d(O_r, O_i) |< d(O_{f_{j*}}, O_i) and
            (∀k < j : D_{k,i} < ∞, | D_{k,i} − d(O_{f_j}, O_{f_k}) |< d(O_{f_{j*}}, O_i)
          then D_{j,i} = d(O_{f_j}, O_i); // we have to compute this distance
        else D_{j,i} = ∞; } // we can avoid this distance computation
      if D_{j,i} < D_{j*,i} then j* = j; // update the nearest sample } } }
```

Figure 5.4: The distance matrix computation algorithm

1. With increasing D, the number of samples, k, decreases, so that the percentage of distances to be computed increases accordingly; this depends on how k is related to the node capacity M (see Section 5.5).

2. Using the L_∞ metric, distances between objects tend to a constant value, for increasing space dimensionality, which reduces the positive effect of having multiple vantage points; as a limit case, for very high dimensionalities, the second optimization technique would compute a higher number of distances than the original algorithm; this would happen when the number of distance computations pruned by using the vantage points is lower than $k(k-1)/2$.

The most surprising result displayed by Figure 5.6 is the initial increasing trend for low dimensionalities for the final optimized algorithm: This shows the effectiveness of the pruning criterion when the distances between data objects have a non-low variance distribution.

5.5 Experimental Results

In this Section we provide experimental results on the performance of the `BulkLoading` algorithm compared to other M-tree insertion techniques. The split policies used are `mM_RAD_2`, `RANDOM_2`, and `M_LB_DIST_1`. For `BulkLoading` we always use $u_{max} = 1$, and both optimization techniques presented in Section 5.4.

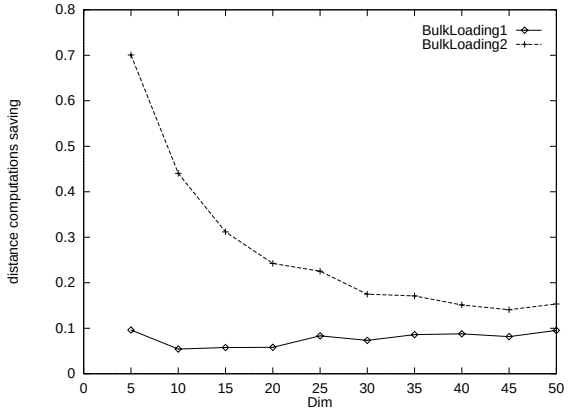

Figure 5.5: Percentage of distance computations saving during construction phase.

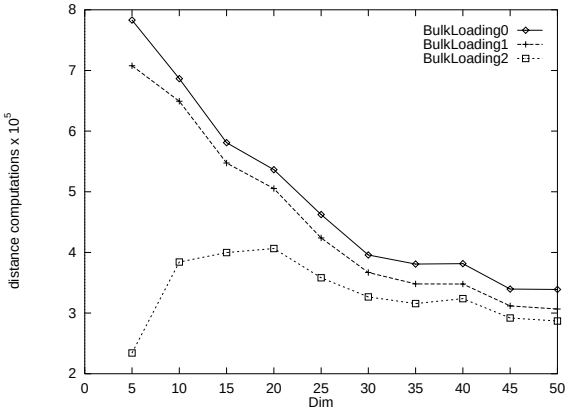

Figure 5.6: Computed distances during construction phase.

5.5.1 The Effect of Sampling Size

First of all, we have to choose the value of k for the algorithm: The first, obvious, choice is to take a value $k = M$, so that we could insert the M samples in a single node obtaining a full root node. If, however, the number of objects is low (i.e. $n \approx M$) we have to compute the distance matrix almost completely, and, since the sets are nearly empty, the redistribution phase could easily end up inserting all objects in a single set, if the distance distribution has a low variance. Thus, a second choice could be to take $k = \min\{M, n/M\}$, obtaining "reasonably" full sets. In this way, though, if $n \approx M$, the root node would have a very low storage utilization, so the final choice for the value of k is $\max\{\min\{M, n/M\}, m\}$.

5.5.2 Minimum Utilization

In the following we will investigate how the storage utilization affects the performance of the `BulkLoading` algorithm. Figures 5.7 and 5.8 show the CPU costs for building the M-tree and for 10-NN queries when the minimum storage utilization threshold, u_{min}, varies in the range $0.1 \div 0.4$. As can be expected, for increasing values of u_{min} the search costs are decreasing, whereas the building costs have an increasing trend. The explanation for this behavior is that higher storage utilizations lead to a better clustering of the objects within each node. Higher utilization thresholds, however, induce higher building costs since it is more likely that the sets associated with the samples would result in a single set because of redistribution of objects in underfilled sets (in this case the distances computed so far are useless and are discarded). This is even more pronounced for $u_{min} = 0.5$ (results are not shown here), where CPU building costs grow dramatically and, sometimes, the

redistribution phase enters an endless loop. Search costs, though, are quite similar to those obtained with $u_{min} = 0.4$, which suggests to use a value of u_{min} between 0.3 and 0.4. In following experiments we will use a value $u_{min} = 0.3$.

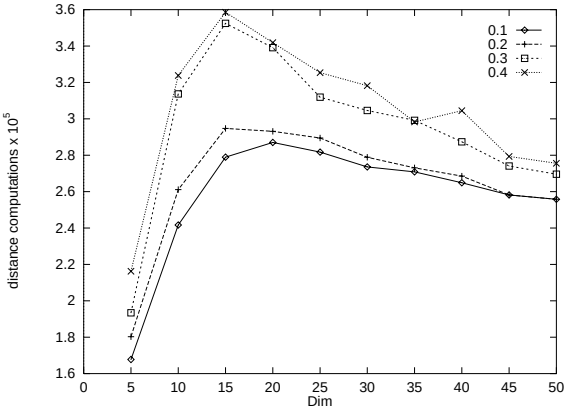

Figure 5.7: Computed distances for building the tree.

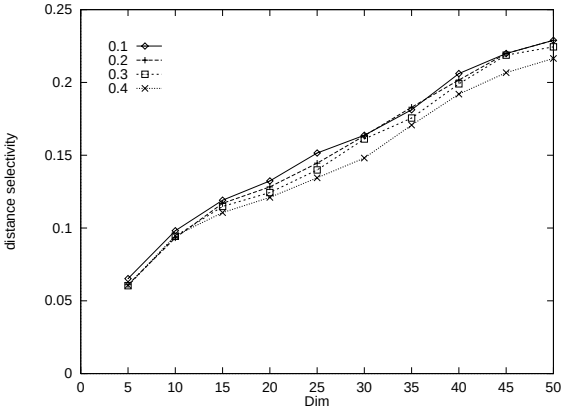

Figure 5.8: Distance selectivity for 10-NN queries.

I/O costs (not shown here) for the building phase are quite similar for different utilization thresholds, whereas higher thresholds lead to lower I/O search costs. This is explained by the lower number of pages of trees built with higher utilization and, as seen before, by the better objects' clustering of such trees, both effects inducing lower I/O costs.

5.5.3 Comparing `BulkLoading` with Standard Insertion Techniques

Now, we consider how the dimensionality of the dataset influences the performance of the proposed bulk loading algorithm. As with standard insertion methods, the number of distances computed by the algorithm decreases with growing dimensionalities, whereas I/O costs have an inverse trend, as shown by Figures 5.9 and 5.10. The reason for this behavior is that increasing D reduces the node capacity, thus reducing the size of the distance matrix to be computed during the clustering phase of the algorithm, and so the number of computed distances, but, of course, leads to larger trees (see also Figure 5.12). The I/O costs for the bulk loading algorithm are, not surprisingly, the lowest, since this method makes massively use of internal memory, e.g. to store the distance matrices at different levels of the tree. It should be noted, however, that basing our implementation on the GiST architecture, we have to keep every intermediate index on secondary storage, while storing them in internal memory we could obtain the minimum cost of writing only the complete M-tree, at the cost of a very increased memory utilization. CPU costs show

that the proposed algorithm is very efficient in the index construction, with costs very similar to, if not lower than, the cheapest `RANDOM_2` split policy. Indeed, Figure 5.10 also shows the effectiveness of the optimization technique to reduce the number of distance computations with low dimensionalities, that can lead to save the 50% of CPU costs for $D = 5$.

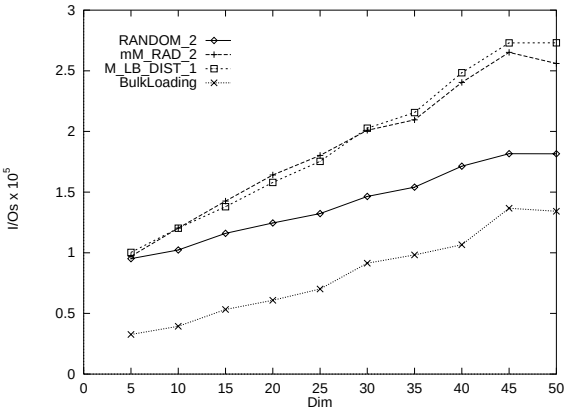

Figure 5.9: I/O costs for building M-tree.

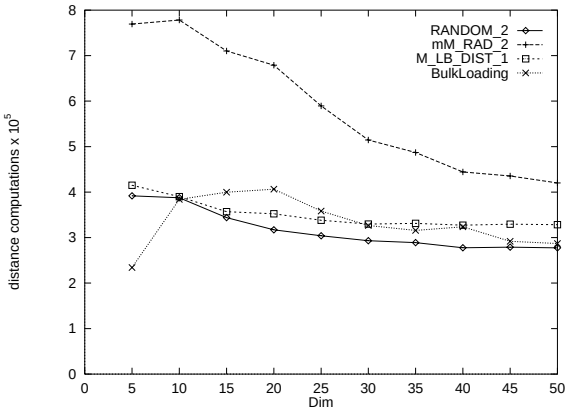

Figure 5.10: Computed distances for building M-tree.

As to the "quality" of tree construction, measured by total covered volume, Figure 5.11 shows that the bulk loading algorithm achieves the proposed goal of optimizing the objects' distribution, by obtaining the lowest overall covered volume. Just as the total covered volume of the M-tree is tied to search performance in terms of distance computations, lower volumes leading to lower search CPU costs, the total number of pages constituting the index is related to search I/O costs, even if the covering volume seems to have a stronger impact, as search performances for `mM_RAD_2` (having the lowest covered volume between the traditional techniques but leading to larger trees) exhibit (see Figures 5.13, 5.14, 5.15, and 5.16). Figure 5.12 shows that the bulk loading algorithm not only attains the lowest covered volume, but leads also to smaller trees, comparable to the cheapest `RANDOM_2` policy.

Performance on 10-NN query processing is summarized in Figures 5.13 and 5.14, where number of page I/O's and distance selectivities are shown, respectively. Figures 5.15 and 5.16 show the I/O and CPU costs for range queries.

Experimental results demonstrate that the good clustering of objects achieved by `BulkLoading` is also reflected by query performance. In fact, the proposed algorithm has CPU and I/O costs very close to, if not better than, `mM_RAD_2` strategy, the "smartest" split policy.

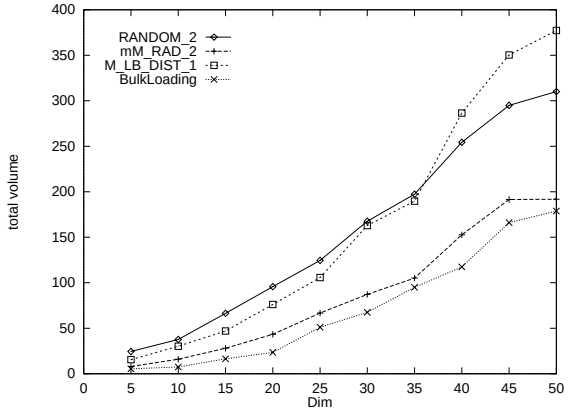

Figure 5.11: Total covered volume.

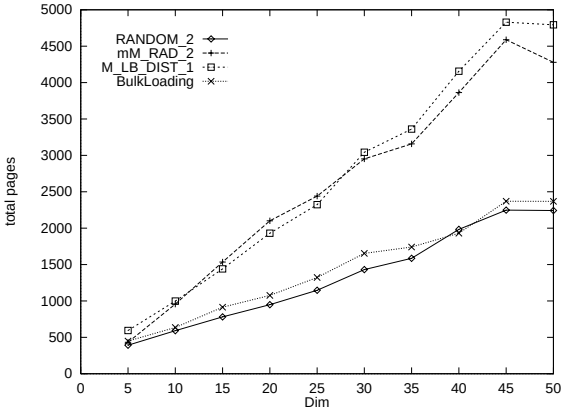

Figure 5.12: Total number of pages.

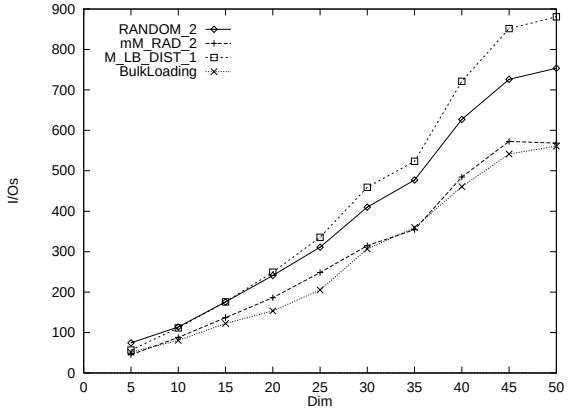

Figure 5.13: I/O costs for processing 10-NN queries.

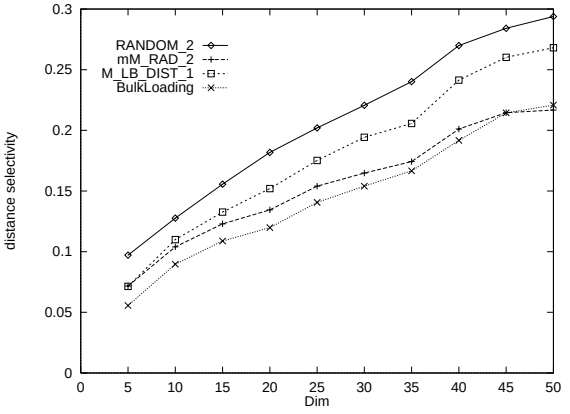

Figure 5.14: Distance selectivity for 10-NN queries.

5.5.4 The Influence of Dataset Size

In Section 4.7.3, we proved that M-tree scales well for increasing dataset sizes, for both construction and search phases. Now we are going to compare the behavior of the `BulkLoading` algorithm against the standard techniques for M-tree construction, for different dataset sizes.

In Figures 5.17 and 5.18 we present the average number of I/O operations and distance computations per inserted object, for 2D datasets whose size varies in the range $10^4 \div 10^5$. Both figures show a logarithmic trend, which is typical of tree-like indices and is mainly due to the increasing height of the tree. As observed in the previous Section, the proposed algorithm is very cheap in terms of I/Os, while its CPU costs are similar to those of the `mM_RAD_2` policy.

Similarly, Figures 5.19 and 5.20 show that both I/O and CPU 10-NN search costs

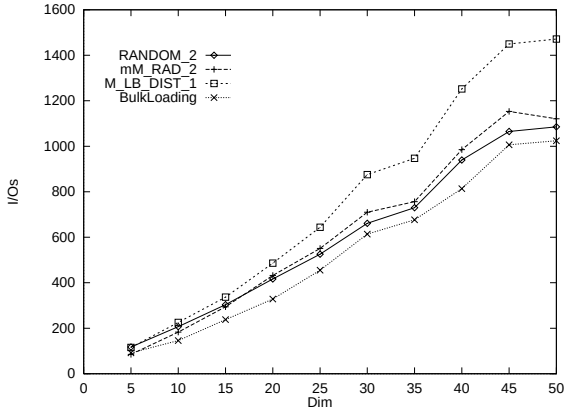

Figure 5.15: I/O costs for processing range queries.

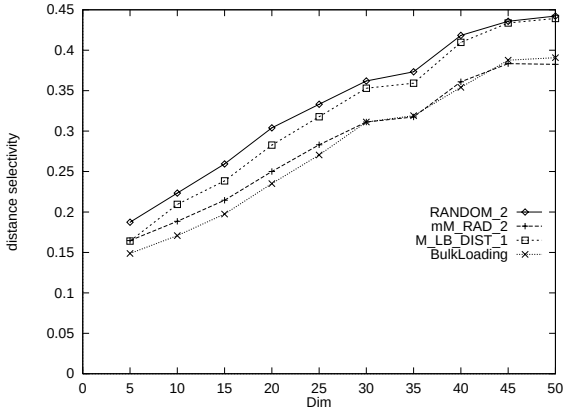

Figure 5.16: Distance selectivity for range queries.

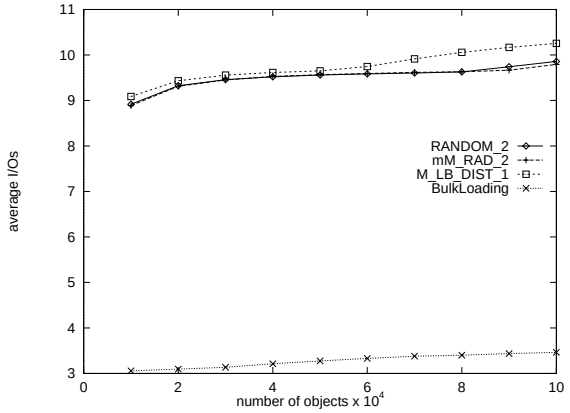

Figure 5.17: Average I/O costs for building the M-tree, as a function of the dataset size.

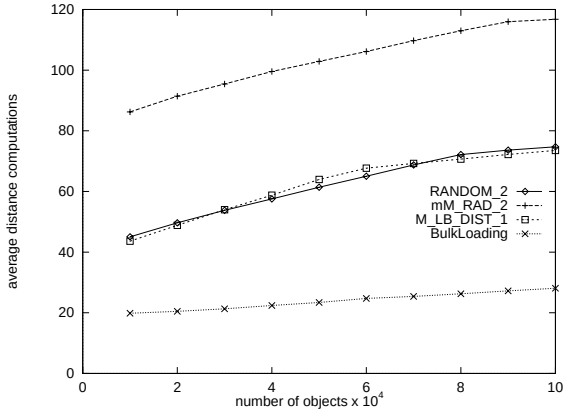

Figure 5.18: Average number of distance computations for building the M-tree, as a function of the dataset size.

grow logarithmically with the number of indexed objects, proving that M-tree scales well in the data set size, and that the dynamic management algorithms do not deteriorate the quality of the search. The bulk loading algorithm achieves the lowest CPU costs, while its I/O costs suffer for the low storage utilization (remember that in these experiments we used $u_{min} = 0.3$).

5.6 Comparing M-tree and mvp-tree

The final set of experiments we present compares the `BulkLoading` algorithm with the mvp-tree access structure [BÖ97]. The mvp-tree was briefly described in Section 3.2.2.

For our experiments we used the following values: $v = 3$ as suggested in [BÖ97],

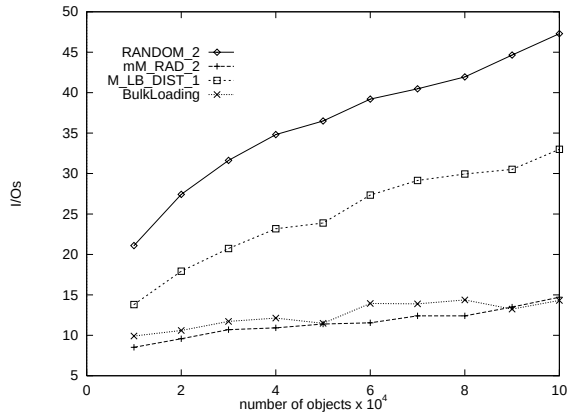

Figure 5.19: I/O costs for processing 10-NN queries as a function of the dataset size.

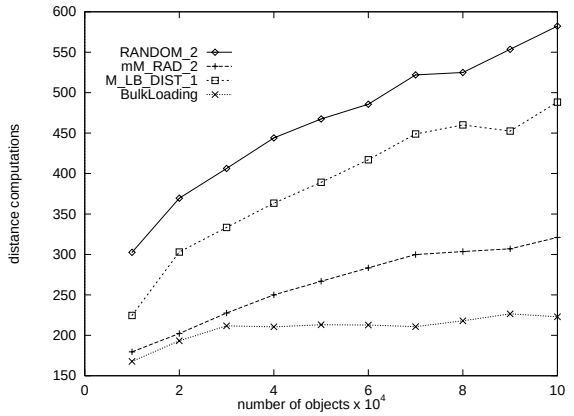

Figure 5.20: Number of distance computations for 10-NN queries as a function of the dataset size.

$f = M$, so that leaves' capacity would be the same as in the M-tree, and $p = 0$, since this optimization, that could be easily inserted in the `BulkLoading` algorithm, will cause consistency problems should the index undergo to re-organizations during a split phase subsequent to an insertion (this problem is not present for mvp-tree, since this is a static index and does not permit insertion and deletion of objects in the database).

Finally, it should be noted that, in the following, I/O costs will be ignored, since mvp-tree implementation does not make use of secondary storage.

Results in Figures 5.21 and 5.22 compare CPU costs to build and search, respectively, M-trees, using the `BulkLoading` algorithm, and mvp-trees.

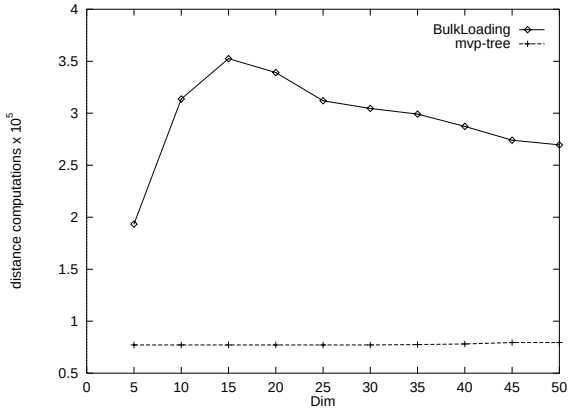

Figure 5.21: Computed distances for loading M- and mvp-trees, as a function of the space dimensionality.

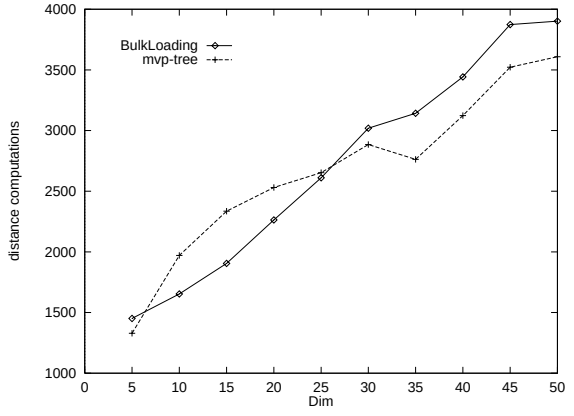

Figure 5.22: Distance computations for range queries.

Figure 5.22 shows the search costs for range queries as a function of the dimensionality

of the vector space. The graphs display quite similar results for both the index structures, with M-tree penalized in higher dimensionalities by a 10% overhead in terms of computed distances, which should be a very good tradeoff for the dinamicity of this indexing method. Construction costs, however, as exposed by Figure 5.21, highly amerce the M-tree, leading to a 350% overhead of distance computations for $D = 15$, even if the gap decreases for increasing dimensionalities, leading to a 250% overhead for $D = 50$. This is because the CPU costs for `BulkLoading`, as seen, are decreasing for higher dimensionalities, while the mvp-tree has a constant, slightly increasing, trend.

Figures 5.23 and 5.24 show the behavior of both index structures for datasets of increasing size ($10^4 \div 10^5$ 5D objects). Figure 5.23 presents the average number of distance computations per inserted object: Both indices exhibit a logarithmic trend, typical of tree-like structures. The CPU overhead for M-tree observed in Figure 5.21 (200% for $D = 5$) is clearly almost independent of the number of indexed objects. Figure 5.24 shows the computed distances for range queries: Performances are very similar, with a difference independent of the dataset size.

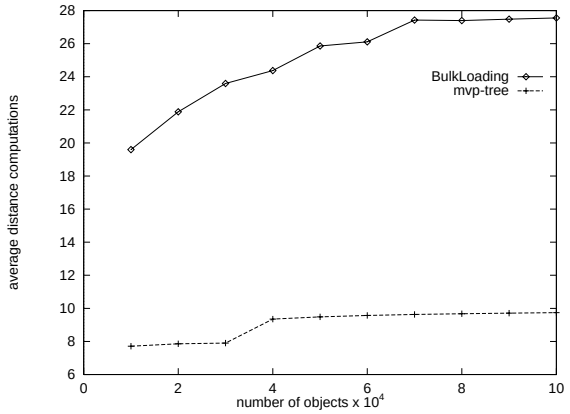

Figure 5.23: Computed distances for building M- and mvp-trees, as a function of the dataset size.

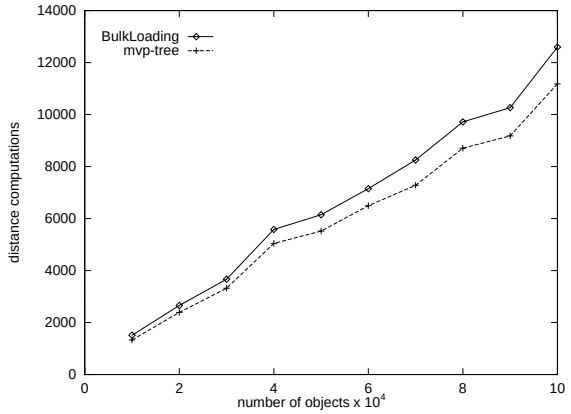

Figure 5.24: Distance computations for range queries.

5.7 Parallelizing `BulkLoading`

It should be noted that the `BulkLoading` algorithm allows a high degree of parallelism. In fact, after the sampling phase, we have to assign each object to its nearest sample; to this end, we have to compute the distance between each object and all the sampled objects, thus obtaining a $k \cdot n$ distance matrix. In order to reduce the overall construction time for such distance matrix, this task can be distributed over a number of available

processors, each processor computing a row (i.e. the distance between a sample object and all the data objects), a column (the distance between a data object and all sample objects), or even a single cell of the matrix, if the number of available processors is very high. It should be noted, though, that the optimization techniques presented in Section 5.4 allow the parallelization of the task of computing the distance matrix only by way of rows, i.e. computing the distances between a sample object and all the data objects.

The assignment of each object to its nearest sample could also be distributed over a number of processors, every processor taking charge of the task of finding the minimum value in an array, this array being a column of the distance matrix. Moreover, the building of each sub-tree could be assigned to a separate processor, thus spreading the utilization of the available processors, since the construction of a sub-tree could entail the building of sub-sub-trees and so on. Finally, the task of appending the sub-trees to the leaves of the super-tree could also be spanned over a number of processors.

Chapter 6

Cost Models for Metric Trees

Although application of metric trees to concrete indexing problems has been proved to be effective [Bri95, BYÖ97, CPZ97], even on "traditional" vector spaces (see also Section 3.2), no theoretical analysis able to predict and justify their performance results is available nowadays. In other terms, *no cost model for metric trees exists yet*, which makes their applicability to a specific dataset still a matter of chance. For instance, given a large set of keywords extracted from a text, to be compared using the edit distance, and an input (query) keyword Q, which is the expected (CPU and I/O) cost to retrieve the, say, 20 nearest neighbors of Q, that is, the 20 strings which are "closest" to Q? Being able to answer questions like this is relevant for database design, query processing, and optimization, since it would provide us with the capability of understanding and tuning a metric access method, and will make it possible to apply optimizers' technology to metric query processing too. In [CPZ98a] we introduced the first *average-case* cost model for metric trees, showing how our approach can be applied to derive cost models for the M-tree and the vp-tree [Yia93] index structures. Then, in [CNP99], we extended the average-case models to derive an effective *query-sensitive* model, i.e. a model able to change its estimates according to the "position" of the query object.

6.1 Cost Models for Spatial Access Methods

Prior to [CPZ98a], no specific work had addressed the problem of estimating costs for queries over generic metric spaces. However, in order to introduce our cost model for metric trees, it is useful to review what has been done in recent years for the case of vector (Cartesian) spaces, which are a subset of metric spaces, with a major focus on the performance of R-tree and its variants.

In [KF93] the authors present a model to estimate I/O costs for range queries as a function of the geometric characteristics of the R-tree's nodes, under the assumption of

uniform distribution of both data and query points. The basic result for this cost model is the following:

Lemma 6.1
The probability that a node N of the R-tree is accessed in a point query is given by its volume.

Proof: This results immediately follows from the assumption of the uniform distribution of point queries in the D-dimensional hypercube. In this case, the probability that a random point falls in a hyper-rectangular region is given by the volume of that region. Therefore, the expected I/O costs for a point query is given by the sum of the covered volume of all the index nodes. □

The result of Lemma 6.1 is then extended to window queries by the following:

Lemma 6.2
The probability that a node N of the R-tree is accessed in a window query is given by the volume of the hyper-rectangle obtained by "inflating" the node region by the dimension of the query region in each dimension.

Proof: To prove this result is sufficient to show that the probability that the node region and the query region overlap is equal to the probability that a random point is inside the "inflated" region. □

Above results are extended in [FK94], by using concepts of fractal theory [Man77], to derive a cost model for R-tree, which does not depend on the assumption of uniform distribution of query points. The obtained cost model is *tree-independent*, in the sense that no statistics on the tree are used, but only information on the fractal dimension of the dataset and on the effective average capacity of a tree node.

The two previous models for R-tree only provide estimates for average costs. Within the context of query optimization, particular relevance have *query-sensitive* cost models, i.e. models able to change their estimates according to the "position" of the query object. In [TS96], a query-sensitive model for predicting I/O costs of range queries on R-tree is presented; the model is based on a D-dimensional histogram which approximates the distribution of the dataset over a D-dimensional vector space. Using such information, the model can predict costs for a specific query, by using the *density* of points around the query object.

In [PM97], the authors extend the model of [KF93] to predict average I/O costs for nearest neighbor queries. The proposed model is limited to the real plane with the Euclidean distance and provides an estimate of the distance between the query point and its nearest neighbor and a lower and an upper bound on the number of accessed pages.

Finally, in [BBKK97] a complete cost model for nearest neighbor queries over generic multi-dimensional spaces indexed by an X-tree is presented. The model relies on the assumption of uniform distribution of query points and exploits statistics on the tree nodes, thus being tree-dependent. Boundary effects are considered by using the concept of *Minkowski sum*, leading to quite accurate estimates, even in high dimensions.

6.2 The Distance Distribution

It has to be remarked that all the models presented in Section 6.1 exploit information about *data distribution*, i.e. about the position of objects within the considered vector space:

- In [KF93] and in [BBKK97] uniformly distributed datasets are considered.
- In [FK94] the fractal dimension of the dataset is used.
- In [TS96] the *density* of points is stored for different regions of the space.

It is clear that, in a generic metric space, *no information on data distribution can be used*. Therefore, above models cannot be applied to metric trees.[1]

Hence, in order to derive a cost model for metric trees, we pursue an approach which does not rely on data distribution, rather it takes a more general view, able to deal whith generic metric spaces, which can be characterized by the following positions:

1. The only information derivable from the analysis of a metric dataset is (an estimate of) the *distance* distribution of objects. No information on *data* distribution is used.
2. A *biased* query model (the distribution of query objects is equal to that of data objects) is considered, with query objects which do not necessarily belong to the indexed dataset.

We claim that the distance distribution is the correct counterpart of data distribution used for vector spaces, since it is the "natural" way to characterize a metric dataset. As to the biased query model, which apparently contradicts the position that no knowledge of the data distribution is assumed, we clarify this point by precisely defining our working scenario.

First of all we have to extend the concept of metric space.

[1] In principle, concepts of fractal theory can be applied to metric spaces. However, their introduction to develop a fractal cost model is left as subject for future work.

Definition 6.1 (Bounded random metric space)
A *bounded random metric* (BRM) space is a quadruple $\mathcal{M} = (\mathcal{D}, d, d^+, S)$, where $\mathcal{D}$ and d are as usual, d^+ is a finite upper bound on distance values, and S is a measure of probability over (a suitable Borel field defined on) $\mathcal{D}$. □

To help intuition, we slightly abuse terminology and call S the *data* distribution over $\mathcal{D}$. Although S has no specific role in our cost model (we do not need to know S and never use it), its existence is postulated both for formal reasons and to account for the nature of the observed datasets (see Section 6.3.1).

Example 6.1
$([0,1]^D, L_2, \sqrt{D}, U([0,1]^D))$ is the BRM space characterized by an uniform distribution of points over the D-dimensional unit hyper-cube, and where distance between points is measured by the Euclidean (L_2) metric. □

Example 6.2
$(\Sigma^m, L_{edit}, m, S)$ is the BRM space whose domain is the set of all the strings of length up to m over the Σ alphabet, whose distance is measured by the *edit* (Levenshtein) metric (see Example 2.3), and with data distribution S, here left unspecified. □

Definition 6.2 (Distance distribution)
The (overall) distribution of distances over $\mathcal{D}$ is defined as:

$$F(x) = \Pr\{d(\mathbf{O_1}, \mathbf{O_2}) \leq x\} \tag{6.1}$$

where $\mathbf{O_1}$ and $\mathbf{O_2}$ are two (independent) S-distributed random points of $\mathcal{D}$. For each $O_i \in \mathcal{D}$, the *relative* distance distribution, RDD, of O_i is obtained by simply setting $\mathbf{O_1} = O_i$ in Equation 6.1, i.e:

$$F_{O_i}(x) = \Pr\{d(O_i, \mathbf{O_2}) \leq x\} \tag{6.2}$$

□

Intuitively, $F_{O_i}(x)$ represents the fraction of objects in $\mathcal{D}$, sampled according to the S data distribution, whose distance from O_i does not exceed x. For what follows it is useful to regard F_{O_i} as the O_i's "viewpoint" of the $\mathcal{D}$ domain, as determined by d and S. The fact that different objects can have different viewpoints is the general rule. Even for an uniform distribution over a bounded Cartesian domain, the center's viewpoint is not the same as the viewpoint an object close to the boundary has. In order to measure how much two viewpoints are (dis-)similar, we introduce the concept of *discrepancy*.

Definition 6.3 (Discrepancy)
The discrepancy of the two RDDs F_{O_i} and F_{O_j} is defined as:

$$\delta(F_{O_i}, F_{O_j}) = \frac{1}{d^+} \int_0^{d^+} |F_{O_i}(x) - F_{O_j}(x)| \, dx \tag{6.3}$$

□

The discrepancy of any pair of RDDs is a real number in the unit interval $[0, 1]$, and equals 0 iff F_{O_i} and F_{O_j} are the same (which does not imply, however, that $O_i \equiv O_j$). Note that δ is a metric on the functional space $\mathcal{F} = \{F_{O_i} : O_i \in \mathcal{D}\}$, as it can be easily verified.

Consider now the case where both $\mathbf{O_1}$ and $\mathbf{O_2}$ are random points. Under this view, $\Delta \stackrel{\text{def}}{=} \delta(F_{\mathbf{O_1}}, F_{\mathbf{O_2}})$ is a random variable, and $G_\Delta(y) = \Pr\{\Delta \leq y\}$ is the probability that the discrepancy of two (random) RDDs is not larger than y. The higher, for a given y, $G_\Delta(y)$ is, the more likely is that two RDDs F_{O_i} and F_{O_j} "behave" the same, up to an y level of discrepancy. Therefore, if $G_\Delta(y) \approx 1$ for a "low" y value, we can say that the BRM space $\mathcal{M}$ from which G is derived is somewhat "homogeneous" as to the viewpoints that objects in $\mathcal{D}$, weighted according to the S distribution, have. This observation is captured by introducing an index of homogeneity for BRM spaces.

Definition 6.4 (Homogeneity of Viewpoints)
The index of "Homogeneity of Viewpoints" of a BRM space $\mathcal{M}$ is defined as:

$$HV(\mathcal{M}) = \int_0^1 G_\Delta(y) \, dy = 1 - E[\Delta] \tag{6.4}$$

□

Example 6.3
Consider the BRM space $\mathcal{M} = (\{0,1\}^D \cup \{(0.5, \ldots, 0.5)\}, L_\infty, 1, U)$, where the domain is the D-dimensional binary hypercube extended with the "midpoint" $C = (0.5, \ldots, 0.5)$, points are uniformly distributed, and $L_\infty(O_i, O_j) = \max_{k=1}^{D}\{|O_i[k] - O_j[k]|\}$. For all $O_i, O_j \in \{0,1\}^D$ it is $\delta(F_{O_i}, F_{O_j}) = 0$, whereas $\delta(F_{O_i}, F_C) = 1/2 - 1/(2^D + 1)$. It follows that $G_\Delta(y) = (2^{2D} + 1)/(2^D + 1)^2$ for $0 \leq y < 1/2 - 1/(2^D + 1)$, and $G_\Delta(y) = 1$ for $1/2 - 1/(2^D + 1) \leq y \leq 1$. Therefore

$$HV(\mathcal{M}) = 1 - \frac{2^{2D} - 2^D}{(2^D + 1)^3} \stackrel{D \to \infty}{\longrightarrow} 1$$

For instance, when $D = 10$, it is $HV(\mathcal{M}) \approx 1 - 0.97 \times 10^{-3} \approx 0.999$. Since all points but C have the same view of $\mathcal{M}$, even for moderately large values of D the presence of C has a negligible effect on $HV(\mathcal{M})$. □

The relevance of HV lies in the fact that, with a single value, we can characterize the whole BRM space with respect to how objects "see" such a space. The higher $HV(\mathcal{M})$ is, the more two random points are likely to have an almost common view of $\mathcal{M}$. Therefore, $HV(\mathcal{M}) \approx 1$ denotes high homogeneity in the $\mathcal{M}$ space as to objects' distance distributions (but not necessarily with respect to data distribution!). As we will show in next Sections, HV can be high even for real datasets.

6.3 Average-case Cost Models for M-tree

In this Section two different models are presented: The Node-based Metric Cost Model (N-MCM) makes use of statistics for each node of the tree, while the simplified Level-based model (L-MCM) exploits only statistics collected on a per-level basis. Relevant symbols and their descriptions are given in Table 6.1.

Symbol	Description
n	number of indexed objects
$F(x)$	distance distribution
$f(x)$	distance density function
Q	query object
r_Q	query radius
k	number of nearest neighbors
M	number of nodes in the M-tree
O_r	routing object
$r(N_r)$	covering radius of node N_r
$e(N_r)$	number of entries in node N_r
L	height of the M-tree
M_l	number of nodes at level l of the M-tree
$\overline{r_l}$	average covering radius of nodes at level l
$nodes(Q)$	expected I/O cost (node accesses) for query Q
$dists(Q)$	expected CPU cost (distance computations) for query Q
$objs(Q)$	expected number of retrieved objects for query Q

Table 6.1: Summary of symbols and respective definitions

Consider a range query $\texttt{range}(Q, r_Q, \mathcal{C})$. A node N_r of the M-tree has to be accessed iff the ball of radius r_Q centered in the query object Q and the region associated with N_r intersect. This is the case iff $d(Q, O_r) \leq r(N_r) + r_Q$, as it can be derived by triangular inequality, which requires that the distance between the two "centers" is not greater than the sum of the two radii. The probability that N_r has to be accessed can therefore be

expressed as:[2]

$$\Pr\{\text{node } N_r \text{ is accessed}\} = \Pr\{d(Q, \mathbf{O}) \leq r(N_r) + r_Q\} = F_Q(r(N_r) + r_Q) \qquad (6.5)$$

where the uncertainty is due to the position in the space of the routing object of N_r, here considered to be a random point.

Equation 6.5 is the starting point for all the proposed cost models. However, it is easy to see that it is unusable in this form. In fact, the probability that a node is accessed is given as a function of the distance distribution relative to the query object Q, that is obviously unknown at query execution time. Hence, what is needed is a way to somehow approximate the unknown distance distribution F_Q. In the following we will present the basic assumptions that led us to develop two different average-case cost models for M-tree.

6.3.1 Dealing with Database Instances

A database *instance* $\mathcal{O} = \{O_1, \ldots, O_n\}$ of $\mathcal{D}$ is, according to our view, an n-sized sample of objects, selected according to the (unknown) S data distribution over $\mathcal{D}$. From this sample, the basic information we can derive about the BRM space $\mathcal{M}$ is an estimate of F, denoted $\widehat{F^n}$, represented by the $n \times n$ matrix of pairwise distances between objects in $\mathcal{O}$.

As we previously saw, for estimating the cost of a query (either range or nearest neighbors), the best thing would be to know F_Q, i.e. the RDD of the query object itself. However, in the general case this is a hopeless alternative, since Q is not restricted to belong to $\mathcal{O}$. What if we use $\widehat{F^n}$ in place of F_Q? As long as the two distributions behave almost the same, we do not expect relevant estimate errors from *any* cost model we could devise, provided the model correctly uses $\widehat{F^n}$.

In order to verify the above possibility, we computed the HV index for several synthetic and real datasets, summarized in Table 6.2. The `clustered` datasets consist of D-dimensional vectors normally-distributed (with σ=0.1) in 10 clusters over the unit hypercube. Text datasets in Table 6.2 are sets of keywords extracted from 5 masterpieces of Italian literature.

For all these datasets we observed HV values always above 0.98, which justifies the following assumption we make for deriving our cost model:

Assumption 6.1
The homogeneity of viewpoints index, HV, is "high" (close to 1), and the relative distance distribution of a query object Q is well approximated by the sampled $\widehat{F^n}$ distance distribution. □

[2]The radius $r(N_r)$ is not defined for the root node. To obviate this we assume that the root has radius $r(N_{root}) = d^+$.

Name	Description	Size	Dim. (D)	Metric
`clustered`	clustered distr. points on $[0,1]^D$	$10^4 - 10^5$	$5 - 50$	L_∞
`uniform`	uniform distr. points on $[0,1]^D$	$10^4 - 10^5$	$5 - 50$	L_∞
`D`	Decamerone	$17,936$		edit
`DC`	Divina Commedia	$12,701$		edit
`GL`	Gerusalemme Liberata	$11,973$		edit
`OF`	Orlando Furioso	$18,719$		edit
`PS`	Promessi Sposi	$19,846$		edit

Table 6.2: Datasets

The second part follows from the facts that:

1. if objects' RDDs almost behave the same, so will do their average, that is $\widehat{F^n}$, and
2. we assume a biased query model.

6.3.2 The Node-based Metric Cost Model

Using Assumption 6.1, we can approximate Equation 6.5 as follows:

$$\Pr\{\text{node } N_r \text{ is accessed}\} = F_Q(r(N_r) + r_Q) \approx F(r(N_r) + r_Q) \tag{6.6}$$

To determine the expected I/O cost for a range query is sufficient to sum above probabilities over all the M nodes of the tree:

$$nodes(\texttt{range}(Q, r_Q, \mathcal{C})) = \sum_{i=1}^{M} F(r(N_{r_i}) + r_Q) \tag{6.7}$$

The number of distance computations (CPU cost) is estimated by considering the probability that a page is accessed multiplied by the number of its entries, $e(N_{r_i})$, thus obtaining:[3]

$$dists(\texttt{range}(Q, r_Q, \mathcal{C})) = \sum_{i=1}^{M} e(N_{r_i})\, F(r(N_{r_i}) + r_Q) \tag{6.8}$$

Finally, the expected number of retrieved objects is estimated as:

$$objs(\texttt{range}(Q, r_Q, \mathcal{C})) = n \cdot F(r_Q) \tag{6.9}$$

[3]The optimization strategies described in Section 4.2 for reducing the number of distance computations are not considered here, and their inclusion in the cost model is left as a subject for future research.

Let us now consider the case of a nearest neighbors query, $\mathtt{NN}(Q, k, \mathcal{C})$, on the assumption that $k < n$. As a first step we determine the expected distance between the query object and its k-th nearest neighbor, which depends on the distance distribution F_Q. Let $\mathbf{nn}_{Q,k}$ be the random variable standing for the distance of the k-th nearest neighbor of Q to the query object itself. The probability that $\mathbf{nn}_{Q,k}$ is at most r equals the probability that at least k objects are inside the ball of radius r centered in Q, that is:

$$
\begin{aligned}
P_{Q,k}(r) &\stackrel{\text{def}}{=} \Pr\{\mathbf{nn}_{Q,k} \leq r\} = \\
&= \sum_{i=k}^{n} \binom{n}{i} \Pr\{d(Q,\mathbf{O}) \leq r\}^i \Pr\{d(Q,\mathbf{O}) > r\}^{n-i} = \\
&= \sum_{i=k}^{n} \binom{n}{i} F_Q(r)^i (1 - F_Q(r))^{n-i} = \\
&= \sum_{i=0}^{n} \binom{n}{i} F_Q(r)^i (1 - F_Q(r))^{n-i} - \sum_{i=0}^{k-1} \binom{n}{i} F_Q(r)^i (1 - F_Q(r))^{n-i} = \\
&= 1 - \sum_{i=0}^{k-1} \binom{n}{i} F_Q(r)^i (1 - F_Q(r))^{n-i} \approx 1 - \sum_{i=0}^{k-1} \binom{n}{i} F(r)^i (1 - F(r))^{n-i}
\end{aligned}
\tag{6.10}
$$

The density function $p_{Q,k}(r)$ is obtained by taking the derivative of $P_{Q,k}(r)$:

$$
\begin{aligned}
p_{Q,k}(r) &= \frac{d}{dr} P_{Q,k}(r) \approx \frac{d}{dr} \left(1 - \sum_{i=0}^{k-1} \binom{n}{i} F(r)^i (1 - F(r))^{n-i} \right) = \\
&= -\sum_{i=0}^{k-1} \binom{n}{i} \left[i \cdot F(r)^{i-1} \; f(r)(1 - F(r))^{n-i} - (n-i) F(r)^i f(r) (1 - F(r))^{n-i-1} \right] = \\
&= \sum_{i=0}^{k-1} \binom{n}{i} F(r)^{i-1} f(r) (1 - F(r))^{n-i-1} \left[(n-i) \; F(r) - i(1 - F(r)) \right] = \\
&= \sum_{i=0}^{k-1} \binom{n}{i} F(r)^{i-1} f(r) (1 - F(r))^{n-i-1} (nF(r) - i)
\end{aligned}
\tag{6.11}
$$

and the expected k-th nearest neighbor distance is computed by integrating $p_{Q,k}(r)$ over all r values:

$$
\begin{aligned}
E[\mathbf{nn}_{Q,k}] &= \int_0^{d^+} r \cdot p_{Q,k}(r) \; dr = \\
&= |r \, P_{Q,k}(r)|_0^{d^+} - \int_0^{d^+} P_{Q,k}(r) \; dr = d^+ - \int_0^{d^+} P_{Q,k}(r) \; dr
\end{aligned}
\tag{6.12}
$$

For $k = 1$, above results simplify as follows:

$$P_{Q,1}(r) \approx 1 - (1 - F(r))^n \tag{6.13}$$

$$p_{Q,1}(r) = \frac{d}{dr} P_{Q,1}(r) \approx n\, f(r)\, (1 - F(r))^{n-1} \tag{6.14}$$

$$E[\mathbf{nn}_{Q,1}] = \int_0^{d^+} r \cdot p_{Q,1}(r)\; dr \approx \int_0^{d^+} r\; n\; f(r)\, (1 - F(r))^{n-1}\; dr = \tag{6.15}$$

$$= -\left| r\, (1 - F(r))^n \right|_0^{d^+} + \int_0^{d^+} (1 - F(r))^n\; dr = \int_0^{d^+} (1 - F(r))^n\; dr$$

and reduce to those derived in [BBKK97] for vector spaces and Euclidean distance. We remark, however, that above formulas are suitable for generic metric spaces, since they do not require the computation of any "Cartesian volume", as done in [BBKK97].

Equation 6.15 shows that the expected nearest neighbor distance can be obtained by integrating over all the possible distance values the n-th power of the complement to 1 of the distance distribution. Note that $\lim_{n\to\infty}(1 - F(r))^n = 0$, thus $E[\mathbf{nn}_{Q,1}]$ goes to zero when the number of objects tends to infinity, as intuition may suggest.

The expected number of page reads can now be obtained by integrating Equation 6.7 over all radius values, each value weighted by its probability to occur, as given by Equation 6.11. For the case $k = 1$ we obtain

$$nodes(\mathtt{NN}(Q, 1, \mathcal{C})) = \int_0^{d^+} nodes(\mathtt{range}(Q, r, \mathcal{C}))\, p_{Q,1}(r)\; dr \approx \tag{6.16}$$

$$\approx \int_0^{d^+} \sum_{i=1}^{M} F(r(N_{r_i}) + r)\; n\; f(r)\, (1 - F(r))^{n-1}\; dr$$

The same principle is applied to determine the expected number of computed distances, for which the number of entries in each node has to be considered:

$$dists(\mathtt{NN}(Q, 1, \mathcal{C})) = \int_0^{d^+} dists(\mathtt{range}(Q, r, \mathcal{C}))\, p_{Q,1}(r)\; dr \approx \tag{6.17}$$

$$\approx \int_0^{d^+} \sum_{i=1}^{M} e(N_{r_i})\; F(r(N_{r_i}) + r)\; n\; f(r)\, (1 - F(r))^{n-1}\; dr$$

6.3.3 The Level-based Metric Cost Model

The basic problem with N-MCM is that mantaining statistics for every node of the tree requires $O(M) = O(n)$ space and the computation of expected values has the same complexity, thus can be very time consuming when the index is (very) large. To obviate this, we consider a simplified model, called L-MCM, which uses only average information

collected for each level of the M-tree. This will intuitively lead to a lower accuracy with respect to N-MCM, but, as shown in Section 6.3.4, estimates are still accurate enough.

For each level l of the tree ($l = 1, \ldots, L$, with the root at level 1 and leaves at level L), L-MCM just uses two information: M_l (the number of nodes at level l), and $\overline{r_l}$ (the average value of the covering radius considering all the nodes at level l). Given these statistics, and referring to Equation 6.7, the number of pages accessed by a range query can be estimated as:

$$nodes(\texttt{range}(Q, r_Q, \mathcal{C})) \approx \sum_{l=1}^{L} M_l \; F(\overline{r_l} + r_Q) \tag{6.18}$$

Similarly, we can estimate CPU costs as:

$$dists(\texttt{range}(Q, r_Q, \mathcal{C})) \approx \sum_{l=1}^{L} M_{l+1} \; F(\overline{r_l} + r_Q) \tag{6.19}$$

where $M_{L+1} \stackrel{\text{def}}{=} n$ is the number of indexed objects. Compared to Equation 6.8, we have exploited the simple observation that the number of nodes at a given level equals the number of entries at the next upper level of the tree.

Correspondingly, I/O and CPU costs for a $\texttt{NN}(Q, 1, \mathcal{C})$ query are estimated as follows:

$$nodes(\texttt{NN}(Q, 1, \mathcal{C})) \;\approx\; \int_0^{d^+} \sum_{l=1}^{L} M_l \; F(\overline{r_l} + r) \; n \; f(r) \; (1 - F(r))^{n-1} \; dr \tag{6.20}$$

$$dists(\texttt{NN}(Q, 1, \mathcal{C})) \;\approx\; \int_0^{d^+} \sum_{l=1}^{L} M_{l+1} \; F(\overline{r_l} + r) \; n \; f(r) \, (1 - F(r))^{n-1} \; dr \tag{6.21}$$

6.3.4 Experimental Evaluation

In order to evaluate the accuracy of the presented cost models, we ran several experiments on both synthetic and real datasets, as described in Table 6.2. Estimates were compared with actual results obtained by the M-tree, which was built using the `BulkLoading` algorithm described in Chapter 5 with a node size of 4 Kbytes and a minimum node utilization of 30%.

The first set of experiments concerns the `clustered` datasets, and investigates accuracy of estimates as a function of the dimensionality D of the space. The distance distribution is approximated by an *equi-width* histogram with 100 bins, respectively storing the values of $\widehat{F^n}(0.01)$, $\widehat{F^n}(0.02)$, and so on.

Figures 6.1 and 6.2 show estimated and real CPU costs and the relative errors (averaged over 1000 queries), respectively, for range queries with radius $\sqrt[D]{0.01}/2$ as a function

of the space dimensionality, while Figures 6.3 and 6.4 present estimated and real I/O costs and the relative errors. It can be seen that N-MCM is very accurate, with a maximum relative error of 4%, while the performance of L-MCM is worse yet still good (with error below 10%). Figures 6.5 and 6.6 show that also query selectivity is well estimated, with errors never exceeding 3%.

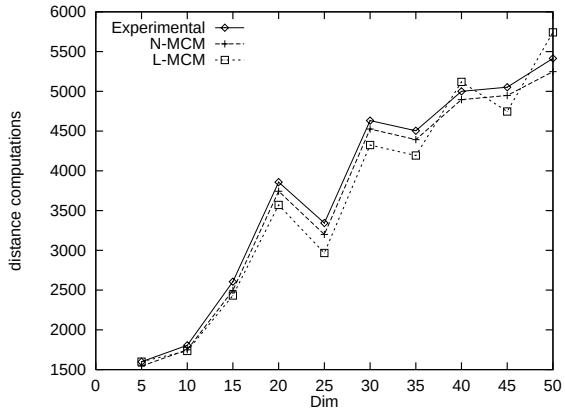

Figure 6.1: Estimated and real CPU costs for range queries.

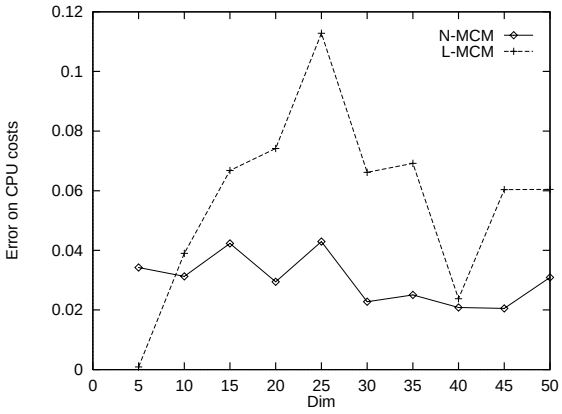

Figure 6.2: Relative errors on CPU costs for range queries.

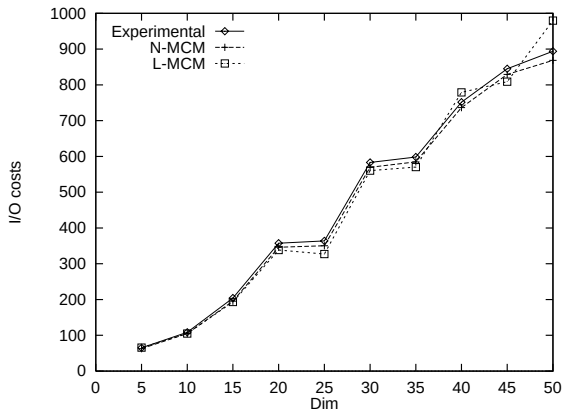

Figure 6.3: Estimated and real I/O costs for range queries.

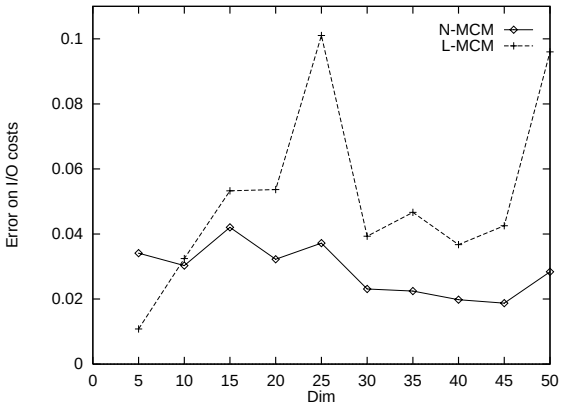

Figure 6.4: Relative errors on I/O costs for range queries.

For the analysis of nearest neighbors queries, we considered the case $k = 1$. Actual costs (averaged over 1000 queries) are contrasted with those estimated by three different models:

1. The L-MCM (Equations 6.20 and 6.21);
2. The costs predicted by L-MCM for a range query, $\texttt{range}(Q, E[\mathbf{nn}_{Q,1}], \mathcal{C})$, with radius equal to the expected NN distance (Equation 6.15);

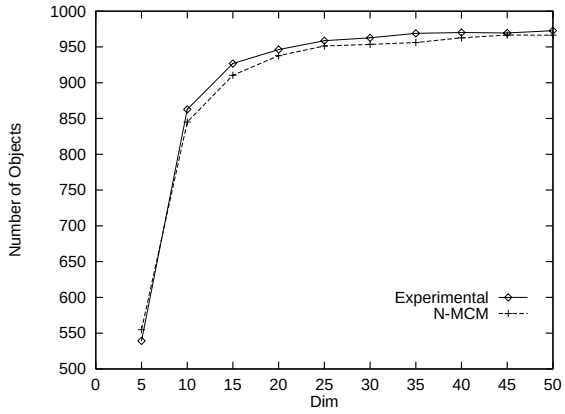

Figure 6.5: Estimated and real cardinality of the result for range queries.

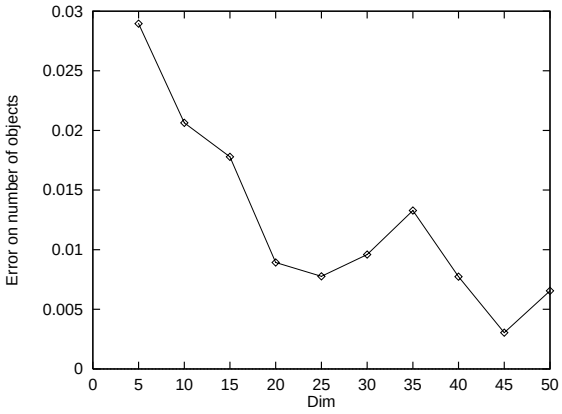

Figure 6.6: Relative errors on the cardinality of the result for range queries.

3. The costs predicted by L-MCM for a range query with a radius such that the expected number of retrieved objects is at least 1, that is, $\texttt{range}(Q, r(1), \mathcal{C})$, $r(1) = \min\{r : n \cdot F(r) \geq 1\}$ (Equation 6.9).

Figures 6.7 and 6.8 show estimated and real CPU costs and the relative errors, respectively, for 1-NN queries, as a function of the space dimensionality, while Figures 6.9 and 6.10 present estimated and real I/O costs and the relative errors. Figures 6.7 and 6.9 demonstrate that cost estimates are highly reliable, even if errors are higher with respect to the range queries case. Figures 6.11 and 6.12, showing actual and estimated NN distances and the relative error, points out how the model based on $r(1)$ can lead to high errors for high D values, which is mainly due to the approximation introduced by the histogram representation.

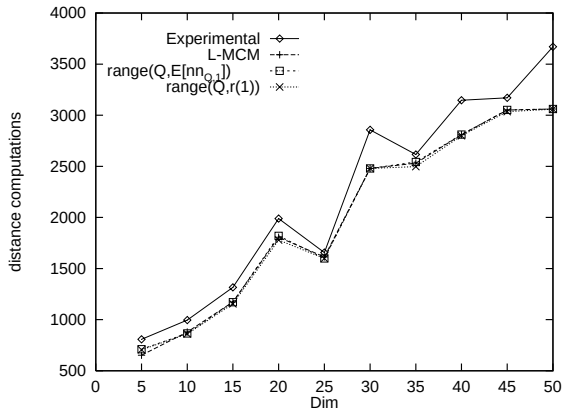

Figure 6.7: Estimated and real CPU costs for NN queries.

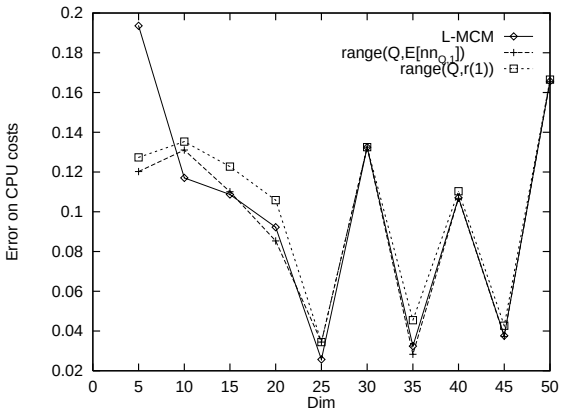

Figure 6.8: Relative errors on CPU costs for NN queries.

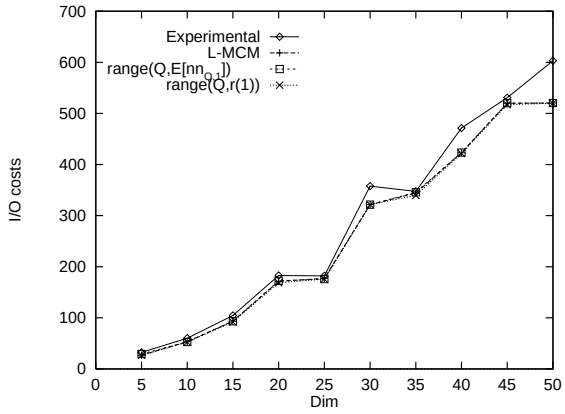

Figure 6.9: Estimated and real I/O costs for NN queries.

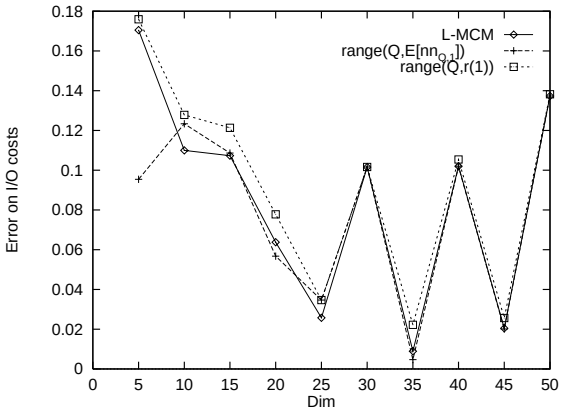

Figure 6.10: Relative errors on I/O costs for NN queries.

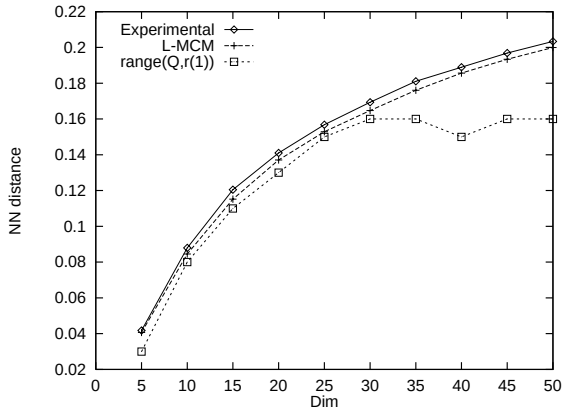

Figure 6.11: Estimated and real distance of the NN.

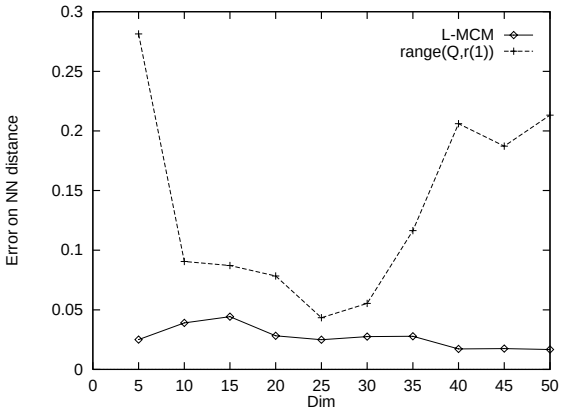

Figure 6.12: Relative errors on the distance of the NN.

Experiments on the real datasets of text keywords (see Table 6.2) were based on 25-bins histograms, since 25 was the maximum observed edit distance. Figures 6.13 and 6.14 compare the analitically predicted CPU and I/O costs, respectively, with those experimentally obtained for 1000 range queries with radius 3. Relative errors are usually below 10% and rarely reach 15%.

Finally, Figures 6.15 and 6.16 compare estimated and real costs for range queries over the `clustered` dataset with $D = 20$ and a variable query radius.

6.4 A Query-sensitive Cost Model

In order to evaluate the accuracy of a cost model, it is important to precisely define how *estimate errors* are assessed. To this end, given an experimental testbed consisting of a

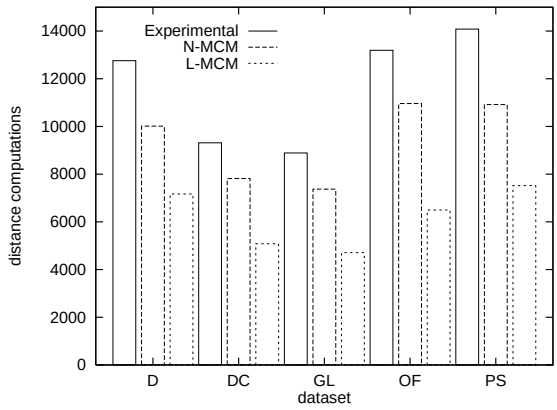

Figure 6.13: Estimated and real CPU costs for range queries for each text dataset.

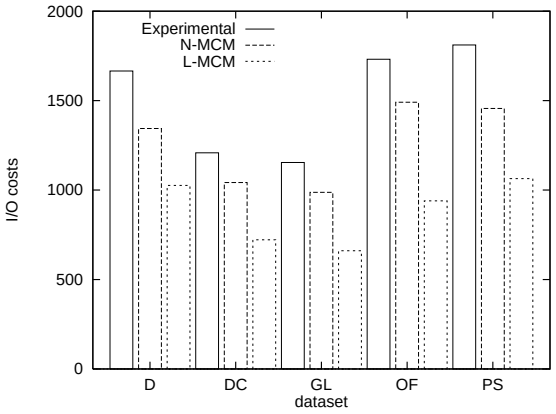

Figure 6.14: Estimated and real I/O costs for range queries for each text dataset.

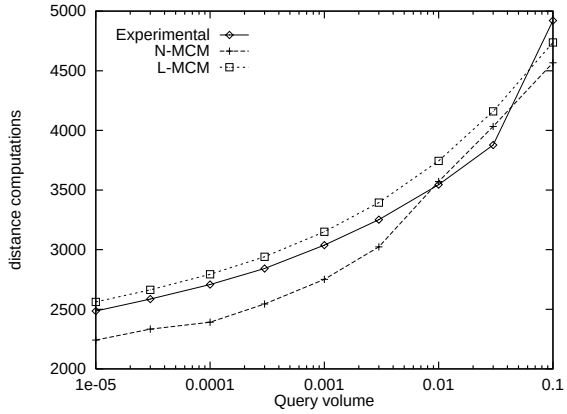

Figure 6.15: Estimated and real CPU costs for range queries as a function of the query volume.

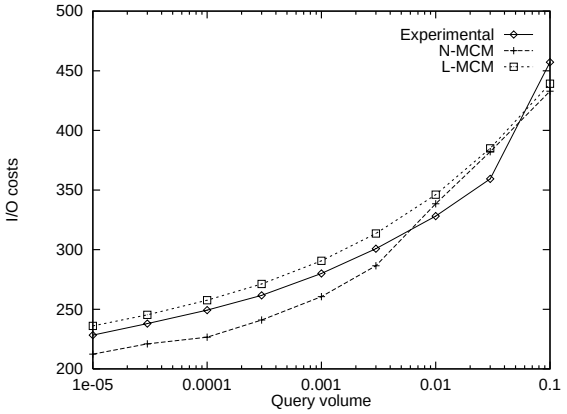

Figure 6.16: Estimated and real I/O costs for range queries as a function of the query volume.

set $\mathcal{Q} = \{q_1, \ldots, q_N\}$ of N queries, we consider three different kinds of error, as explained in the following.

- *Average absolute relative error*, defined as:

$$\texttt{AvgErr} = \frac{1}{N} \sum_{q \in \mathcal{Q}} \left| \frac{\widehat{c}_q - c_q}{c_q} \right| \tag{6.22}$$

  where c_q is the cost of query q and $\widehat{c}_q$ is its estimate.

- *Maximum absolute relative error*, defined as:

$$\texttt{MaxErr} = \max_{q \in \mathcal{Q}} \left\{ \left| \frac{\widehat{c}_q - c_q}{c_q} \right| \right\} \tag{6.23}$$

- *Absolute relative error on average costs*, defined as:

$$\texttt{AvgCaseErr} = \left| \frac{\widehat{c}_{avg} - c_{avg}}{c_{avg}} \right| \tag{6.24}$$

where $c_{avg} = \frac{1}{N} \sum_{q \in \mathcal{Q}} c_q$ is the average cost due to the execution of the n queries and $\widehat{c}_{avg}$ is the model estimate for the average execution cost.

Note that for average-case cost models it is $\widehat{c}_q = \widehat{c}_{avg}, \forall q \in \mathcal{Q}$, and model's performance is typically evaluated by the `AvgCaseErr` measure (see [FK94, BBKK97, CPZ98a]). In this light, as shown in Section 6.3.4, the average-case M-tree cost model performs well both on real and synthetic datasets, with `AvgCaseErr` assuming values typically around 10%-15%.

It is a fact that, for optimization purposes, one is mainly interested in obtaining good estimates for the *cost of each specific query* and not for the average cost relative to the execution of several queries. So, as a first step of our work, we have examined the behavior of the existing model in this new context: Given a certain query type, we executed several queries of the same type but varying the query object and compared the estimate of the average-case L-MCM model with the real costs obtained for each query.

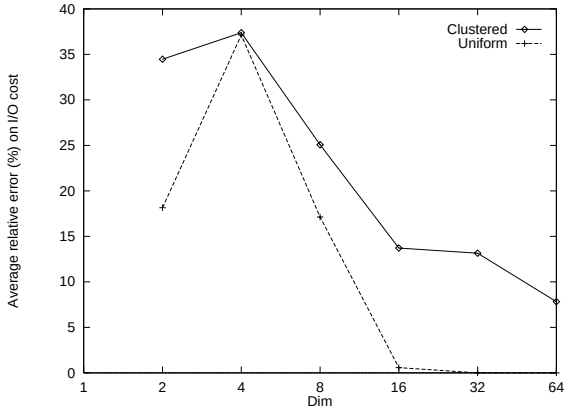

Figure 6.17: `AvgErr` for the average-case L-MCM model — I/O costs for range queries on synthetic datasets.

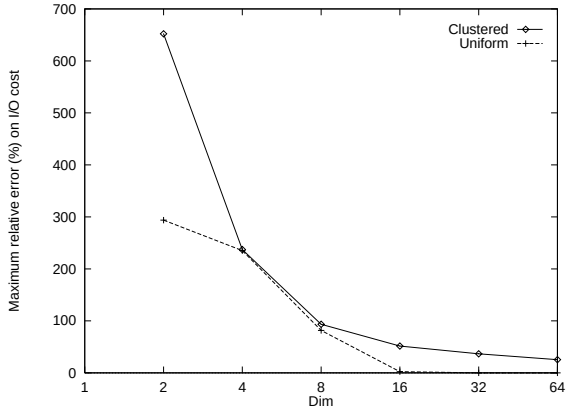

Figure 6.18: `MaxErr` for the average-case L-MCM model — I/O costs for range queries on synthetic datasets.

According to the results obtained we can say that the average-case L-MCM model (similar results were obtained for the N-MCM model) is inadequate for estimating the costs of every single query. For instance, Figures 6.17 and 6.18 show, respectively, the values of `AvgErr` and `MaxErr` observed from the execution of 500 range queries on synthetic datasets (see also Table 6.2). It can be seen that the average-case estimate of the model

compared with each real cost leads to values of `AvgErr` generally around 20%-30% and sometimes close to 40%. Moreover, `MaxErr` assumes high values, tipically around 100%-200%, with peaks near 700%. As Figure 6.17 shows, however, the accuracy of the estimates of the average-case model increases as the space dimensionality increases. This trend is due to the fact that, for high dimensionalities, the "Homogeneity of Viewpoints" of the metric space (see Definition 6.4) is very high, i.e. distance distributions relative to different objects are very similar; thus, the main approximation of Equation 6.6, that is, using (the estimate of) the overall distribution F in place of the distribution relative to the query object Q, F_Q, has a minor impact on the performance of the model. The performance of the model for uniform datasets, however, has a different explanation: In high dimensional spaces, the *dimensionality curse* is such that, when $D \geq 16$, for (almost) every query the whole index has to be accessed (see also Section 3.1.2). It is, therefore, pretty easy to predict this behavior, and even the average-case model shows very good performance, with errors very close to 0%. Due to this trend, in subsequent analyses we will therefore mainly concentrate on clustered datasets.

To obviate the inadequacy of performance of the existing model, hence, results show that we have to better estimate the distance distribution relative to the query object. If we would know the distance distribution F_Q of the query object Q, the cost of a query could be better estimated by using it in Equation 6.5.

In order to have an idea of the behavior of cost estimates obtained when F is replaced by F_Q, we show in Figures 6.19 and 6.20, respectively, the values of `AvgErr` and `MaxErr`. The tests refer to range queries on synthetic clustered datasets and are contrasted with the estimates of the average-case L-MCM model.

As it can be seen, when F_Q is exactly known our model is very accurate: According to the tests considered, `AvgErr` rarely exceeds 10% and `MaxErr` is generally below 30%-40%. These values are considerably lower than the respective ones exhibited by the average-case model, as Figures 6.19 and 6.20 clearly show.

From these results, it seems evident that the major problem of the model is the "loose" approximation of F_Q with F. What we propose is a way to better estimate F_Q, since it is clear that such distance distribution is unknown at query execution time.

As we saw in Section 6.1, in [TS96] the distribution of objects in the considered D-dimensional space is approximated by way of a D-dimensional histogram where the *density* of points is stored. In a generic metric space, such approach is clearly impracticable: To keep track of the different possible views of $\mathcal{M}$, we propose to store, for different regions of the space, a specific distance distribution. Then, at query execution time, these distance distributions are somehow combined to obtain a distribution sufficiently similar to that

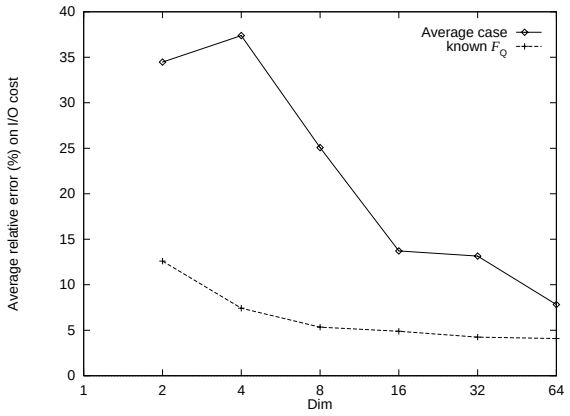

Figure 6.19: `AvgErr` for the model with known F_Q and for the average-case L-MCM model — I/O costs for range queries on synthetic clustered datasets.

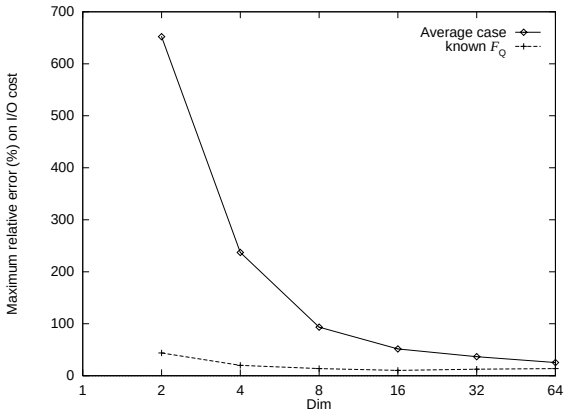

Figure 6.20: `MaxErr` for the model with known F_Q and for the average-case L-MCM model — I/O costs for range queries on synthetic clustered datasets.

of the query object, and such computed distribution is used in Equation 6.5 to estimate query costs.

To give a concrete form to above argumentation, we introduce the following concept.

Definition 6.5 (Witness)
A witness is a point of $\mathcal{D}$ which collects information about the distribution of objects lying around it; in particular, every witness W_j observes its own relative distance distribution, defined as:

$$F_{W_j}(x) = \Pr\{d(W_j, \mathbf{O}) \leq x\} \tag{6.25}$$

where $\mathbf{O}$ is a random object of the dataset $\mathcal{O}$. □

The central idea is to have several witnesses (chosen in some way among the objects in $\mathcal{O}$, in order to reflect their "distribution"), each one with its relative distance distribution; all these observations are then combined in order to give a more accurate estimate of the cost for a given query, depending on the "position" of the query object Q with respect to all the witnesses (see Figure 6.21).

Starting from the notion of witness, we now have to cope with two different problems, in order to obtain a good estimate of F_Q:

1. how witnesses have to be chosen among all the objects of the dataset, and

2. how their relative distributions have to be combined.

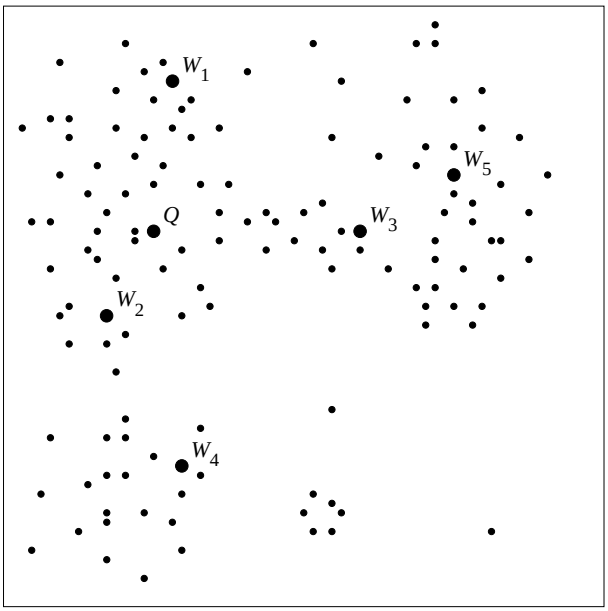

Figure 6.21: The distance distribution of query object Q is approximated by using distance distributions of witnesses W_j.

6.4.1 How to Choose Witnesses

The choice we make about which objects of the dataset have to be designated as witnesses has its own importance, since it affects the way the metric space is "covered" by them: A bad choice, for instance, could lead to have regions of the metric space within which the relative distance distributions are (highly) different and not enough witnesses are present to capture this variability.

A related topic is also the choice for the number nw of witnesses to use: We expect the estimates of the model to be more accurate with a growing number of them, since more information can be exploited.

Ideally, we should select witnesses in such a way that, for every "possible" query object Q, a witness with a distance distribution arbitrarily close to F_Q exists. The basic heuristics we consider is to minimize the distance between each possible query object, Q, and the set of witnesses, by assuming that close objects would have similar distance distributions. To this end, witnesses should provide an appropriate "coverage" of the data space. With this in mind, we propose two basic criteria to choose the witnesses; they are respectively called 'Random' and 'GNAT'.

'Random' – we choose nw objects within the dataset in a random way;

'GNAT' – nw witnesses are chosen among all the objects of the dataset in a way similar

to the one used in the GNAT access method [Bri95] to designate "split points". In practice, the 'GNAT' method first extracts from the dataset a random sample of $3 \cdot nw$ objects, called *candidate* objects; then, within this sample, nw witnesses are chosen far apart each other. More specifically, this is done as follows: A first witness is picked at random within the set of candidate objects; then we choose the candidate point which is farthest away from this one; then we pick the candidate point which is the farthest from these two (that is, its minimum distance from the two is maximized), and so on.

Of course the 'Random' method has the advantage of being much easier and faster; moreover, since witnesses are distributed like objects in $\mathcal{O}$, it is very likely that each query object will have a "near" witness, under the assumption of a *biased* query model, i.e. indexed and query objects follow the same distribution (see also Section 6.2). On the other hand, the 'GNAT' method has the purpose to "cover" the region of the metric space relative to the dataset in a somewhat homogeneous way, avoiding the "crowding" of witnesses in dense regions of the space; in this way, we try to minimize the maximum possible distance between a query object and its nearest witness.

6.4.2 How to Combine Relative Distance Distributions

Starting from the relative distance distributions observed by several witnesses, the next problem consists in how to combine this information in order to give a proper estimate of F_Q. Again, the basic rationale is that close objects have similar distance distributions.

We consider two main criteria to cope with this problem; moreover, we also propose a specific variant for the second one.

'Nearest Witness' Method

This method estimates F_Q as follows:

$$F_Q(x) \simeq F_{W_{NW}}(x) \qquad \text{with } d(W_{NW}, Q) \leq d(W_j, Q),\ j = 1, \ldots, nw \tag{6.26}$$

that is, the unknown distribution relative to the query object Q is approximated with the one relative to its nearest witness. This method is quite easy to use, since it only requires to estabilish which is the nearest witness and no new distance distribution has to be computed.

'Distance Weighted' Method

This method estimates F_Q as follows:

$$F_Q(x) \simeq \frac{\sum_{j=1}^{nw} F_j(x) \cdot \alpha_j}{\sum_{j=1}^{nw} \alpha_j} \tag{6.27}$$

In other terms, F_Q is estimated as a weighted average of *all* the relative distance distributions observed by the witnesses, with generic weights α_j. Of course, different choices for the weights lead to different performance for the model. Our assumption, however, is that witnesses closer to Q are supposed to be more "reliable", since their distance distribution is more similar to that of the query object itself. Therefore, weights α_j in Equation 6.27 should be inversely related to the distance between the query object Q and the witnesses W_j. Our choice is to use the Exp-th power of the inverse of the distance between a witness and Q, that is:

$$\alpha_j = d(W_j, Q)^{-Exp} \tag{6.28}$$

We point out that the 'Nearest Witness' method is the limit of the 'Distance Weighted' method when Exp goes to infinity. On the other end, for $Exp = 0$ we obtain the classic arithmetic average, which means that we equally weigh the contribution given by each witness.

'Distance Weighted', Adaptive Method

The 'Distance Weighted' method is dependent on the parameter Exp, so different choices for the value of the exponent lead to different results (as we will see in Section 6.4.3). It would be, therefore, desirable to find a way to dynamically compute a "proper" value for Exp. Here we propose an *adaptive* variant of the 'Distance Weighted' method which computes a value for Exp as a function of the query object at hand.

The basic idea of this method is to choose a value for Exp as a function of the distances between witnesses and the query object. When, on the average, these distances are all somewhat "high", it does not make sense relying on the nearest witness, so we choose a low value for Exp. On the other hand, when, on the average, witnesses are very close to Q, we can rely more on the nearest witness, thus choosing a high value for Exp.

We define the average distance of witnesses from Q, normalized to maximum distance d^+, as follows:

$$m_{dw} = \sum_{j=1}^{nw} \frac{d(W_j, Q)}{d^+ \cdot nw} \tag{6.29}$$

Now, for a given query, Exp can be computed as:

$$Exp = (1 - m_{dw}) \cdot MaxExp \tag{6.30}$$

where $MaxExp$ has to be thought as that value of Exp for which the two methods, 'Distance Weighted' and 'Nearest Witness', give very similar estimates. Experimentally we found out that an acceptable value is $MaxExp = 10$; this is also the value adopted in all the tests we carried out.

6.4.3 Experimental Evaluation

In order to evaluate the accuracy of our cost models, we ran several experiments on both synthetic and real datasets (see Table 6.2). Estimates are compared with actual results obtained by the M-tree, which, again, was built using the `BulkLoading` algorithm described in Chapter 5 with a node size of 4 Kbytes and a minimum node utilization of 30%.

For each test we ran, 500 similarity queries were executed; unless otherwise stated, for range queries we used a radius $r_Q = \sqrt[D]{0.01}/2$ for synthetic datasets and a radius $r_Q = 3$ for real datasets. For k-nearest neighbor queries we considered only $k = 1$, which is the most common case.

For each distance distribution needed in the experiments we ran, an estimate of its density function f was obtained from an analysis of the dataset $\mathcal{O}$. In particular, for the overall distance distribution we sampled all the $n(n-1)/2$ pairwise distances between all the n objects of $\mathcal{O}$; for each distance distribution relative to a single witness we considered all the $n - 1$ distances between this witness and any other object of $\mathcal{O}$.

In both cases, starting from this sample we built a 100 bins equi-width histogram of type ASH (Averaged Shifted Histogram, as described in [Sco92]) which represents an approximation of the density function f.

6.4.4 Experimental Results

In this Section we present some results showing the performance of our query-sensitive cost model; we also compare its different methods with the previous average-case cost model. The reported graphs, to keep it short, only refer to I/O costs, since errors on estimates of CPU costs show a very similar trend.

First of all, in Figures 6.22 and 6.23 we present some results concerning the incidence on estimates of how witnesses are chosen and of their number, respectively. For simplicity, we consider only the values of `AvgErr` for the 'Nearest Witness' method relative to range queries on synthetic clustered datasets.

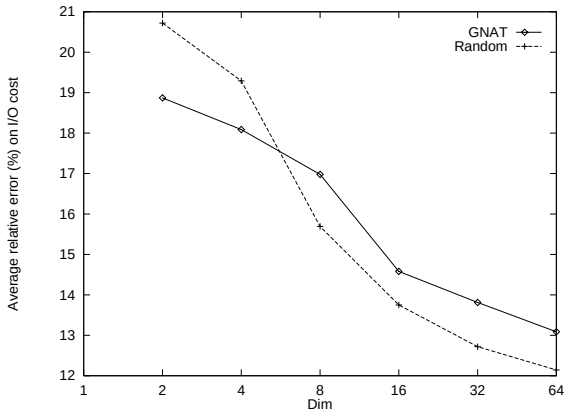

Figure 6.22: `AvgErr` for range queries. 'Nearest Witness' method: 'GNAT' vs. 'Random'.

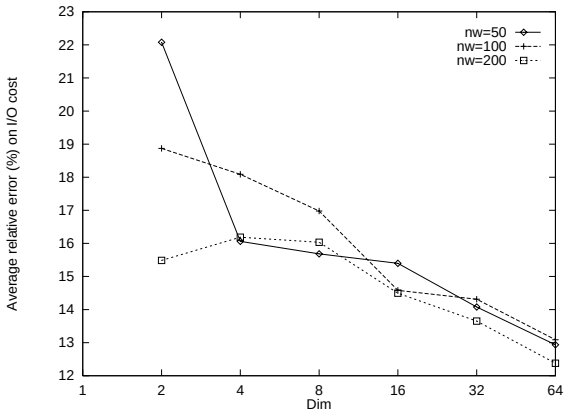

Figure 6.23: `AvgErr` for range queries. 'Nearest Witness' method: Effect of the number of witnesses ('GNAT' chosen).

Figure 6.22 shows that usually we obtain more accurate estimates when witnesses are chosen in a 'GNAT' way, rather than using the 'Random' criterion. The explanation for this is that the 'GNAT' method typically leads to a lower average distance between the query object and its nearest witness, as compared to the distance obtained by the 'Random' method. This trend, however, is inverted for higher dimensionalities of the space, with estimate differences lower than 1%.

In Figure 6.23 errors obtained by varying the number of witnesses are shown. As expected, by increasing the number of witnesses the estimates of the model improve; anyway, it can be seen that this improvement is not directly proportional to the increase introduced and sometimes it is not really appreciable.

In the following tests we analyze the behavior of the different variants of our query-sensitive model, comparing them with the average-case model. All these tests were carried out using 100 witnesses chosen in a 'GNAT' way.

The first set of experiments concerns the synthetic datasets. Figures 6.24 and 6.25 show relative errors of query-sensitive methods, compared with those of the average-case L-MCM model for range queries.

From the results shown in Figures 6.24 and 6.25 we can point out what follows:

- In several cases query-sensitive methods exhibit a great improvement over the average-case model.

- The most important thing is that when average-case estimates are affected by high errors, query-sensitive methods allow an effective reduction of these errors (best estimates of query-sensitive methods generally exhibit values of `AvgErr` between

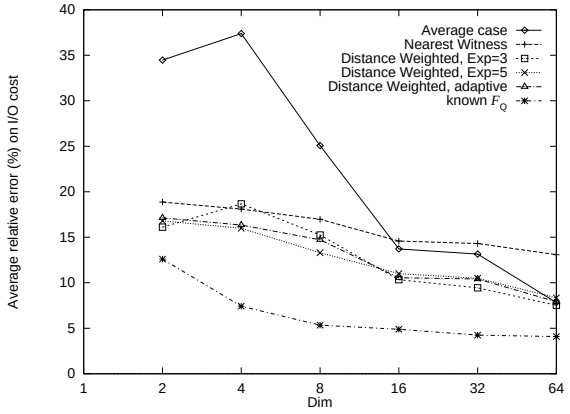

Figure 6.24: `AvgErr` for range queries on synthetic datasets.

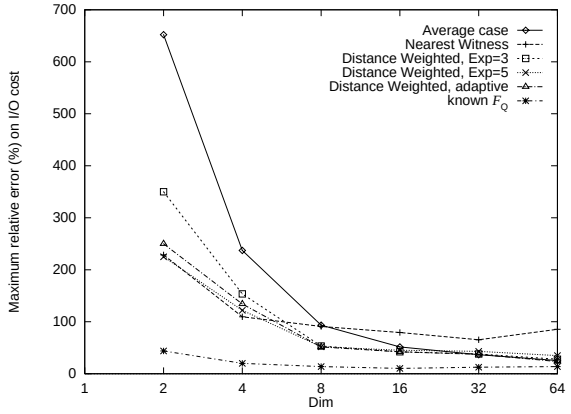

Figure 6.25: `MaxErr` for range queries on synthetic datasets.

10% and 20%).

- 'Distance Weighted' usually performs better than 'Nearest Witness'.
- The adaptive variant of 'Distance Weighted' exhibits good results, often close to the best estimates over all query-sensitive methods.

To analyze the effect of query selectivity on performance of the proposed models, in Figures 6.26 and 6.27 we compare the estimates of two query-sensitive methods — 'Nearest Witness' and the adaptive variant of 'Distance Weighted' — with the ones of the average-case model. We consider I/O costs for range queries on a clustered dataset with $D = 4$, and vary the query volume between 0.0025 and 0.025 (note that all previous results refer to a query volume of 0.01).

From the figures, the improvement of the query-sensitive cost model over the average-case cost model is evident. In the specific case, it can also be seen that the adaptive method performs better than 'Nearest Witness', as regards `AvgErr`. Considering `MaxErr`, instead, we observe exactly the opposite behavior.

Now, let us consider the results of experiments on real datasets. Figures 6.28 and 6.29 show errors for range queries. Concerning `AvgErr`, it is interesting to observe that, in this case, the average-case model exhibits quite good estimates on single queries, with relative errors between 10% and 16%. Anyway, our query-sensitive model performs even better: The adaptive variant of 'Distance Weighted' method and the 'Nearest Witness' method are very accurate, limiting `AvgErr` between 6% and 10%.

As to nearest neighbor queries, Figures 6.30 and 6.31, displaying results for synthetic and real datasets respectively, show that the difference between query-sensitive estimates

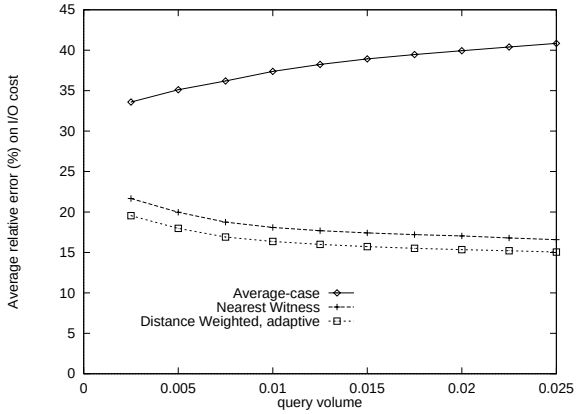

Figure 6.26: `AvgErr` for range queries on the 4-D clustered dataset as a function of the query volume.

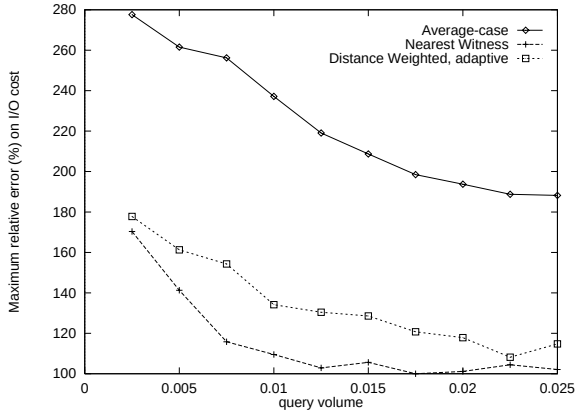

Figure 6.27: `MaxErr` for range queries on the 4-D clustered dataset as a function of the query volume.

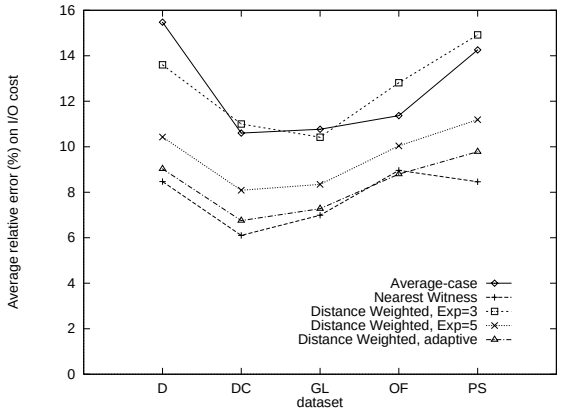

Figure 6.28: `AvgErr` for range queries on real datasets.

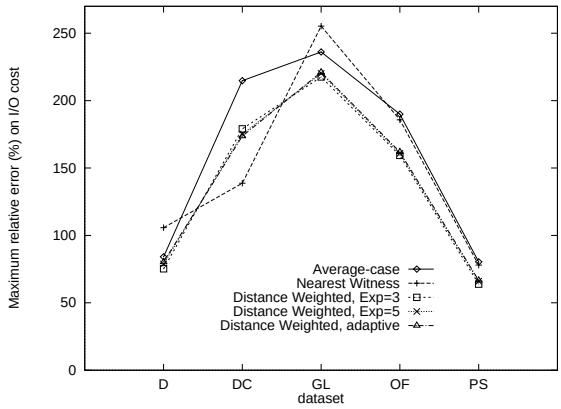

Figure 6.29: `MaxErr` for range queries on real datasets.

and those of average-case model reduces. In fact, in this case, the errors on average-case estimates are somewhat better than the respective ones for range queries. Anyway, it can be seen that query-sensitive methods still reduce relative errors, particularly when they reach fairly high values.

In this Section we have insisted on the usefulness of the proposed model in estimating execution costs for specific queries with M-tree. Issues concerning optimization of the algorithm and of the used structures, e.g. histograms compression, are left as subject for future work.

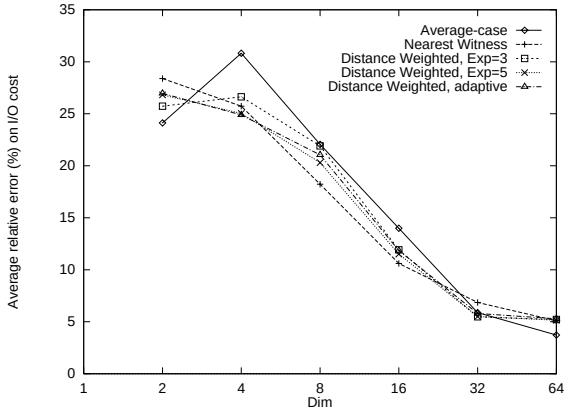

Figure 6.30: `AvgErr` for nearest neighbor queries on synthetic datasets.

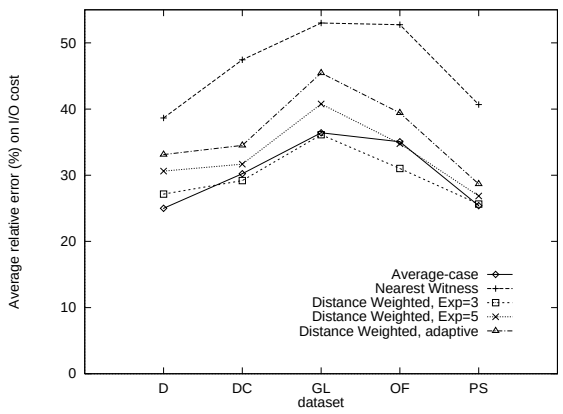

Figure 6.31: `AvgErr` for nearest neighbor queries on real datasets.

6.5 Extending the Approach to Other Metric Trees

In order to show how our approach could be extended to other metric trees, in this Section we discuss how an average-case cost model for range queries over vp-trees [Yia93] could be derived.[4] To this end, we consider the same basic principles used for M-tree, that is:

- The (overall) distance distribution is known.
- The *biased* query model is used.
- The homogeneity of viewpoints is high.

Consider a range query $\texttt{range}(Q, r_Q, \mathcal{C})$ on an m-way vp-tree.[5] Starting from the root, the system computes the distance between the query object Q and the vantage point O_v, then descends only those branches whose region intersects the query region. Thus, the i-th child of the root, N_{r_i}, has to be accessed, and the distance between the corresponding vantage point and Q computed,[6] iff $\mu_{i-1} - r_Q < d(Q, O_v) \leq \mu_i + r_Q, (i = 1, \ldots, m$, where $\mu_0 = 0$ and $\mu_m = d^+)$. Thus, the probability that N_{r_i} has to be accessed is:

$$\begin{aligned} \Pr\{N_{r_i} \text{ accessed}\} &= \Pr\{\mu_{i-1} - r_Q < d(Q, \mathbf{O_v}) \leq \mu_i + r_Q\} = \\ &= F_Q(\mu_i + r_Q) - F_Q(\mu_{i-1} - r_Q) \approx F(\mu_i + r_Q) - F(\mu_{i-1} - r_Q) \end{aligned} \tag{6.31}$$

[4] The vp-tree is briefly described in Section 3.2.1.

[5] The extension to nearest neighbors queries follows the same principles and is not presented here for the sake of brevity.

[6] Since the vp-tree is not paged, in the following we will assume that the index is stored in main memory, thus ignoring I/O costs.

where, as in Equation 6.5, the uncertainty is due to the position of the vantage point and the approximation relies on Assumption 6.1.[7] Figure 6.32 shows the probability to access the second child of the root in a 3-way vp-tree.

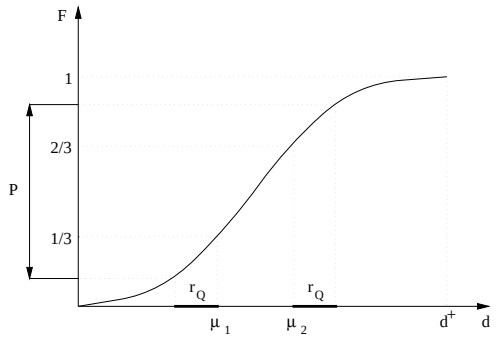

Figure 6.32: P is the probability to access the second child of the root in a 3-way vp-tree.

The homogeneity assumption also allows us to estimate the cutoff values without actually building the tree. In fact, each μ_i can be estimated as the i/m quantile of F, that is $F^{-1}(i/m)$.[8] It follows that Equation 6.31 can be rewritten as:

$$\Pr\{N_{r_i} \text{ accessed}\} \approx F(F^{-1}(i/m) + r_Q) - F(F^{-1}((i-1)/m) - r_Q) \tag{6.32}$$

Therefore, among the m children of the root,

$$\sum_{i=1}^{m} F(F^{-1}(i/m) + r_Q) - F(F^{-1}((i-1)/m) - r_Q) \tag{6.33}$$

nodes have to be accessed, on the average.

Above arguments are not directly applicable to the lower levels of the tree, because of constraints on the distance distribution. In fact, suppose the i-th child of the root, N_{r_i}, is accessed. The distance between the objects in the corresponding sub-tree is bounded by the triangle inequality to be lower than or equal to $2\mu_i$, as Figure 6.33 shows.

Since the probability of accessing the j-th child of N_{r_i}, denoted $N_{r_{i,j}}$, can be computed as:

$$\Pr\{N_{r_{i,j}} \text{ accessed}\} = \Pr\{N_{r_{i,j}} \text{ accessed} | N_{r_i} \text{ accessed}\} \cdot \Pr\{N_{r_i} \text{ accessed}\} \tag{6.34}$$

the problem is to determine $\Pr\{N_{r_{i,j}} \text{ accessed} | N_{r_i} \text{ accessed}\}$. For this Equation 6.32 cannot be directly applied, since the maximum distance is now bounded by $2\mu_i$. Therefore, the

[7] Of course, the reasoning of Section 6.4 can be also applied to this case, thus obtaining a query sensisitve cost model for the vp-tree.

[8] For simplicity of notation, here we assume that F is invertible.

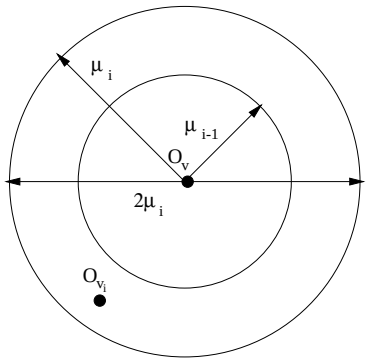

Figure 6.33: The distance between the objects in the sub-tree rooted at N_{r_i} cannot exceed $2\mu_i$.

distance distribution has to be "normalized" to the new bound, thus obtaining the distance distribution:

$$F_i(x) = \begin{cases} \dfrac{F(x)}{\min\{1, F(2\mu_i)\}} & \text{if } x \leq 2\mu_i \\ 1 & \text{if } x > 2\mu_i \end{cases} \tag{6.35}$$

Thus, the probability of accessing $N_{r_{i,j}}$ is obtained by substituting F_i, as given by Equation 6.35, for F in Equation 6.32:

$$\Pr\{N_{r_{i,j}} \text{ accessed} | N_{r_i} \text{ accessed}\} \approx F_i(F_i^{-1}(j/m) + r_Q) - F_i(F_i^{-1}((j-1)/m) - r_Q) \tag{6.36}$$

Following this approach it is possible to compute the probability of accessing every node of the vp-tree, thus obtaining a cost formula similar to Equation 6.8, with $e(N_{r_i}) = 1$. The intuitive complexity of such a formula would suggest, as done for M-tree, to derive a level-based cost model. However, due to the "asymmetry" of the vp-tree — the probability of accessing a node depends on the specific path to the node itself — this appears to be a difficult problem.

Chapter 7

Complex Queries

In Chapter 2, we showed how simple similarity queries can be transformed, by means of a correspondence function h, into distance-based queries. Then, in Chapters 3 and 4, we saw how such simple distance queries can be efficiently evaluated with distance-based access methods (SAMs and metric trees).

In this Chapter, we consider the relevant case where *complex* similarity queries — queries consisting of more than one similarity predicate — are defined. The problem of efficiently processing complex similarity queries has been highlighted only by recent works [CG96, Fag96, FW97]. The basic lesson is that, since the "similarity score" (*grade*) an object gets for the whole query depends on how the scores it gets for the single predicates are combined, predicates cannot be independently evaluated.

Example 7.1
Consider an image database where objects can be retrieved by means of predicates on `shape` and `color` features, and assume that the two sets of feature values are separately indexed. In order to retrieve the best match for the query

```
(shape = 'circular') and (color = 'red')
```

it is *not* correct to retrieve *only* the best match for `color` (using an index on `color`) and the best match for `shape` (using an index on `shape`), since the best match for the *overall* query needs not to be the best match for the single conjuncts. □

In this Chapter we first concentrate on a relevant class of complex similarity queries, which arises when all the similarity predicates refer to a single feature, then, in Section 7.5, we will extend our approach to the general multi-feature case. It is important to note that single-feature queries are an interesting subset of generic complex queries [CPZ98b].

Example 7.2
Consider an image database where objects can be retrieved using a *Query-by-Sketch*

modality (see also Example 2.1). When a user draws a shape on the screen, the system searches the DB, and returns those, say, 10 images which contain a shape best matching (according to given similarity criterion for shapes) the user's input. The user can then "refine" the search by selecting those objects which are similar to what he/she had in mind and which are actually not. Suppose two "positive" and one "negative" samples are specified. Now, the system has to search the DB for those 10 objects which are most similar to *both* positive samples, and, at the same time, *not* similar to the negative one. This interactive process can be iterated several times, until the user gets satisfied with system's output. □

An interactive retrieval process, such as the one sketched above, typically occurs when querying multimedia repositories [Jai96], where the user has no clear idea on how to express what he/she is looking for, and relies on previous results to improve the effectiveness of subsequent requests.[1]

7.1 The Problem

In Section 2.1 we introduced the basic ingredients to deal with simple similarity queries, i.e. the concepts of feature, similarity predicate, and similarity score. Since, now, our objective is to deal with *complex* similarity queries, we need a language $\mathcal{L}$ which allows multiple predicates to be combined into a *similarity formula*, f. The nature of the specific language is uninfluential to our arguments. We only require the existence of a *scoring function* [Fag96] computing the overall score of an object with respect to the complex similarity formula f, considering all the scores of the object itself with respect to the predicates of f.

Definition 7.1 (Scoring function)
If $f = f(p_1, \ldots, p_n)$ is a formula of $\mathcal{L}$, then the similarity of an object O with respect to f, denoted $s(f, O)$, is computed through a corresponding *scoring function*, s_f, which takes as input the scores of O with respect to the predicates of formula f, that is:

$$s(f(p_1, \ldots, p_n), O) = s_f(s(p_1, O), \ldots, s(p_n, O)) \tag{7.1}$$

□

Shortly, we will introduce three specific sample languages to construct similarity formulae. For the moment, we provide the following definitions which exactly specify the kinds of queries we are going to deal with.

[1] Although some connections with the *relevance feedback* techniques applied to textual document retrieval [Har92] can be observed, the scenario we envision has a broader context.

Definition 7.2 (Complex range query)
Given a similarity formula $f \in \mathcal{L}$ and a minimum similarity threshold α, the query $\texttt{range}(f, \alpha, \mathcal{C})$ selects all the objects in $\mathcal{C}$ (with their scores) such that $s(f, O) \geq \alpha$, that is, objects whose overall score with respect to f, as determined by the language $\mathcal{L}$, is not less than α. □

Definition 7.3 (Complex nearest neighbors (k-NN) query)
Given a similarity formula f and an integer $k \geq 1$, the k-NN query $\texttt{NN}(f, k, \mathcal{C})$ selects the k objects in $\mathcal{C}$ having the highest similarity scores with respect to f. In case of ties, they are arbitrarily broken. □

7.1.1 Similarity Languages

A similarity language $\mathcal{L}$ comes with a syntax, specifying which are valid (well-formed) formulae, and a semantics, telling us how to evaluate the similarity of an object with respect to a complex query. Although the results we present are language-independent, it also helps intuition to consider specific examples.

The first two languages we consider, $\mathcal{FS}$ (fuzzy standard) and $\mathcal{FA}$ (fuzzy algebraic), share the same syntax and stay in the framework of *fuzzy logic* [Zad65, KY95]. The third language, $\mathcal{WS}$ (weighted sum), does not use logical connectives at all, but allows *weights* to be attached to the predicates, in order to reflect the importance the user wants to assign to each of them.

The language $\mathcal{FS}$

The language $\mathcal{FS}$ is based on the "standard" semantics of fuzzy logic [Zad65]. Formulae of $\mathcal{FS}$ are defined by the following grammar rule:

$$f ::= p | f \wedge f | f \vee f | \neg f | (f) \tag{7.2}$$

where p is a similarity predicate. The semantics of a formula f is given by the following set of recursive rules:

$$\begin{aligned} s(f_1 \wedge f_2, O) &= \min\{s(f_1, O), s(f_2, O)\} \\ s(f_1 \vee f_2, O) &= \max\{s(f_1, O), s(f_2, O)\} \\ s(\neg f, O) &= 1 - s(f, O) \end{aligned}$$

The language $\mathcal{FA}$

The language $\mathcal{FA}$ has the same syntax as $\mathcal{FS}$, as defined in Equation 7.2, but it uses an "algebraic" semantics for logical operators [KY95], which are defined as follows:

$$\begin{aligned} s(f_1 \wedge f_2, O) &= s(f_1, O) \cdot s(f_2, O) \\ s(f_1 \vee f_2, O) &= s(f_1, O) + s(f_2, O) - s(f_1, O) \cdot s(f_2, O) \\ s(\neg f, O) &= 1 - s(f, O) \end{aligned}$$

The language $\mathcal{WS}$

The last language we consider, $\mathcal{WS}$, aims to show the generality of the presented approach, and is based on the well-known model of "list-of-keywords". A formula f has the form:

$$f ::= \{(p_1, \theta_1), (p_2, \theta_2), \ldots, (p_n, \theta_n)\}$$

where each p_i is a similarity predicate, the θ_i's are positive weights, and $\sum_{i=1}^{n} \theta_i = 1$. The semantics of a $\mathcal{WS}$ formula f is simply:

$$s(f, O) = \sum_{i=1}^{n} \theta_i \cdot s(p_i, O)$$

Although the subject of deciding on which is the "best" language is not in the scope of this work, it is important to realize that any specific language has some advantages and drawbacks, thus making the choice a difficult problem. For instance, it is known that if two *negation-free* formulae f_1 and f_2 are equivalent under Boolean semantics, then they are also equivalent according to $\mathcal{FS}$, which is clearly a desirable property from the optimization point of view. As an example, $p_1 \vee p_1 \wedge p_2 = p_1$ is a correct equivalence in $\mathcal{FS}$. On the other hand, it is *not* correct under $\mathcal{FA}$ semantics, as it can be easily shown. On the other side, $\mathcal{FS}$ is *single-operand dependent*, meaning that $s(f_1 \wedge f_2, O)$ (as well as $s(f_1 \vee f_2, O)$) is always equal either to $s(f_1, O)$ or to $s(f_2, O)$. This suggests that $\mathcal{FS}$ is not the best choice if one wants the final score an object obtains to be a "combination" of the scores of all the predicates.

We also remark that above languages are only a selected sample of the many one can conceive to formulate complex queries, and that our approach is not limited only to them. In particular, our results also apply to fuzzy languages, such as $\mathcal{FS}$ and $\mathcal{FA}$, when they are extended with weights, as shown in [FW97].

Example 7.3
Assume that we want to retrieve objects which are similar to both query values v_1 and v_2. With the $\mathcal{FS}$ and $\mathcal{FA}$ languages we can use the formula $f_1 = p_1 \wedge p_2$, where $p_i : F \sim v_i$.

With $\mathcal{WS}$, assuming that both predicates have the same relevance to us, the formula $f_2 = \{(p_1, 0.5), (p_2, 0.5)\}$ is appropriate. Given objects' scores for the two predicates p_1 and p_2, Table 7.1 shows the final scores, together with the relative rank of each object.

			$\mathcal{FS}$		$\mathcal{FA}$		$\mathcal{WS}$	
Object	$s(p_1, O_j)$	$s(p_2, O_j)$	$s(f_1, O_j)$	rank	$s(f_1, O_j)$	rank	$s(f_2, O_j)$	rank
O_1	0.9	0.4	0.4	4	0.36	3	0.65	1
O_2	0.6	0.65	0.6	1	0.39	2	0.625	3
O_3	0.7	0.5	0.5	3	0.35	4	0.6	4
O_4	0.72	0.55	0.55	2	0.396	1	0.635	2

Table 7.1: Similarity scores for complex queries.

It is evident that objects' ranking highly depends on the specific language (see object O_1) — this can affect the result of nearest neighbors queries — and that the score of an object can be very different under different languages — this can influence the choice of an appropriate threshold for range queries. □

Above example also clearly shows that determining the best match (the object with rank 1 in Table 7.1) for a complex query cannot be trivially solved by considering only the best matches for the single predicates. For instance, the best match for formula f_1 under $\mathcal{FA}$ semantics is object O_4, which is neither the best match for p_1 nor for p_2.

Similar considerations can be done for complex range queries too. Refer again to Table 7.1, and consider the query $\texttt{range}(f_2, 0.63, \mathcal{C})$, to be evaluated under $\mathcal{WS}$ semantics. Given the threshold value 0.63, which leads to select objects O_1 and O_4, which are (if any) appropriate thresholds for the single predicates such that the correct answer could still be derived?

7.2 Existing Approaches

With the concepts at our hand, we are now ready to solve the problem of *any* complex query by sequentially evaluating it over $\mathcal{C}$. The following definition links together the main concepts needed to this end.

Definition 7.4 (Distance-based similarity environment)
A distance-based similarity environment is a quadruple $\mathcal{DS} = (\mathcal{D}, d, h, \mathcal{L})$, where $\mathcal{D}$ is a domain of feature values, d is a metric distance over $\mathcal{D}$, h is a correspondence function, and $\mathcal{L}$ is a similarity language. □

Given any similarity environment $\mathcal{DS}$, we are now ready to perform sequential evaluation of arbitrarily complex similarity queries. The algorithm for range queries is described in Figure 7.1; the one for nearest neighbors queries is based on the same principles, but it is not shown here for brevity.

```
Range-Seq(DS: similarity_environment, range(f, α, C): query)
{ ∀O ∈ C do:
  { ∀ predicate p_i : F ~ v_i of f, compute d_i = d(v_i, O.F);
    Let s_i = h(d_i), i = 1, ..., n;
    If s(f, O) ≜ s_f(s_1, ..., s_n) ≥ α then add (O, s(f, O)) to the result;
  } }
```

Figure 7.1: The algorithm for sequential evaluation of complex range queries.

Example 7.4
Consider the environment $\mathcal{DS} = (\Re^2, L_1, 1 - 0.1 \cdot x, \mathcal{FS})$, and the query Q : `range`$(p_1 \wedge p_2, 0.8, \mathcal{C})$, with $p_i : F \sim v_i$ $(i = 1, 2)$. Refer to Figure 7.2, where $v_1 = (3, 2)$ and $v_2 = (5, 3)$, and consider the point (feature vector) $v = (3.5, 1)$. To evaluate its score, we first compute $d_1 = L_1(v_1, v) = |3 - 3.5| + |2 - 1| = 1.5$ and $d_2 = L_1(v_2, v) = |5 - 3.5| + |3 - 1| = 3.5$. Then, we apply the correspondence function $h(x) = 1 - 0.1 \cdot x$ to the two distance values, thus obtaining $s_1 = h(d_1) = 0.85$ and $s_2 = h(d_2) = 0.65$. Finally, since we are using the $\mathcal{FS}$ semantics, we have to take the minimum of the two scores to compute the overall score, i.e. $s(p_1 \wedge p_2, O) = \min\{s_1, s_2\} = 0.65$. Since this is less than the threshold value 0.8, point v does not satisfy the range query Q. □

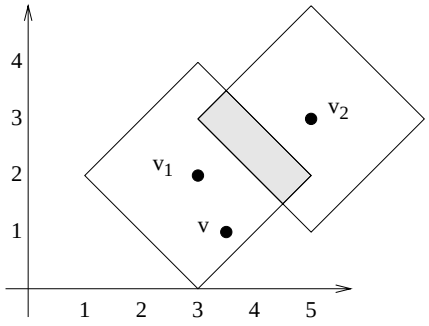

Figure 7.2: The region of the query `range`$((F \sim v_1) \wedge (F \sim v_2), 0.8, \mathcal{C})$ is shaded.

It is important to observe that the choice of a specific correspondence function can affect the result of similarity queries. This is easily shown by referring to the above

example, and redefining h as $h(x) = 1 - 0.05 \cdot x$. After simple calculations, it is derived that $s(p_1 \wedge p_2, v) = 0.825$, thus point v will be part of the result.

Besides above argumentations on the influence of each component of $\mathcal{DS}$ on the result of a query, it is easy to see that sequential processing is not an efficient solution, particularly for large objects' collections. In Chapter 3 we showed how an index can be effectively exploited in order to efficiently resolve simple similarity queries. The question now is: How one or more indices built over a set of features can be used to deal with (arbitrarily) complex queries? The traditional approach independently evaluates the predicates and then combines the partial results *outside* of the indices themselves. The case of nearest neighbors queries has been analyzed in [Fag96]. Here the problem is that the best match for a complex query cannot be determined by looking only at the best matches of the single predicates (see also Example 7.3).

The major result of [Fag96] is the algorithm $\mathcal{A}_0$ returning the correct answer for a k-nearest neighbors query under the assumption that the scoring function for the query formula is monotonic, i.e. $s_f(s_1, \ldots, s_n) \leq s_f(s'_1, \ldots, s'_n)$, if $s_i \leq s'_i$ for every i. The $\mathcal{A}_0$ algorithm is described in Figure 7.3.[2]

$\mathcal{A}_0$(NN$(f, k, \mathcal{C})$: query)
{ $\forall p_i$ of f, open a *sorted access* index scan and insert objects
in the set X^i, stopping when there are at least k objects
in the intersection $L = \cap_i X^i$;
$\forall O \in \cup_i X^i$ compute $sim(f, O)$;
return the k objects in $\cup_i X^i$ with the highest overall scores; }

Figure 7.3: The $\mathcal{A}_0$ algorithm.

In the first step of the algorithm, *sorted access* means that the index scan will return, one by one, objects in decreasing score order with respect to p_i, stopping when the intersection L of objects returned by each scan contains at least k objects.

The approach of independently evaluating predicates, besides being inefficient because it leads to access parts of the index more than once, cannot be applied at all for generic complex queries. In fact, in the case of complex range queries, independent evaluation is possible only under the strict assumption that a distance constraint for each single predicate in the query can be derived from the overall minimum similarity threshold, which is not always the case.

[2]We have slightly changed notation and terminology to better fit our scenario. In particular, we access data through index scans, whereas in [Fag96] generic independent *subsystems* are considered.

Example 7.5
Consider Example 7.4. In order to process the query $\texttt{range}(p_1 \wedge p_2, 0.8, \mathcal{C})$, by independently evaluating predicates p_1 and p_2, we can proceed as follows. Since we are using the $\mathcal{FS}$ semantics and the correspondence function h, it has to be $\min\{1-0.1\cdot d(v_1, O.F), 1-0.1\cdot d(v_2, O.F)\} \geq 0.8$. This can also be expressed as $\max\{d(v_1, O.F), d(v_2, O.F)\} \leq 2$, where an *explicit* distance threshold is now present. It can be easily verified that if $O.F$ satisfies above inequality, then O lies in the shaded query region of Figure 7.2. Since above constraint can be also written as

$$(d(v_1, O.F) \leq 2) \wedge (d(v_2, O.F) \leq 2)$$

the complex query Q can be evaluated by independently performing two simple range queries, taking the intersection of objects' results, and then computing the final scores. □

Example 7.6
Assume now that the correspondence function has the form $h(x) = e^{-x}$, and consider the query $\texttt{range}(\{(p_1, 0.4), (p_2, 0.6)\}, 0.5, \mathcal{C})$ in the $\mathcal{WS}$ language. The similarity constraint is:

$$0.4 \cdot e^{-d(v_1, O.F)} + 0.6 \cdot e^{-d(v_2, O.F)} \geq 0.5$$

which cannot be decomposed into two *bounded* simple range queries. Indeed, if O is in the result, then O necessarily satisfies the two constraints (each using a single query value) $0.4 \cdot e^{-d(v_1, O.F)} + 0.6 \geq 0.5$ and $0.4 + 0.6 \cdot e^{-d(v_2, O.F)} \geq 0.5$, which are obtained by setting, respectively, $d(v_2, O.F) = 0$ and $d(v_1, O.F) = 0$. However, since the first constraint is satisfied by *any* $d(v_1, O.F)$ value, the corresponding simple range query is $d(v_1, O.F) \leq \infty$, which amounts to access the whole data collection. □

The work by Chaudhuri and Gravano [CG96] addresses issues similar to [Fag96]. The strategy the authors propose to transform complex (multi-feature) nearest neighbors queries into a conjunction of simple range queries could in principle be also applied to our framework. However, this requires some knowledge of data and distance distributions, which might not be always available. Furthermore, and more important, it only applies if distance constraints can be derived for the single range queries, which is not always the case (see Example 7.6).

7.3 Extending Distance-based Access Methods

The second possibility of evaluating complex queries is the one we proposed in [CPZ98b], and suggests that the index should process complex queries *as a whole*. Of course, since the

index is built on a single feature F, this approach is restricted on single-feature complex queries only, which, however, represent a non-trivial case, as we saw in previous Sections. We first show how queries in the two examples of Section 7.2 would be managed by the new approach, then we generalize to generic similarity environments.

Example 7.7
Consider Example 7.5, and assume, without loss of generality, that feature values are indexed by an M-tree. We can prune a node N with routing object O_r and covering radius $r(O_r)$ if its region, $Reg(N)$, only contains points O such that

$$\min\{1 - 0.1 \cdot d(v_1, O.F), 1 - 0.1 \cdot d(v_2, O.F)\} < 0.8 \tag{7.3}$$

Because of the triangular inequality and non-negativity properties of d, the following lower bound on $d(v_i, O.F)$ can be derived:

$$d(v_i, O.F) \geq d_{min}(v_i, Reg(N)) \stackrel{\text{def}}{=} \max\{d(v_i, O_r.F) - r(O_r), 0\} \qquad i = 1, 2$$

If we substitute such lower bounds into (7.3), we obtain

$$\min\{1 - 0.1 \cdot d_{min}(v_1, Reg(N)), 1 - 0.1 \cdot d_{min}(v_2, Reg(N))\} < 0.8$$

From this, we can immediately decide whether node N has to be accessed or not. □

Example 7.8
Consider now Example 7.6. We can adopt the same approach as in Example 7.7. Node N can be pruned if each point v in its region satisfies

$$0.4 \cdot e^{-d(v_1, O.F)} + 0.6 \cdot e^{-d(v_2, O.F)} < 0.5$$

By using the $d_{min}(v_i, Reg(N))$ lower bounds, it is obtained

$$0.4 \cdot e^{-d_{min}(v_1, Reg(N))} + 0.6 \cdot e^{-d_{min}(v_2, Reg(N))} < 0.5$$

Once again, checking above constraint is all that is needed to decide if node N has to be accessed. □

In order to generalize our approach to generic similarity environments and arbitrarily complex queries, we need a preliminary definition, extending the concept of monotonicity introduced in the previous Section.

Definition 7.5 (Monotonicity)
We say that a scoring function $s_f(s(p_1, v), \ldots, s(p_n, v))$ is monotonic increasing (respectively decreasing) in the variable $s(p_i, v)$ if, given any two n-tuples of scores' values

$(s_1, \ldots, s_i, \ldots, s_n)$ and $(s_1, \ldots, s'_i, \ldots, s_n)$ with $s_i \leq s'_i$, it is $s_f(s_1, \ldots, s_i, \ldots, s_n) \leq s_f(s_1, \ldots, s'_i, \ldots, s_n)$ (resp. $s_f(s_1, \ldots, s_i, \ldots, s_n) \geq s_f(s_1, \ldots, s'_i, \ldots, s_n)$). If a scoring function s_f is monotonic increasing (resp. decreasing) in all its variables, we simply say that s_f is monotonic increasing (resp. decreasing). □

Monotonicity is a property which allows us to somewhat predict the behavior of a scoring function in a certain data region, which is a basic requirement for deciding whether or not the corresponding node in the index should be accessed. Note that both queries in Examples 7.7 and 7.8 are monotonic increasing.

Before presenting our major result, it has to be observed that *a scoring function can be "monotonic in all its arguments" without being neither monotonic increasing nor monotonic decreasing* (on the other hand, the converse is true). For instance, $s(p_1, v) \cdot (1 - s(p_2, v))$, which is the scoring function of $p_1 \wedge \neg p_2$ in the $\mathcal{FA}$ language, is monotonic increasing in $s(p_1, v)$ and monotonic decreasing in $s(p_2, v)$.

In case a certain predicate occurs more than once in a formula, we need to distinguish its occurrences. For instance, the formula $f : p_1 \wedge \neg p_1$ with $p_1 : F \sim v_1$, has to be rewritten as, say, $p_1 \wedge \neg p_2$, with $p_2 : F \sim v_2$, and $v_1 \equiv v_2$. Under the $\mathcal{FA}$ semantics, say, the scoring function of f, that is $s(p_1, v) \cdot (1 - s(p_2, v))$, is now monotonic increasing in $s(p_1, v)$ and monotonic decreasing in $s(p_2, v)$.

By distinguishing single occurrences of predicates, it can be seen that the $\mathcal{WS}$ language can only generate formulae having monotonic increasing scoring functions, whereas all scoring functions of formulae of languages $\mathcal{FS}$ and $\mathcal{FA}$ are guaranteed to be monotonic in all their arguments.

We are now ready to state our major result.

Theorem 7.1
Let $\mathcal{DS} = (\mathcal{D} = dom(F), d, h, \mathcal{L})$ be a similarity environment, $f = f(p_1, \ldots, p_n) \in \mathcal{L}$ $(p_i : F \sim v_i,\ i = 1 \ldots, n)$ a similarity formula such that each predicate occurs exactly once, and $\mathcal{C}$ a collection of objects indexed by a distance-based tree $\mathcal{T}$ on the values of feature F. Let $s_f(s(p_1, v), \ldots, s(p_n, v))$ $(v \in \mathcal{D})$ be the scoring function of f.

If s_f is monotonic in all its variables, then a node N of $\mathcal{T}$ can be pruned if

$$s_{max}(f, Reg(N)) \stackrel{\text{def}}{=} s_f(h(d_B(v_1, Reg(N))), \ldots, h(d_B(v_n, Reg(N)))) < \alpha \tag{7.4}$$

where

$$d_B(v_i, Reg(N)) = \begin{cases} d_{min}(v_i, Reg(N)) & \text{if } s_f \text{ is monotonic increasing in } s(p_i, v) \\ d_{max}(v_i, Reg(N)) & \text{if } s_f \text{ is monotonic decreasing in } s(p_i, v) \end{cases} \tag{7.5}$$

with $d_{min}(v_i, Reg(N))$ ($d_{max}(v_i, Reg(N))$) being a lower (upper) bound on the minimum (maximum) distance from v_i of any value $v \in Reg(N)$, and where α is

- *the user-supplied minimum similarity threshold, if the query is* $\texttt{range}(f, \alpha, \mathcal{C})$*;*
- *the k-th highest similarity score encountered so far, if the query is* $\texttt{NN}(f, k, \mathcal{C})$*. If less than k objects have been evaluated, then* $\alpha = 0$*.*

Proof: Assume that $Reg(N)$ contains a point v^* such that $s_f(h(d(v_1, v^*)), \ldots, h(d(v_n, v^*))) \geq \alpha$. By construction, it is $d(v_i, v^*) \geq d_B(v_i, Reg(N))$, if s_f is monotonic increasing in $s(p_i, v)$, and $d(v_i, v^*) \leq d_B(v_i, Reg(N))$, if s_f is monotonic decreasing in $s(p_i, v)$. Since h is a monotonic decreasing function, it is also

$$h(d(v_i, v^*)) \leq (\geq) h(d_B(v_i, Reg(N))) \qquad \text{if } d(v_i, v^*) \geq (\leq) d_B(v_i, Reg(N))$$

Since s_f is monotonic in all its arguments, it is impossible to have

$$s_f(h(d(v_1, v^*)), \ldots, h(d(v_n, v^*))) > s_f(h(d_B(v_1, Reg(N))), \ldots, h(d_B(v_n, Reg(N))))$$

which proves the result. □

Theorem 7.1 generalizes to complex queries the basic technique used to process simple range and nearest neighbors queries. It does so by considering how a (single occurrence of a) predicate can affect the overall score, and by using appropriate bounds on the distances from the query values. These are then used to derive an upper bound, $s_{max}(f, Reg(N))$, on the maximum similarity score an object in the region of node N can get with respect to f, that is:

$$s_{max}(f, Reg(N)) \geq s(f, v), \ \forall v \in Reg(N)$$

Example 7.9

A query which has been proved in [Fag96] to be a "difficult one" is $\texttt{NN}(p_1 \wedge \neg p_1, k, \mathcal{C})$, with $p_1 : F \sim v_1$. This can be processed as follows. First, rewrite the formula as $p_1 \wedge \neg p_2$ ($p_2 : F \sim v_2, v_2 \equiv v_1$). Without loss of generality, assume the standard fuzzy semantics $\mathcal{FS}$, and the correspondence function $h(x) = 1 - 0.1 \cdot x$. The scoring function can therefore be written as

$$\min\{s(p_1, v), 1 - s(p_2, v)\}$$

By substituting bounds on distances and applying the correspondence function we finally get:

$$s_{max}(p_1 \wedge \neg p_1, Reg(N)) = \min\{1 - 0.1 \cdot d_{min}(v_1, Reg(N)), 0.1 \cdot d_{max}(v_1, Reg(N))\}$$

where we have turned back to the original v_1 notation. □

Theorem 7.1 provides a general way to handle complex queries in generic similarity environments, using *any* distance-based index. The only part specific to the index at hand is the computation of the $d_{min}(v_i, Reg(N))$ and $d_{max}(v_i, Reg(N))$ bounds, since they depend on the kind of data regions managed by the index. For instance, in M-tree above bounds are computed as $\max\{d(v_i, O_r) - r(O_r), 0\}$ and $d(v_i, O_r) + r(O_r)$, respectively (see Chapter 4). Simple calculations are similarly required for other metric trees (see Section 3.2), as well as for spatial access methods, such as R-tree (see Section 3.1).

7.3.1 False Drops at the Index Level

The absence of any specific assumption about the similarity environment and the access method in Theorem 7.1 makes it impossible to guarantee the absence of "false drops" at the level of index nodes. More precisely, if inequality of Equation 7.4 is satisfied, it is guaranteed that node N cannot lead to qualifying objects, and can therefore be safely pruned. This is also to say that $Reg(N)$ and the query region do not intersect. On the other hand, if Equation 7.4 is *not* satisfied (i.e. $s_{max}(v, Reg(N)) \geq \alpha$) it can still be the case that $Reg(N)$ and the query region do not intersect.

Example 7.10
Consider the environment $\mathcal{DS} = (\Re^2, L_2, e^{-x}, \mathcal{FS})$, and the query $\texttt{range}(p_1 \wedge p_2, 0.5, \mathcal{C})$, with $p_i : F \sim v_i$, $v_1 = (1, 2)$ and $v_2 = (2, 2)$. Consider the M-tree data region:

$$Reg(N) = \{v : d(v_r = (1.5, 1), v) \leq r(v_r) = 0.43\}$$

It can be seen in Figure 7.4 that $Reg(N)$ does not intersect the query region, represented by the intersection of the two circles of radius $\ln(1/0.5)$ centered in v_1 and v_2, respectively. However, the maximum possible similarity for $Reg(N)$ is estimated as

$$\min\{e^{-(d(v_1,v_r)-r(v_r))}, e^{-(d(v_2,v_r)-r(v_r))}\} \approx 0.502 > 0.5$$

Therefore, node N cannot be pruned. □

Although the phenomenon of false drops can lead to explore unrelevant parts of the tree, thus affecting the efficiency of the retrieval, it does not alter at all the correctness of the results, since, at the leaf level, we evaluate the actual similarities of the objects, for which no bounds are involved and actual distances are measured.

Resolving the false drop problem for generic similarity environments appears to be a difficult task. In order to derive a tighter $s_{max}(v, Reg(N))$ bound, the $n \cdot (n-1)/2$ relative distances between the n query values could be taken into account. However, without specific assumptions on the similarity environment, in particular with no knowledge of

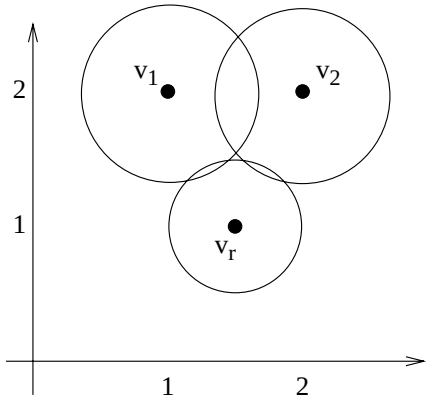

Figure 7.4: The false drops phenomenon.

the specific metric space, additional hypotheses on the scoring functions (such as differentiability) seem to be needed to obtain major improvements. We leave this problem as a future research activity.

In the case of spatial access methods, which only manage similarity environments of type $\mathcal{DS}_{sam} = (\Re^n, L_p, h, \mathcal{L})$, that is, vector spaces with L_p (Euclidean, Manhattan, etc.) metrics,[3] the similarity bound established by (7.4) could be improved by trying to exploit the geometry of the Cartesian space. However, for arbitrarily complex queries this still remains a difficult task [HM95, SK97].

7.4 Extending M-tree

As we saw in Section 4.6, our M-tree implementation is based on the GiST package. The only GiST method used during the search phase is `Consistent`. Therefore, only this method has to be modified to support complex queries.

The new version of the `Consistent` method we have developed is based on the results obtained in the previous Section, and is fully parametric in the similarity environment $\mathcal{DS}$. The overall architecture of the method is shown in Figure 7.5.

The input of the `Consistent` method is an entry $Reg(N) \equiv (O_r, r(O_r))$, representing the region of node N, and a query $Q \equiv (f, \alpha)$, where $f = f(p_1, \ldots, p_n)$ is a (suitable encoding of a) formula of language $\mathcal{L}$, and α is a minimum similarity threshold. In order to optimize nearest neighbors queries, the new version of `Consistent` also returns an upper bound, $s_{max}(f, Reg(N))$, on the similarity between the objects in the region $Reg(N)$ and the formula f. At each step of the k-NN algorithm, the node with the

[3]Indeed, they can also manage quadratic distance functions, as shown in [SK97], but this does not make a substantial difference.

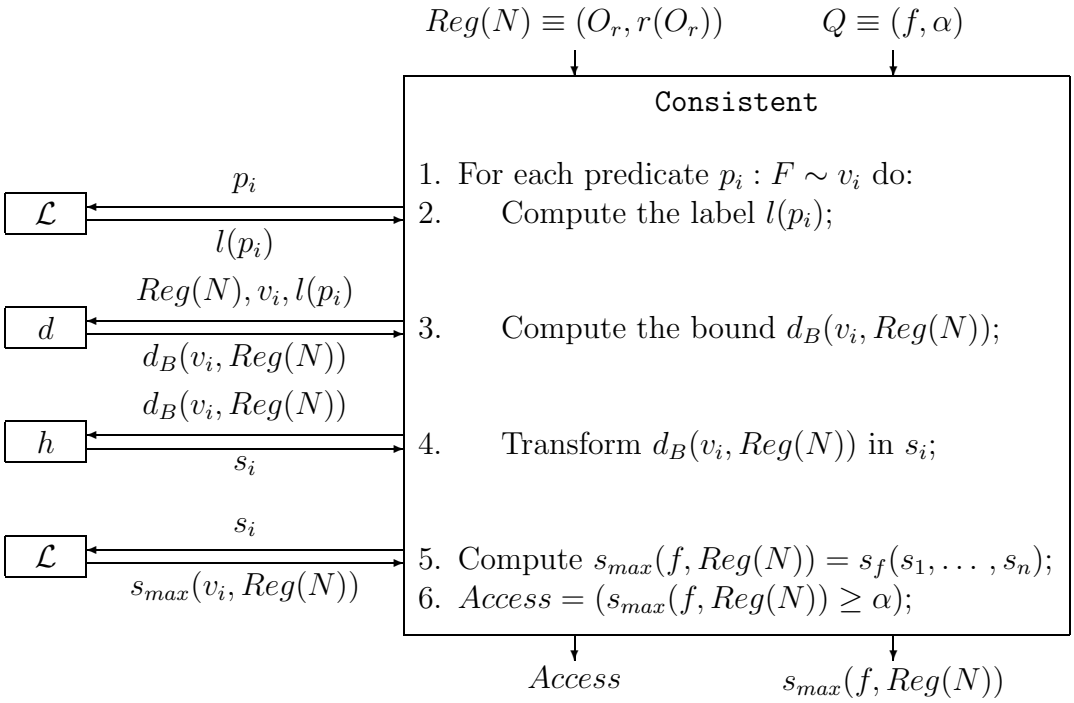

Figure 7.5: The `Consistent` method.

highest bound is selected and fetched from disk.

The architecture of `Consistent` is independent of the similarity environment $\mathcal{DS}$, since all specific computations are performed by external modules implementing each component of the environment (these are shown on the left side in Figure 7.5).

In particular, the two modules denoted with $\mathcal{L}$ are those which encode language-specific information. The execution flow closely follows the logic of Theorem 7.1 (refer to Figure 7.5):

- At step 2, we compute a Boolean *label* for each predicate p_i, to determine if the scoring function s_f is monotonic increasing or decreasing in the variable $s(p_i, v)$.
- Then, distance bounds are computed, depending on the value of $l(p_i)$.
- At step 4, the latter bounds are transformed, by using the correspondence function h, into similarity bounds s_i.
- The overall upper bound $s_{max}(f, Reg(N))$ is then computed, by applying the scoring function s_f to the bounds obtained for all the predicates.
- Finally, if $s_{max}(f, Reg(N))$ is lower than α ($Access = false$) N can be pruned from the search.

7.4.1 Experimental Results

In this Section we compare the performance of the extended M-tree with that of other search techniques. For the sake of definiteness, we consider the specific similarity environment $\mathcal{DS} = ([0,1]^5, L_\infty, 1-x, \mathcal{FS})$. The results we present refer to 10-NN conjunctive queries $f : p_1 \wedge p_2 \wedge \ldots$, evaluated over a collection of 10^4 clustered objects (see Table 6.2). Again, the M-tree implementation uses a node size of 4 Kbytes and the tree is built using the `BulkLoading` algorithm described in Chapter 5.

The alternative search algorithms against which we compare M-tree are a simple linear scan of the objects — the worst technique for CPU costs, but not necessarily for I/O costs — and the $\mathcal{A}'_0$ algorithm [Fag96], a variant of the general $\mathcal{A}_0$ algorithm, presented in Section 7.2, and suitable for conjunctive queries under $\mathcal{FS}$ semantics, which is briefly described in Figure 7.6.

$\mathcal{A}'_0$(NN$(f, k, \mathcal{C})$: query)
{ $\forall p_i$ of f, open a *sorted access* index scan and insert objects
    in the set X^i, stopping when there are at least k objects
    in the intersection $L = \cap_i X^i$;
  $\forall v \in L$ compute $sim(f, v)$;
  let v_0 be the object in L having the least score,
    and p_{i_0} the predicate such that $sim(f, v_0) = sim(p_{i_0}, v_0)$;
  $\forall$ *candidate* $v_c \in X^{i_0}$, such that $sim(p_{i_0}, v_c) \geq sim(p_{i_0}, v_0)$, compute $sim(f, v_c)$;
  return the k candidates with the highest overall scores; }

Figure 7.6: The $\mathcal{A}'_0$ algorithm.

The scan i_0 is the one which returned the object v_0 with the least score in L (third step of the algorithm). For all the *candidates* [Fag96], that is, objects v_c returned by such a scan *before* v_0 ($sim(p_{i_0}, v_c) \geq sim(p_{i_0}, v_0)$), in the fourth step the overall score is computed.

Since the M-tree does not implement yet a sorted access scan, to evaluate the costs of algorithm $\mathcal{A}'_0$ we simulated its behavior by repeatedly performing a k_i-nearest neighbors query for each predicate, with increasing values of k_i, until 10 common objects were found in the intersection. The sorted access costs are then evaluated as the costs for the last n queries (one for each predicate). Note that this is an optimistic cost estimate, since it is likely that a "real" sorted access scan would cost more than a single k_i-nearest neighbors query which "magically" knows the right value of k_i. The step of computing the score for the candidate objects is charged only with CPU costs, since we assume that all the

candidates are kept in main memory.

Figures 7.7 and 7.8 compare I/O and CPU costs, respectively, for 10-NN queries consisting of the conjunction of two predicates, $f : p_1 \wedge p_2$, as a function of the distance between the two query objects. As usual, CPU costs are simply evaluated as the number of distance computations, and I/O costs are the number of page reads. As the graphs show, $\mathcal{A}'_0$ performs considerably better when the query objects are relatively "close", because in this case it is likely that the two query objects will have almost the same neighbors, thus leading to cheaper costs for the sorted access phase. On the other hand, the M-tree approach is substantially unaffected by the distance between the query objects. When query objects are "close" (i.e. the user asks for a conjunction of similar objects) the CPU costs for both approaches are very similar, while I/O costs for $\mathcal{A}'_0$ tend to be twice those of our approach. Comparison with linear scan shows that our approach is highly effective in reducing CPU costs, which can be very time-consuming for complex distance functions, and also lowers I/O costs. $\mathcal{A}'_0$, on the other hand, is much worse than linear scan for "distant" query objects.

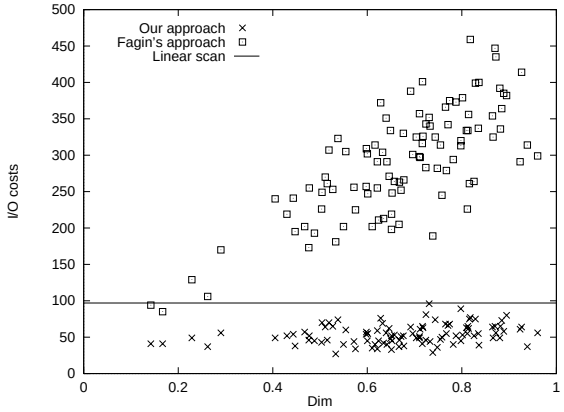

Figure 7.7: I/O costs. $f : p_1 \wedge p_2$. 10 clusters.

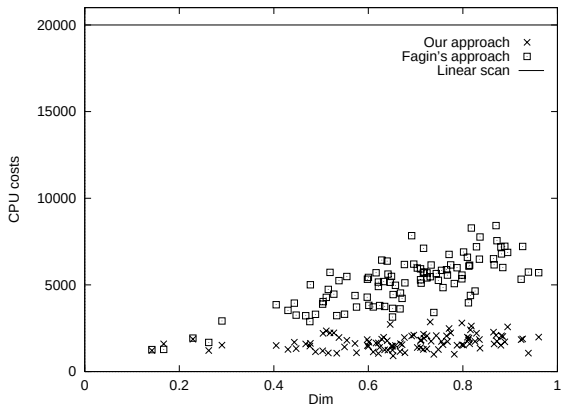

Figure 7.8: CPU costs. $f : p_1 \wedge p_2$. 10 clusters.

Figures 7.9 and 7.10 show the effect of varying data distribution, by generating 10^3 clusters. Now the distribution of objects' relative distances has a lower variance with respect to the previous case, thus making more difficult the index task. Major benefits are still obtained from reduction of CPU costs, whereas I/O costs of M-tree are comparable to that of a linear scan only for not too far query objects.

We now consider the case where one of the two predicates is negated i.e. $f : p_1 \wedge \neg p_2$. In this case, as Figures 7.11 and 7.12 show, the trend of index-based algorithms is somewhat inverted with respect to the previous cases, thus favoring, as to I/O costs, the linear scan when query objects are close. The performance degradation of M-tree in this case

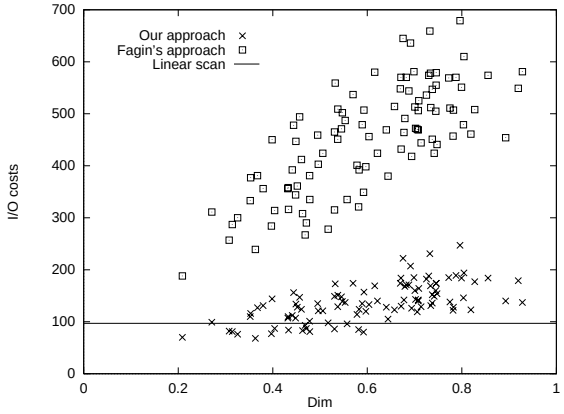

Figure 7.9: I/O costs. $f : p_1 \wedge p_2$. 10^3 clusters.

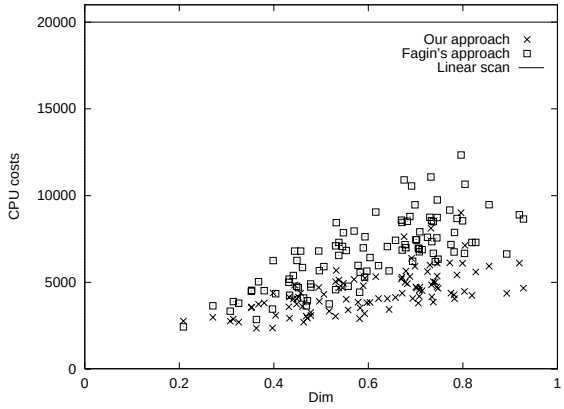

Figure 7.10: CPU costs. $f : p_1 \wedge p_2$. 10^3 clusters.

is because, due to negation, best matches are far away from both the query objects, thus leading to access a major part of the tree.

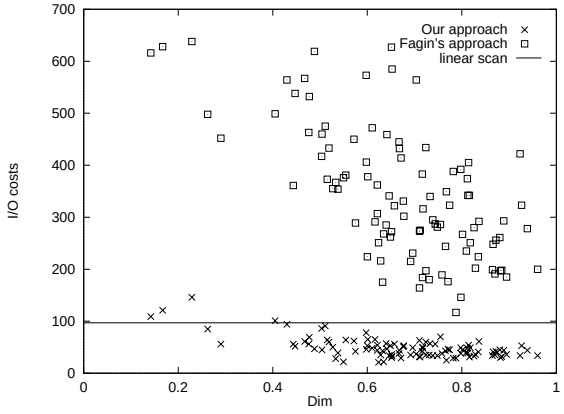

Figure 7.11: I/O costs. $f : p_1 \wedge \neg p_2$. 10 clusters.

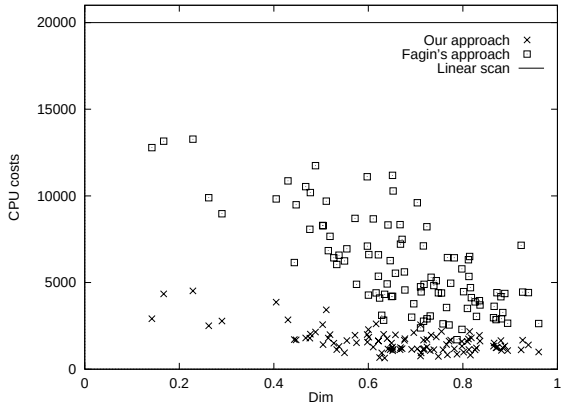

Figure 7.12: CPU costs. $f : p_1 \wedge \neg p_2$. 10 clusters.

The last experiment we show compares M-tree with $\mathcal{A}_0'$ in the case of n positive conjuncts, that is $f : p_1 \wedge \ldots \wedge p_n$. Figure 7.13 shows the relative CPU and I/O savings obtained from M-tree with respect to $\mathcal{A}_0'$, as a function of n. The slight increase in the I/O curve indicates that our approach improves its relative performance with the complexity of the formula, arriving at 95% reduction of I/O costs for 5 predicates. On the other hand, CPU savings have a decreasing trend (but never less than 40% in the considered range). This is explained by observing that, at each call of the `Consistent` method, we evaluate distances with respect to all the predicates. On the other hand, $\mathcal{A}_0'$ algorithm does this only for the *candidate* objects, as above explained.

The overall conclusions we can draw from above results can be so summarized:

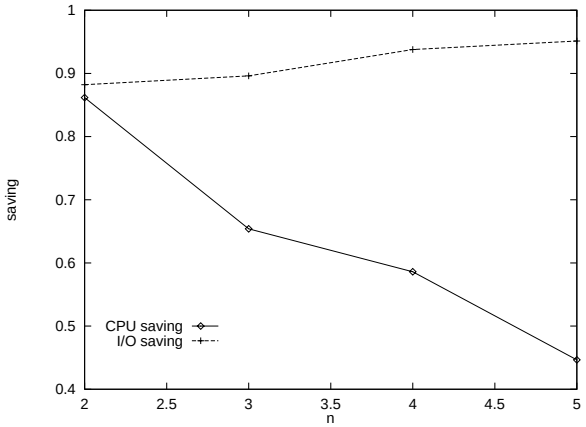

Figure 7.13: CPU and I/O costs savings with respect to $\mathcal{A}_0'$. $f : p_1 \wedge \ldots \wedge p_n$. 10 clusters.

1. Processing complex queries as a whole is *always* better than performing multiple sorted access scans (as $\mathcal{A}_0'$ does), both as to I/O and CPU costs.

2. For a given formula, our approach is almost insensitive to the specific choice of the query objects, thus leading to stable performance. This is not the case for the $\mathcal{A}_0'$ algorithm.

3. In some cases linear scan can be preferable as to I/O costs, but our approach leads in any case to a drastic reduction of CPU costs, which can become the dominant factor for CPU-intensive distance functions typical of multimedia environments.

7.5 The Multi-feature Case

Analysis of the general case of complex queries over multiple features can heavily rely on results derived in Section 7.3. Indeed, from a formal point of view, *no significant difference with respect to the case of single-feature queries exists*. For instance, it is easy to see that if an access method is developed and used to resolve single-feature queries, then the same access method can in principle be used to deal with multiple-feature queries, e.g. by using it in the $\mathcal{A}_0$ algorithm. This is not to say, however, that multi-feature query processing is the same as single-feature query processing, rather no new aspect is introduced as to the "power" of access methods.

A point for which further clarification is needed concerns the "indexability" of multiple domains. In order to apply results of Section 7.3 and process multiple-feature queries *as a whole*, we have to show that an access method can be designed to index values from multiple domains.

We consider two basic cases, depending on the nature of the features' domains. In the first case it is assumed that, for each feature F_i, $dom(F_i) \equiv \Re^{n_i}$ is a vector space and that the corresponding distance function d_{F_i}, is an L_p metric.[4]

The simple observation exploited to deal with multi-feature formulae over vector spaces is that $\Re^{n_1} \times \ldots \times \Re^{n_m} \equiv \Re^n$, with $n = \sum_i n_i$. In other terms, if the m considered features are vectors with n_i elements each, their combination is a vector with n elements. The fact that each feature uses its own distance is not a problem at all, as the following example shows.

Example 7.11
Consider the query $\texttt{range}(f, \alpha, \mathcal{C})$, where $f = p_1 \wedge p_2$, with $p_1 : F_1 \sim v_1$ and $p_2 : F_2 \sim v_2$, and the two similarity environments (see Definition 7.4):

$$\begin{aligned} \mathcal{DS}(R.F_1) &= (\Re^2, L_2, 1 - 0.1 \cdot x, \mathcal{FA}) \\ \mathcal{DS}(R.F_2) &= (\Re^3, L_1, e^{-x}, \mathcal{FA}) \end{aligned}$$

Evaluation of the query as a whole by means of, say, a 5-dimensional R-tree would be as follows. Given a node N of the R-tree, we first compute $L_{2_{\min}}(v_1, Reg(N))$ and $L_{1_{\min}}(v_2, Reg(N))$, that is, the minimum distance bounds from the query values. Note that each bound uses the distance function specific for the feature at hand. After this, we can directly compute $s_{\max}(f, Reg(N))$ as:

$$s_{\max}(f, Reg(N)) = (1 - 0.1 \cdot L_{2_{\min}}(v_1, Reg(N))) \cdot e^{-L_{1_{\min}}(v_2, Reg(N))}$$

The final step consists in comparing $s_{\max}(f, Reg(N))$ with α, from which we can decide whether or not node N can be pruned. □

The second case concerning features' domains and distance functions covers all other possibilities, with the only assumption that generic metric spaces are considered. In this case the question of "indexability" of the *heterogeneous* domain is immediately raised. Since, as far as we know, no existing access method can do this, the question is interesting per se, thus, regardless of the specific context we are considering here.

In order to show that even heterogeneous domains can be indexed, in Section 8.2 we sketch the basic principles of a *new* access method, the M^2-tree (*Multi-Metric* tree) we have designed for this purpose.

[4] Again, nothing would prevent us to use "quadratic form functions" [SK97]; our choice simplifies the presentation without affecting at all the substance of the arguments.

7.5.1 Combining Scores from Multiple Domains

In this Section we address a specific yet important problem, which concerns the meaningful integration of similarity scores when predicates are over multiple feature domains. The following example clarifies the problem.

Example 7.12
Consider an image database, where images can be retrieved by means of `color` and `texture` features. Now, suppose the user wants to retrieve, say, 10 grassland images. The specified query would be $\texttt{NN}(p_1 \wedge p_2, 10, \mathcal{C})$, with $p_1 = \texttt{color} \sim \texttt{green}$ and $p_2 = \texttt{texture} \sim \texttt{grass}$, and where $\mathcal{C}$ is the set of images. Let $d_{\texttt{color}}$ and $d_{\texttt{texture}}$ be the distance functions used to measure color and texture similarity, respectively, and $h_{\texttt{color}}$ and $h_{\texttt{texture}}$ their correspondence functions. Since each h_{F_i} has only to satisfy minimal requirements specified in Definition 2.6, in principle any choice would do the job. A closer analysis, however, reveals that the exact form of the correspondence functions, besides altering objects' scores, can also modify objects' ranking, thus changing the result of the query. □

Altough it can be argued that the choice of the correspondence functions should be either left to the system's designer or to the user, we believe that a principled approach is needed. The one we suggest is applicable provided data statistics are available, and has the pleasant property that gives an immediate and intuitive characterization of what similarity scores represent.

Consider a feature F, a metric d_F defined over $dom(F)$, and a collection $\mathcal{C}$. Assume that the (cumulative) distance distribution, G_F, of d_F over $\mathcal{C}$ is known (see Section 6.2). Therefore, we can estimate, for each distance value x, the probability that two random objects of $\mathcal{C}$ will have a distance not exceeding x, that is (see also Equation 6.1):

$$G_F(x) = \Pr\{d_F(O_i.F, O_j.F) \leq x\}$$

We have the following simple yet powerful result.

Lemma 7.1
Let G_F be the continuous and invertible distance distribution of feature F over the collection $\mathcal{C}$. If the correspondence function has the form

$$h_F(x) = 1 - G_F(x)$$

then the probability distribution of the similarity scores for the feature F is uniform over $[0, 1]$, that is:

$$\Pr\{s(O_i.F, O_j.F) \leq \alpha\} = \alpha$$

Proof: Since $s(O_i.F, O_j.F) = h_F(d_F(O_i.F, O_j.F)) = 1 - G_F(d_F(O_i.F, O_j.F))$, it has to be proved that $\Pr\{1 - G_F(d_F(O_i.F, O_j.F)) \leq \alpha\} = \alpha$. The detailed steps are as follows:

$$\begin{aligned}
\Pr\{1 - G_F(d_F(O_i.F, O_j.F)) \leq \alpha\} &= \Pr\{G_F(d_F(O_i.F, O_j.F)) \geq 1 - \alpha\} \\
&= \Pr\{d_F(O_i.F, O_j.F) \geq G_F^{-1}(1 - \alpha)\} \\
&= 1 - \Pr\{d_F(O_i.F, O_j.F) \leq G_F^{-1}(1 - \alpha)\} \\
&= 1 - G_F(G_F^{-1}(1 - \alpha)) = 1 - (1 - \alpha) = \\
&= \alpha
\end{aligned}$$

□

Let us briefly comment above result. If we set $h_F(x) = 1 - G_F(x)$, then we know that a simple range query $\texttt{range}(F \sim v, \alpha, \mathcal{C})$ will retrieve, on average, a fraction (1 - α) of the objects in $\mathcal{C}$. In other terms, uniformity of similarity scores provides a clear way to relate similarity thresholds to selectivity of (simple) range queries.

A second important aspect is that above choice indeed allows a better discrimination on the distance domain. For this, refer to Figures 7.14 and 7.15. In Figure 7.14, most of the distance values are in the range 20–30, but in this range the h correspondence function does not exhibit substantial changes. This implies that small changes in the similarity threshold represent indeed large changes in the query result. The opposite is true if the similarity threshold is changed but still remains quite high. This can be summarized by saying that there is no clear way to determine what a difference of, say, 0.1 between two similarity scores actually represents. Consider now Figure 7.15, where $h(x) = 1 - G(x)$. It can be easily seen that above problems are now disappeared, thus a clear intuition of the meaning of absolute similarity scores is provided. We can synthetically characterize the good behavior of h by saying that "it changes where it is needed to change".

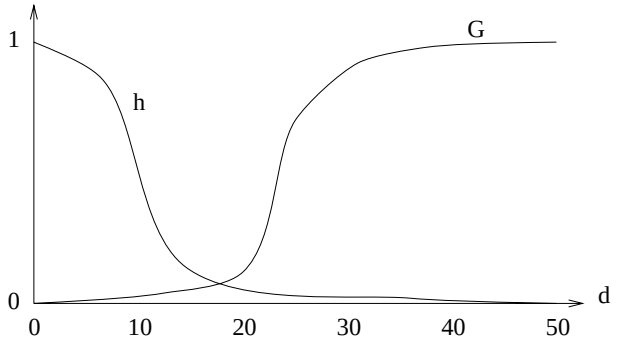

Figure 7.14: A "bad" correspondence function.

We believe that the idea of relating correspondence functions to distance distributions is also relevant from the query optimization point of view, in that the induced uniformity

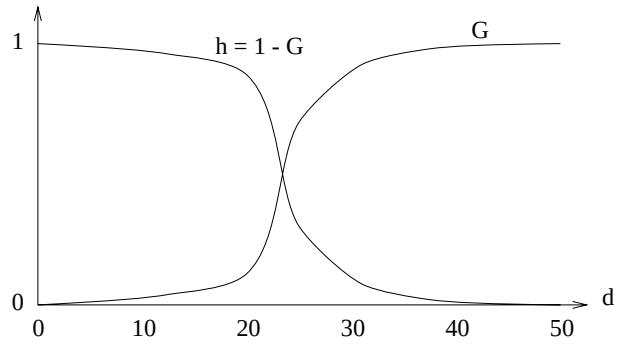

Figure 7.15: The correspondence function $h(x) = 1 - G(x)$.

of similarity scores tends to simplify the task of estimating query cardinalities. The fact that the distance distribution is used, rather than the more common "data distribution", should not be a surprise at all, since distance is the basic information we need to assess similarity and to predict performance of distance-based access methods, as shown in Chapter 6.

Chapter 8

Limitations and Extensions of M-tree

In Chapter 4 we showed the effectiveness of the M-tree access structure for the efficient indexing of generic metric spaces. We also pointed out that, unlike the R-tree family of index methods, the M-tree is not restricted to vector spaces. The conclusion that M-tree is a generalization of R-tree is, however, not true, as explained by the following points:

- First of all, R-tree-like indices can take advantage of the use of objects' coordinates to organize the space; of course, such information is not available in a generic metric space.
- SAMs are easily extendible to deal with user-adaptable similarity queries, i.e. with queries referring to user-defined distance functions [SK97]. From the definition of the M-tree given in Chapter 4, it seems that the only supported distance function for queries is the same metric used to build the tree.

In this Chapter, we will "extend" the M-tree to deal with queries using a different metric with respect to that used to build the tree. Then, we will present the M^2-tree, a novel index structure generalizing both the M-tree and the R-tree access methods. Such index structure can be effectively used to deal with complex queries referring to multiple domains (see Section 7.5).

8.1 Using Different Metrics with M-tree

In Section 4.2 we proved, by way of Lemma 4.1, that if the distance between the query object Q and the routing object O_r of a node is greater than the sum of the query radius r_Q and of the covering radius $r(O_r)$ of the node, that is if $d(Q, O_r) > r_Q + r(O_r)$, then the sub-tree rooted at that node, i.e. $T(O_r)$, can be safely pruned from the search, thus guaranteeing the absence of *false dismissals*, i.e. objects satisfying the query but

not included in the result set. This, as stated in Section 1.1, is one of the fundamental properties for the similarity search process. If we are to generalize the M-tree access method in order to make it able to deal with distance functions different from that used to build the tree, we should, therefore, guarantee that, in any case, no false dismissal is present. To this end, we start by precisely defining our reference scenario.

In the general case, three different metrics can be used with an M-tree:

1. the *indexing* distance function, d_I, that is used to build the tree,
2. the *query* distance function, d_q, used to issue queries to the system, and
3. the *comparison* distance function, d_c, used to compare the query object and the objects stored in the tree during the search phase.

For pruning sub-parts of the tree during the search phase, we have to find a pruning criterion similar to that of Lemma 4.1. This is provided by the following

Lemma 8.1
If d_c is a lower bounding distance function for both d_I and d_q and $d_c(O_r, Q) > r_Q + r(O_r)$, then, for each object O_j in $T(O_r)$, it is $d_q(O_j, Q) > r_Q$. Thus, $T(O_r)$ can be safely pruned from the search.

Proof: We have to prove that, if $d_c(O_r, Q) > r_Q + r(O_r)$ and $d_I(O_r, O_j) \leq r(O_r)$, then it is $d_q(Q, O_j) > r_Q$. In fact, it is

$$\begin{aligned} d_q(Q, O_j) &\geq d_c(Q, O_j) && \text{(def. of l.b. distance function)} \\ &\geq d_c(Q, O_r) - d_c(O_r, O_j) && \text{(triangle inequality)} \\ &\geq d_c(Q, O_r) - d_I(O_r, O_j) && \text{(def. of l.b. distance function)} \\ &\geq d_c(Q, O_r) - r(O_r) && \text{(def. of covering radius)} \\ &> r_Q + r(O_r) - r(O_r) && \text{(by hypothesis)} \\ &= r_Q \end{aligned} \tag{8.1}$$

□

From Lemma 8.1, we see that, in order to search without false dismissals the M-tree using a distance function different from that used to build the tree, it is sufficient (and also necessary as it can be easily proven) to provide a comparison function that is a lower bound for both the indexing and the query metrics (see Definition 3.1).

For each internal node, therefore, we compute the comparison distance between the query object Q and the routing object of the node O_r and apply Lemma 8.1. In order

to compute $d_c(Q, O_r)$, however, it has to be $\mathcal{D}_c \equiv \mathcal{D}_I$, since the M-tree stores only the features needed to compute d_I, i.e. the representation of each object in the $\mathcal{D}_I$ domain.

When the leaf level is reached, however, the absence of false drops cannot be guaranteed, since the condition $d_c(Q, O) \leq r_Q$ it is not sufficient to guarantee that $d_q(Q, O) \leq r_Q$. On the other end, if it is $\mathcal{D}_q \equiv \mathcal{D}_I$, we can compute the exact query distance $d_q(Q, O)$, since the features needed to compute that distance are stored in the M-tree; therefore, in the latter case, no objects' false drops are present, since we can access nodes in the upper levels of the tree by using the d_c metric, and check objects at leaf level using the exact d_q metric. If, however, it is $\mathcal{D}_q \not\equiv \mathcal{D}_I$, the result of a simple range search is a set of *candidate* objects: For each object in the set we have to compute the actual d_q distance with respect to the query object in order to see if it qualifies for the query result (thus obtaining a *filter and refine* search process). For k-NN queries, the optimal algorithm described in [SK98] can be used.

Given the two constraints $d_c \leq d_I$ and $d_c \leq d_q$, we consider six cases:

1. $d_c = d_q = d_I$. This is the basic case.

2. $d_c < d_q = d_I$. In this case, we use an unexpensive d_c metric to check if a node can be pruned. Of course, if $d_c(Q, O_r) \leq r_Q + r(O_r)$, it can still be the case that $d_q(Q, O_r) > r_Q + r(O_r)$, thus we access a node whose sub-tree cannot contain objects satisfying the query (*index false drop*). In this case, however, since it is $\mathcal{D}_q \equiv \mathcal{D}_I \equiv \mathcal{D}_c$, we can easily compute the exact distance $d_q(Q, O_r)$ to see if the node can be pruned. The condition $d_c(Q, O_r) > r_Q + r(O_r)$, thus, can be used as a pre-test for node pruning, after which the exact test $d_q(Q, O_r) > r_Q + r(O_r)$ is performed.

3. $d_c = d_q < d_I$. In this case, as in the following ones, we search the M-tree using a distance function that is different from the metric used to build the tree. Since it is $d_q = d_c$, it is $\mathcal{D}_q \equiv \mathcal{D}_I$, therefore no objects false drops are present. This case is that of *partial-match queries*, where we query the system using a distance function "simpler" than d_I.

4. $d_c = d_I < d_q$. In this case, we index the objects using a distance which is simpler with respect to the metric used for querying the DB. This is the technique used in the GEMINI approach [ZCF+97, Chapter 12] for indexing multimedia databases. Again, objects false drops are present.

5. $d_c < d_I < d_q$. In this case, as in the following one, we use three completely different distance functions for indexing, comparison and query.

6. $d_c < d_q < d_I$. As for the previous case, this situation presents no relevant properties.

8.1.1 False Drops at the Index Level

Another problem arising when using different metrics is that of *index false drops*. We have an index false drop during the search phase when we access a branch of the tree that cannot lead to any qualifying object. This problem is not present in the basic case when $d_c = d_q = d_I$, since the condition of Lemma 4.1 is also a necessary condition for pruning a sub-tree. In order to prove that, we need a preliminary definition.

Definition 8.1 (Overlap of regions of a metric space)
Let $Reg(O_1) = (O_1, r(O_1))$ and $Reg(O_2) = (O_2, r(O_2))$ be two regions (balls) of a metric space $\mathcal{M} = (\mathcal{D}, d)$ defined as

$$Reg(O_i) = \{x \in \mathcal{D} \ : \ d(O_i, x) \leq r(O_i)\} \tag{8.2}$$

We say that $Reg(O_1)$ and $Reg(O_2)$ overlap, if it cannot be excluded that

$$\exists x \in \mathcal{D} \ : \ x \in Reg(O_1) \wedge x \in Reg(O_2)$$

□

Note that, in the general case, we cannot say that two regions of a metric space are not overlapping if $\nexists x \in \mathcal{D} \ : \ x \in Reg(O_1) \wedge x \in Reg(O_2)$. As an example, see Figure 8.1, representing the overlap of two regions in the $(\mathbb{N}^2, L_2)$ metric space: In this case the two regions overlap, but there is no object of the space belonging to both regions, i.e. the two regions are not intersecting. However, since the absence of objects in the intersection of the two regions cannot be guaranteed for a generic metric space, for indexing purposes we say that the two regions of Figure 8.1 actually overlap.

In order to exclude false drops, since the condition for node pruning is based on the overlap between the node and the query regions, we have to prove that every accessed node overlaps with the query region. In the exact case, i.e. when $d_c = d_q = d_I$, no index false drops are present, since the condition of Lemma 4.1 is not only sufficient but also necessary to guarantee that two regions of the metric space do not overlap, as is specified by the following

Theorem 8.1
Consider a query region $Reg(Q) = (Q, r_Q)$ and a node region $Reg(O_r) = (O_r, r(O_r))$ of a metric space $\mathcal{M} = (\mathcal{D}, d)$. Then it is

$$d(Q, O_r) > r_Q + r(O_r) \Leftrightarrow Reg(Q) \ \neg overlaps \ Reg(O_r) \tag{8.3}$$

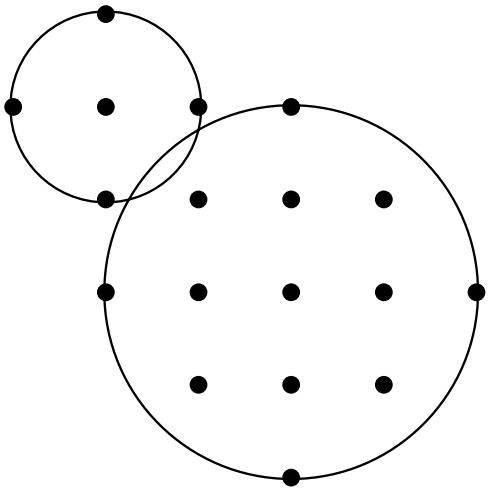

Figure 8.1: Two regions of the $(\mathbb{N}^2, L_2)$ metric space.

Proof:
$\Rightarrow$ This is given by Lemma 4.1.
$\Leftarrow$ We have to prove that if every object in $Reg(O_r)$ cannot belong to $Reg(Q)$ (or vice versa), then it is $d(Q, O_r) > r_Q + r(O_r)$. If $O \in Reg(O_r)$, it is $d(O_r, O) \leq r(O_r)$; since $O \notin Reg(Q)$, it is $d(Q, O) > r(Q)$. It follows

$$\begin{aligned} d(Q, O) &\geq d(Q, O_r) - d(O_r, O) \quad \text{(triangle inequality)} \\ &\geq d(Q, O_r) - r(O_r) \qquad\quad \text{(by hypothesis)} \end{aligned} \tag{8.4}$$

Therefore it is

$$\begin{cases} d(Q, O) > r_Q & \text{(by hypothesis)} \\ d(Q, O) \geq d(Q, O_r) - r(O_r) & \text{(Equation 8.4)} \end{cases} \tag{8.5}$$

Since the conditions of Equation 8.5 should be met for any object $O \in Reg(O_r)$, it is $d(Q, O_r) - r(O_r) > r_Q$. Therefore, it is $d(Q, O_r) > r_Q + r(O_r)$, which proves the result. □

In the general case, when it is $d_c < d_q$ or $d_c < d_I$, Lemma 8.1 ensures that no false dismissals are present, i.e. that $d_c(Q, O_r) > r_Q + r(O_r) \Rightarrow Reg(Q)$ ¬overlaps $Reg(O_r)$. The converse, however, is not true, since, in this case, we cannot obtain an inequality similar to that of Equation 8.4. Therefore, when it is $d_c < d_q$ or $d_c < d_I$, we cannot exclude index false drops. The following example clarifies the situation.

Example 8.1
Suppose we have indexed a set of objects in the $(\Re^2, L_2)$ metric space using an M-tree (therefore, nodes regions are circularly shaped). Now, we want to search the M-tree using the L_∞ metric, obtaining squared search regions. In order to see if a node has to be

accessed, we compute the L_∞ distance between the query object and the routing object of the node. If this distance is higher than $r_Q + r(O_r)$, we can safely prune the node. Therefore, both the query radius and the node covering radius are considered with respect to the d_c metric function, L_∞ in this case. In the case of Figure 8.2, the query region and the node region are not overlapping. However, when the node region is "inflated" using the L_∞ metric, it overlaps with the query region; therefore, the node cannot be pruned from the search and we access a node that cannot lead to qualifying objects.

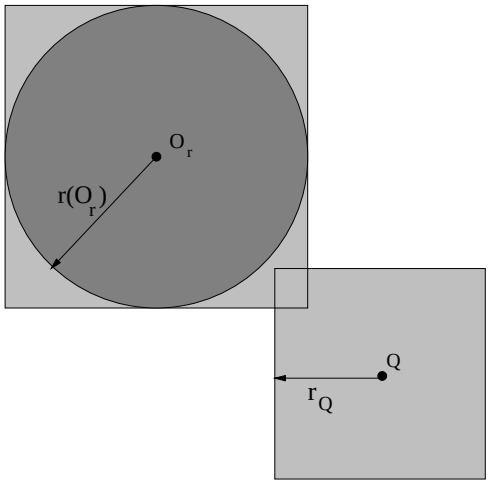

Figure 8.2: An index false drop arising when we use, to query the M-tree, a distance function that is different from that used to build the tree.

□

8.2 The M^2-tree

The M-tree is able to index objects drawn from a metric space $\mathcal{M}$. In order to extend this access method to deal with multi-feature queries (see Section 7.5), we need to precisely define our working scenario.

Definition 8.2 (Multi-dimensional metric space)
If $\{\mathcal{M}_i = (\mathcal{D}_i, d_i),\ i = 1, \ldots, n\}$ is a set of metric spaces, we define the *multi-dimensional metric space* as $\mathcal{M}^n = (\mathcal{D}_1 \times \ldots \times \mathcal{D}_n, (d_1, \ldots, d_n))$. □

In practice, a set of metric spaces defines a multi-dimensional metric space, whose domain is given by the cartesian product of the domains of the original metric spaces. On this domain, we can use the original distances to compare objects.

8.2.1 Regions of a Multi-Dimensional Metric Space

A region of a multi-dimensional metric space $\mathcal{M}^n$ can be defined by way of a set of distance constraints, as the following examples demonstrate.

Example 8.2
Consider the multi-dimensional vector space $\mathcal{M}^2 = ([0,1] \times [0,1], (d_1, d_2))$, where $d_i(x,y) = |x-y|,\ (i = 1,2)$, and an object $Q = (0.3, 0.5) \in [0,1] \times [0,1]$. A region of $\mathcal{M}^2$ around Q can be defined as:

$$Reg(Q) = \{O \in [0,1] \times [0,1] : (1 - d_1(Q_1, O_1))\,(1 - d_2(Q_2, O_2)) \geq \alpha\} \tag{8.6}$$

Figure 8.3 displays the region defined by Equation 8.6. Note that the specification of $Reg(Q)$ is equivalent to the specification of the complex range query $\texttt{range}(f, \alpha, \mathcal{C})$, where $f = (x \sim 0.3) \wedge (y \sim 0.5)$, under the $\mathcal{FA}$ semantics with $h(d) = 1 - d$. □

Example 8.3
Consider, again, the multi-dimensional vector space $\mathcal{M}^2 = ([0,1] \times [0,1], (d_1, d_2))$, where $d_i(x,y) = |x-y|,\ (i = 1,2)$, and an object $Q = (0.7, 0.5) \in [0,1] \times [0,1]$. Now, let us define a region of $\mathcal{M}^2$ around Q as:

$$Reg(Q) = \{O \in [0,1] \times [0,1] : |d_1(Q_1, O_1) - d_2(Q_2, O_2)| \leq \epsilon\} \tag{8.7}$$

Figure 8.4 displays the region defined by Equation 8.7. □

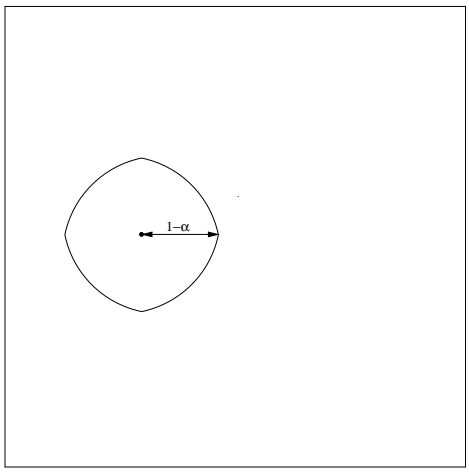

Figure 8.3: A region of $\mathcal{M}^2$.

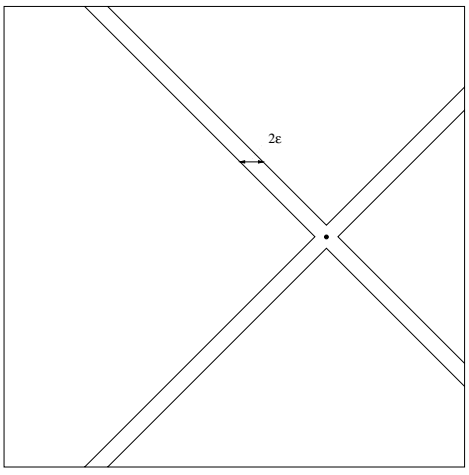

Figure 8.4: Another region of $\mathcal{M}^2$.

Of course, arbitrarily complex specifications of a region in the multi-dimensional metric space are possible.

8.2.2 Nodes of the M^2-tree

In order to index a multi-dimensional metric space, we present the principles of a new access structure, the M^2-tree. The basic idea which underlies the M^2-tree design is simple yet powerful. If we have n value domains with corresponding distance functions, we can still use the basic organizing principle of the M-tree provided the definition of a node region takes into account information from all the n functions. This is to say that regions associated with nodes of the M^2-tree are not simple *balls*, as in M-tree, rather they constrain the heterogeneous space in a more complex way. Note that this is made possible since only relative distances are considered to partition the metric space(s), rather than absolute coordinate values as done by spatial access methods. Therefore, each M^2-tree node is associated to a region in a multi-dimensional space, where each dimension corresponds to a different metric space.

If we choose a reference point O_r, a metric space can be seen as an half-line departing from O_r.[1] If we now consider n different features $F_1, \ldots, F_n$, with their correspondent metrics $d_1, \ldots, d_n$, and a routing point $O_r = (O_{r_1}, \ldots, O_{r_n}) \in dom(F_1) \times \ldots \times dom(F_n)$, the "viewpoint" of O_r over the associated multi-dimensional metric space $\mathcal{M}^n$ can be seen as the positive quadrant of an n-dimensional vector distance space.

In principle, a node N of the M^2-tree specifies an arbitrary region of such a space. A general way to specify this region is to use p constraints

$$f_i(d_1(O_{r_1}, O.F_1), \ldots, d_n(O_{r_n}, O.F_n)) \leq 0, \quad i = 1, \ldots, p \tag{8.8}$$

where O is an object in the sub-tree rooted at N.

Example 8.4
Consider Example 8.2. The graphic representation of a node whose region is specified through Equation 8.6 is given by Figure 8.5. □

Example 8.5
Consider Example 8.3. The graphic representation of a node whose region is specified through Equation 8.7 is given by Figure 8.6. □

If both the node region and the query region are defined by means of arbitrarily complex constraints, the task of deciding if a node of the M^2-tree overlaps the query region (or, using the GiST [HNP95] terminology, if the node is `Consistent` with the query) could become very difficult to solve, without specific information on the underlying multi-dimensional metric space. Just consider, as an example, the two regions defined by

[1] Or as a line segment if the metric space is bounded (see Definition 6.1)

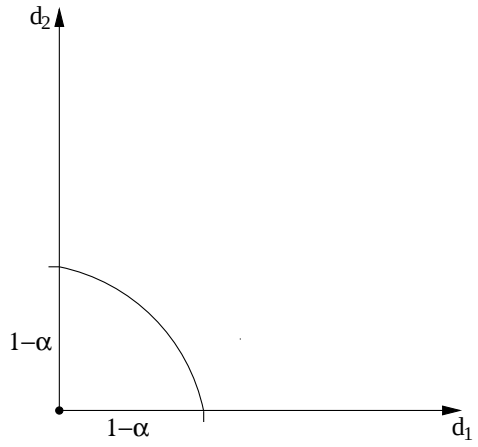

Figure 8.5: The node region specified by Equation 8.6.

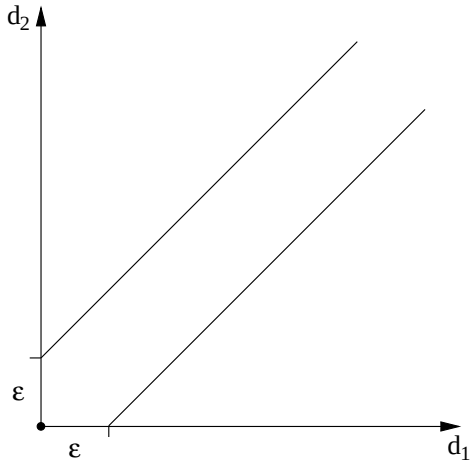

Figure 8.6: The node region specified by Equation 8.7.

Equation 8.6 and by Equation 8.7. Thus, it is hard to check if a node of the tree has to be accessed. The simplest way to define the constraints of Equation 8.8 is to specify a distinct covering radius for each component space:

$$d_i(O_{r_i}, O.F_i) \leq r_i(N), \quad i = 1, \ldots, n \tag{8.9}$$

In this way, the region associated with node N is an hyper-rectangle in the n-dimensional distance space defined by the routing object O_r, as Figure 8.7 shows.

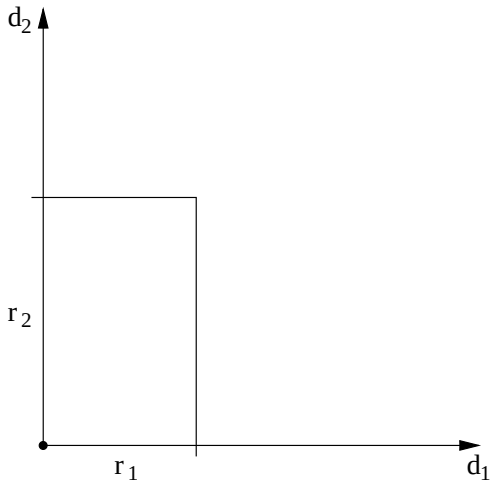

Figure 8.7: A M^2-tree node region specified by way of Equation 8.9 ($n = 2$).

When nodes are defined in this way, the R-tree access structure becomes a particular case of the M^2-tree, when each component space of the multi-dimensional metric space is $(\Re, |x - y|)$.

Having defined how regions associated to M^2-tree nodes are specified, we are now ready to show how to search the tree. Given the query specification, thus, we have to specify a criterion to prune sub-parts of the tree that cannot lead to qualifying objects. In order to simplify the presentation, in the following we will only consider queries specified through a similarity formula f, as defined in Section 7.1. In this scenario, Theorem 7.1 can easily be extended in order to be applied to M^2-tree nodes.

Theorem 8.2
Let $\mathcal{DS}^n = (\mathcal{D} = dom(F_1) \times \ldots \times dom(F_n), (d_1, \ldots, d_n), (h_1, \ldots, h_n), \mathcal{L})$ be a multi-similarity environment where similarity between objects can be assessed by way of n different distance functions d_i on the domain $\mathcal{D}$, each with the respective correspondence function h_i; let $f = f(p_1, \ldots, p_m) \in \mathcal{L}$ ($p_j : F_{i_j} \sim v_j,\ j = 1, \ldots, m,\ i_j \in \{1, \ldots, n\}$) be a similarity formula such that each predicate occurs exactly once, and d_{i_j} the metric used to assess predicate p_j; let $\mathcal{C}$ be a collection of objects indexed by an M^2-tree $\mathcal{T}$ on the values of features $F_1, \ldots, F_n$. Let $s_f(s(p_1, v), \ldots, s(p_m, v))$ ($v \in \mathcal{D}$) be the scoring function of f.

If s_f is monotonic in all its variables, then a node N of $\mathcal{T}$ can be pruned if

$$s_{max}(f, Reg(N)) \stackrel{\text{def}}{=} s_f(h_{i_1}(d_{B,i_1}(v_1, Reg(N))), \ldots, h_{i_m}(d_{B,i_m}(v_m, Reg(N)))) < \alpha \quad (8.10)$$

where

$$d_{B,i_j}(v_j, Reg(N)) = \begin{cases} d_{min,i_j}(v_j, Reg(N)) & \text{if } s_f \text{ is monotonic increasing in } s(p_j, v) \\ d_{max,i_j}(v_j, Reg(N)) & \text{if } s_f \text{ is monotonic decreasing in } s(p_j, v) \end{cases} \quad (8.11)$$

with $d_{min,i_j}(v_j, Reg(N))$ ($d_{max,i_j}(v_j, Reg(N))$) being a lower (upper) bound on the minimum (maximum) distance from v_j of any value $v \in Reg(N)$, and where α is

- *the user-supplied minimum similarity threshold, if the query is* $\texttt{range}(f, \alpha, \mathcal{C})$*;*
- *the k-th highest similarity score encountered so far, if the query is* $\texttt{NN}(f, k, \mathcal{C})$*. If less than k objects have been evaluated, then $\alpha = 0$.*

Proof: Follows the same steps of Theorem 7.1. □

The major problem, now, is the computation of the bounds $d_{B,i_j}(v_j, Reg(N))$ on the distance from each v_j of the query to any object $O \in Reg(N)$, which can be a quite difficult task if the region associated to node N is defined through p general constraints, as in Equation 8.8, while it is pretty easy if we have n covering radii, as specified in Equation 8.9:

$$d_{min,i_j}(v_j, Reg(N)) = \max\{d_{i_j}(O_{r_{i_j}}, v_j) - r_{i_j}(N), 0\} \quad (8.12)$$

$$d_{max,i_j}(v_j, Reg(N)) = d_{i_j}(O_{r_{i_j}}, v_j) + r_{i_j}(N) \quad (8.13)$$

Apart from technicalities related to index maintenance and similar problems (efficient algorithms to insert entries in the tree and to split nodes should be investigated), from above argumentations it should be clear that the definition of M^2-tree makes it indeed possible to search over multiple metric spaces with a single access structure, thus solving the problem of evaluation of multi-feature complex queries (see Section 7.5).

Chapter 9

Conclusions

In this thesis we presented an approach for resolving similarity queries in multimedia databases. We focused on the efficient and effective processing of similarity queries, showing how distance-based access structures can be proficiently exploited to reduce search costs.

The main conclusions we can draw from our work are the following:

- Basic similarity search operations can be modeled as search operations on metric spaces, following similarity theories developed by pshychologists.

- Similarity (range and nearest neighbors) queries over metric spaces can be efficiently processed using distance-based access structures, such as Spatial Access Methods and metric trees.

- Both SAMs and metric trees present some drawbacks, preventing their use in generic large-size complex environments. To overcome such problems, the M-tree access structure has been presented. Experimental results show that the M-tree can be proficiently used to index generic metric spaces. The effectiveness of M-tree is also demonstrated by the fact that the index is used for several real-world application, ranging from indexing of genomic DBs [CA97] to data mining [EKS+98].

- For query optimization purposes, cost models for distance-based access methods have to be developed; in this field, particular relevance assume query-sensitive cost models. To this end, we have presented three different cost models for the M-tree. These are, as far as we know, the first cost models for metric trees.

- In most cases, the problem of single-feature complex similarity queries can be efficiently resolved by using distance-based access methods.

- For some "pathological" spaces, existing access methods are inefficient for solving similarity queries; in such cases (e.g. in high-dimensional vector spaces) a simple linear scan of the DB is a quicker solution. It has to be noted, however, that this situation can be the norm for some relevant problems (e.g. when indexing images).
- The case of multi-feature complex queries can be resolved by using the same results obtained for the single-feature case, provided that "powerful enough" access methods are available. To this end, we introduced the M^2-tree, a novel access structure able to index multiple heterogeneous domains.

9.1 Future Directions

Throughout this thesis we pointed out several interesting issues for future research. These include:

- We plan to analyze the efficiency of access structures using the concept of *distance distribution* (see Section 6.2). This, besides its obvious contribution to a better explanation of the problem of the *dimensionality curse* (see Section 3.1.2), could also help in developing new access structures able to index such "pathological" spaces.
- The problem of approximate similarity search has been recently addressed [AMN+94, SZ+96, ZSAR98] in order to speed-up the search phase by giving up some precision in the query result. We plan to develop an approximate search technique for the M-tree access method, along with a cost model to predict search costs.
- We intend to extend our approach to develop a cost model for complex similarity queries (see Chapter 7).
- In [Cia98] an algebra for similarity queries is presented, along with some issues for query optimization using index structures. We plan to specify a complete set of optimization rules in order to derive an algebraic optimizer.
- Complete specification and optimization, along with an experimental evaluation, of the M^2-tree access structure are needed.
- Finally, we also intend to apply our approach to some real-life problems, e.g. content-based image retrieval, fingerprint databases, and text retrieval.

Appendix A

Implementation of M-tree

As we saw in Section 4.6, our M-tree implementation is based on the Generalized Search Tree (GiST) C++ package [HNP95]. In this Chapter we will discuss about the structure of the code.[1]

A.1 Classes Overview

The basic block of our structure is the concept of *object*. To our purposes, an object is simply the description of a feature value of the $\mathcal{D}$ space (see Section 2.1). The basic method of the `Object` class is the `distance` method, i.e. the function assessing the distance between two different feature values. Thus, in defining the `Object` implementation for a particular application, the user should provide all and only those features that will be used by the `distance` method. A `maxDist` function is also needed, in order to specify the maximum possible distance between two objects.

M-tree nodes store entries composed by a `MTkey` and a page pointer, referencing the root node of the corresponding sub-tree for internal entries and the corresponding DB object for entries in leaf nodes. Each `MTentry` also stores a pointer to the corresponding node of the tree, along with the position of the entry inside that node and the level of the node itself. The `MTentry` class should also provide the `Compress` method, used to store on disk the information about each entry, and the inverse `Decompress` method. The `Penalty` method of the GiST `GiSTentry` base class has also been redefined in order to apply the optimization technique of Section 4.3.

The `MTkey` class stores the description of an `Object`, the covering radius of the region (0 for leaf keys) and the distance between the routing object and its relative parent object, i.e. the routing object of the parent node (an undefined value for keys in the root node).[2]

[1] The code of M-tree is freely available at URL `http://www-db.deis.unibo.it/~patella/MMindex.html`.

[2] In order to ensure compatibility for different versions of M-tree, the value of the minimum radius, i.e.

A node of the M-tree is an entity of the `MTnode` class. This class implements all the split and insertion methods, along with some search functions. The main methods for splitting are `PromotePart` and `PromoteVote`, implementing the unconfirmed and the confirmed promotion algorithms, respectively. The `Split` method partitions of the entries of the overflown node among the two nodes, by choosing between the balanced and the generalized hyperplane strategies. All the choices for the split strategies are expressed by setting the value of a few variables, namely `PROMOTE_PART_FUNCTION`, specifying the promotion strategy for node splitting, `SECONDARY_PART_FUNCTION`, for the splitting of the root node, `SPLIT_FUNCTION`, specifying the strategy for entries' partition, and `MIN_UTIL`, specifying the minimum node utilization for the generalized hyperplane unbalanced strategy.

Searching in the M-tree is allowed by using the `RangeSearch` method of the `MTnode` class and the `TopSearch` of the `MT` class. The `RangeSearch` method, applied to the root of the M-tree, recursively descend along the active paths of the tree, by applying the `Consistent` method to all the children entries of the current node. If the current node is a leaf, the entries consistent with the query are added to the results' list, whereas if the current node is an internal one, the `RangeSearch` method is recursively applied to the nodes corresponding to consistent entries. The `TopSearch` method implements the k nearest neighbors search. Here, the k-NN query is transformed into a range query with radius given by the distance between the query and the k-th nearest neighbor obtained so far. Then, the `Consistent` method is used to prune out sub-parts of the tree. Active nodes are mantained in a list and sorted for increasing d_{min} (see Section 4.2). Entries in the current node are analyzed in sorted order, starting from those entries whose distance from the routing object O_r is closest to the distance between O_r and the query. This strategy, as stated in [BFM+96], reduces the number of operations needed for entries' evaluation.

Similarity queries that can be submitted to M-tree belong to two basic types: Range queries are defined through the `SimpleQuery` class, whereas nearest neighbors queries are defined by the `TopQuery` class. Both classes reference to a `MTpred` object, specifying the (complex) predicate of the query; the `SimpleQuery` class has also a reference to a real value for the query radius, while the `TopQuery` class uses an integer number for the value of k, i.e. the number of requested neighbors. The `MTpred` class is a virtual class whose only purpose is the declaration of the pure virtual `distance` method, used to compute the distance between an object and the predicate itself. Starting from the base `MTpred` class, we derived the `Pred` class specifying simple predicates. An object of the `Pred` class has a reference to an `Object`, i.e. the query object, and the `distance` virtual method is

the distance between the routing object and the nearest object stored in the covering tree of the routing object itself, is also stored, having a constant value of 0.

simply redefined to compute the distance between the two objects. To specify arbitrarily complex predicates, using the syntax of $\mathcal{FS}$ and $\mathcal{FA}$ similarity languages (see Section 7.1.1), we derived 3 other classes from the base `MTpred` class, as can be seen in Figure A.1. These are the `AndPred`, `OrPred`, and `NotPred` classes. All these classes reference two (one in the case of the `NotPred` class) `MTpred` objects, specifying the subpredicates of the predicate itself. In the case of the `NotPred` class, the distance value is easily computed as:

$$d(\neg p, O) = h^{-1}(1 - h(d(p, O)))$$

whereas the actual implementation of the `distance` method for the `AndPred` and the `OrPred` classes depends on the used fuzzy language. As an example, under the $\mathcal{FA}$ language, the overall distance for the `OrPred` class is given by:

$$d(p_1 \vee p_2, O) = h^{-1}(h(d(p_1, O)) + h(d(p_2, O)) - h(d(p_1, O)) \cdot h(d(p_2, O)))$$

where h is the used correspondence function (see Definition 2.6). The actual implementation of h and h^{-1} is given by the `Dist2Sim` and the `Sim2Dist` functions respectively.[3] The overall architecture is parametric in both the correspondence function and the language used, the former being specified by the `hfunction` variable and the latter by `query_language`. A general framework for expanding M-tree to deal with generic complex expressions, i.e. expressions combining different range and k-NN queries, is subject of current research.

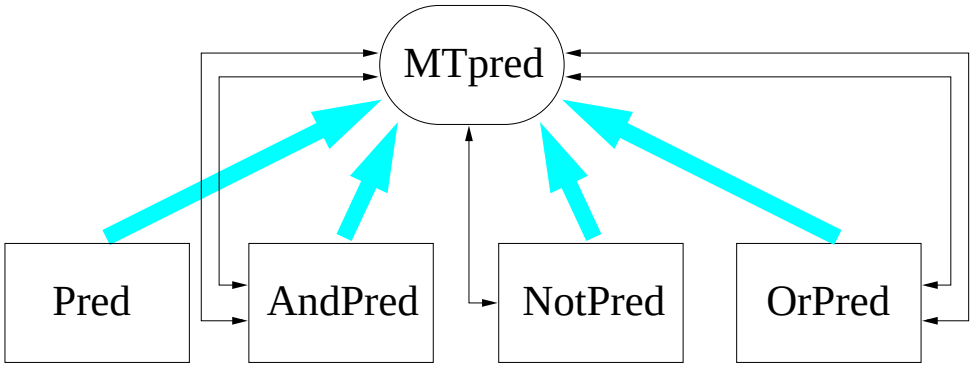

Figure A.1: Hierarchy schema for the `MTpred` class.

[3] In our implementation, we always suppose that h is invertible.

Appendix B

The Colors Application

In this Chapter we introduce a prototype application that demonstrate the effectiveness of the similarity search techniques developed in this thesis on a real-world problem, namely the content-based retrieval of images by means of color features.

The main objective of the Colors prototype is to show both the generality and the power of the approach presented in Chapter 7 for the optimization of *complex* content oriented requests. The software architecture, being parametric in the similarity environment (see Definition 7.4), could be, in principle, applied to a generic distance-based scenario, but we chose the image retrieval environment for its immediate visual impact.

B.1 Defining the Similarity Environment

The dataset used in the Colors application consists of 11,650 real-color JPEG compressed [Wal91] thumbnails of size 180x120 pixels. The used distance function is that defined in [SO95], where the average, variance and skewness of hue, saturation, and brightness components are extracted for each image, and a weighted L_1 metric is used to compare the 9-dimensional feature vectors. It should be noted that the evaluation of the effectiveness of the similarity function is definitely out of the scope of the application. The same approach can be used with *any* similarity function used to compare images, possibly including texture and/or spatial information.

Feature vectors extracted from the images were indexed using an M-tree, obtaining an index consisting of 632 pages of 4 Kbytes arranged on 3 levels. A sequential file of feature vectors was also created, consisting of 219 pages.

B.2 System Architecture

The system architecture of the Colors prototype is composed of five sub-systems, as sketched in Figure B.1:

1. The Image Database consisting of the 11,650 JPEG images.
2. The Feature Extractor that, given an image, computes the corresponding 9-dimensional feature vector.
3. The Query Engine that, given the query specification issued by the user, transforms it in a standard format and queries the DB using the specified method.
4. The Distance-Based Access Method, providing the way to access the DB (we implemented M-tree and a sequential scan as access methods).
5. The User Interface, used by the system to present the query results and by the user to specify queries.

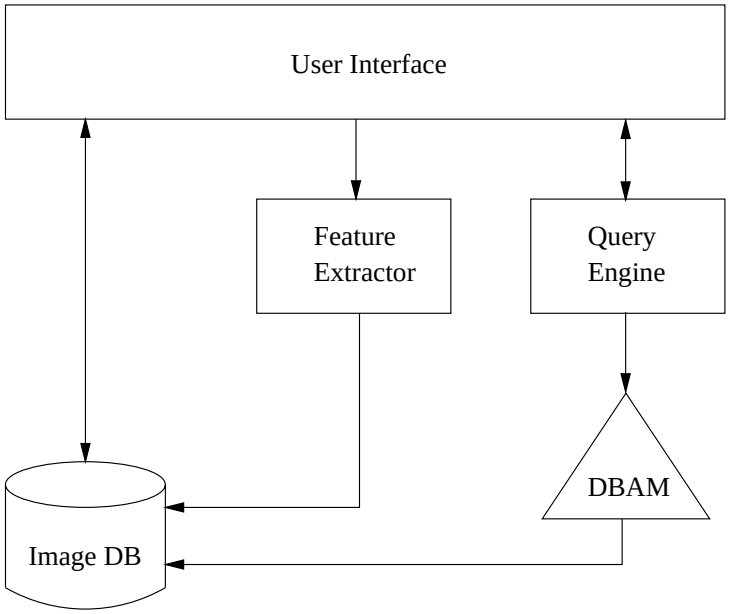

Figure B.1: The system architecture of the Colors application.

B.3 Query Specification

The user can issue queries to the system through the User Interface using three different modalities:

1. By choosing a starting image (selecting **File**, then **Open**, and specifying the path of an existing JPEG image, see Figure B.2).

2. By selecting a color (clicking on **File**, then on **New**, and choosing an uniform color from the color dialog, see Figure B.3).

3. By specifying a (complex) query using the result images of a previous query (clicking on each query image and then choosing **File**, then **Requery**).

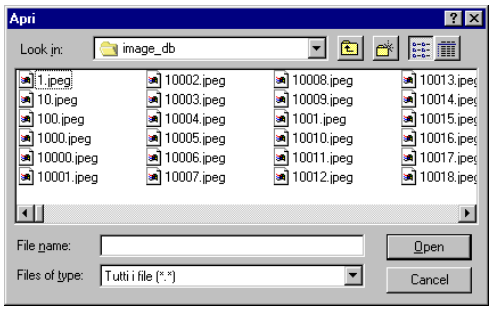

Figure B.2: The user can query the system for images similar to an existing one.

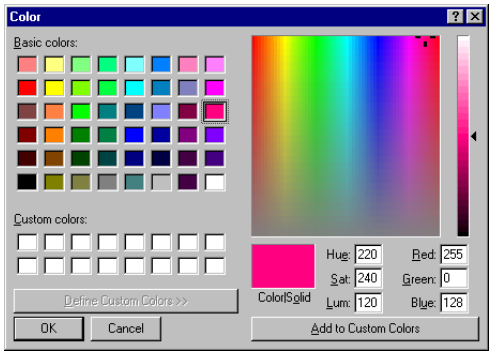

Figure B.3: The user can query the system for images similar to an image consisting of an uniform color (variance = skewness = 0).

When the user has specified the query, using one of the three different modalities, the system asks the user for the number of requested nearest neighbors by way of the Neighbors dialog (see Figure B.4).

The query engine, then, processes the query using the DBAM, retrieving the result images from the Image DB. Finally, the images are presented to the user through the User Interface, sorted in decreasing order of similarity with respect to the query (see Figure B.5). In the title bar of the result window, the system shows, along with some information

Figure B.4: The Neighbors dialog.

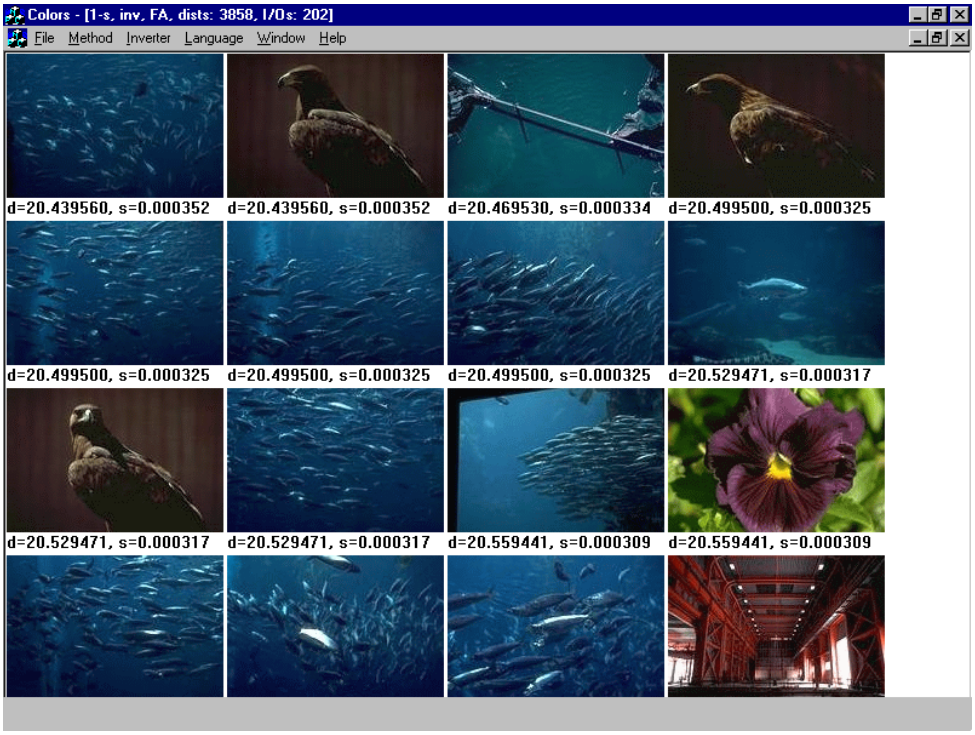

Figure B.5: The result of a query.

about the search method and the used similarity environment, the number of computed distances and of page I/Os (for a page size of 4 Kbytes).

When the user issues a complex query using the result of a previous one, he can specify both positive and negative examples. Positive examples are selected by clicking on the image; the system shows a blue frame around the image and the predicate is conjuncted to the query using an `and` operator. Negative examples are selected by clicking on the image with the Ctrl key pressed; the system shows a red frame around the image and the predicate is conjuncted to the query using `and not`. Figure B.6 show an example of a query; in this case two positive and one negative examples are specified.

Figure B.6: A complex query example.

B.4 Search Methods

The Query Engine can access the DB using one out of four different search methods, that can be specified by the user at run time by way of the **Method** menu:

1. **1-scan** is the approach presented in Chapter 7 applied to the M-tree access method.

2. **n-scan** is the $\mathcal{A}_0'$ algorithm [Fag96] applied to the M-tree as described in Section 7.4.1.

3. **Average** is a simple approach that can be exploited only if the feature space $\mathcal{D}$ is a vector space and the user has specified only positive examples for his complex query; in this case, the Average approach simply computes an average vector by equally weighing all the query vectors and performs a simple k-NN query on the underlying access method (M-tree in this case) using the average vector as query object. Of course, the results obtained in this way are different with respect to those obtained with other methods, which are computed using the user-specified query language, as can be seen in Figure B.7.

4. **Sequential** simply performs a sequential scan of the feature vectors file.

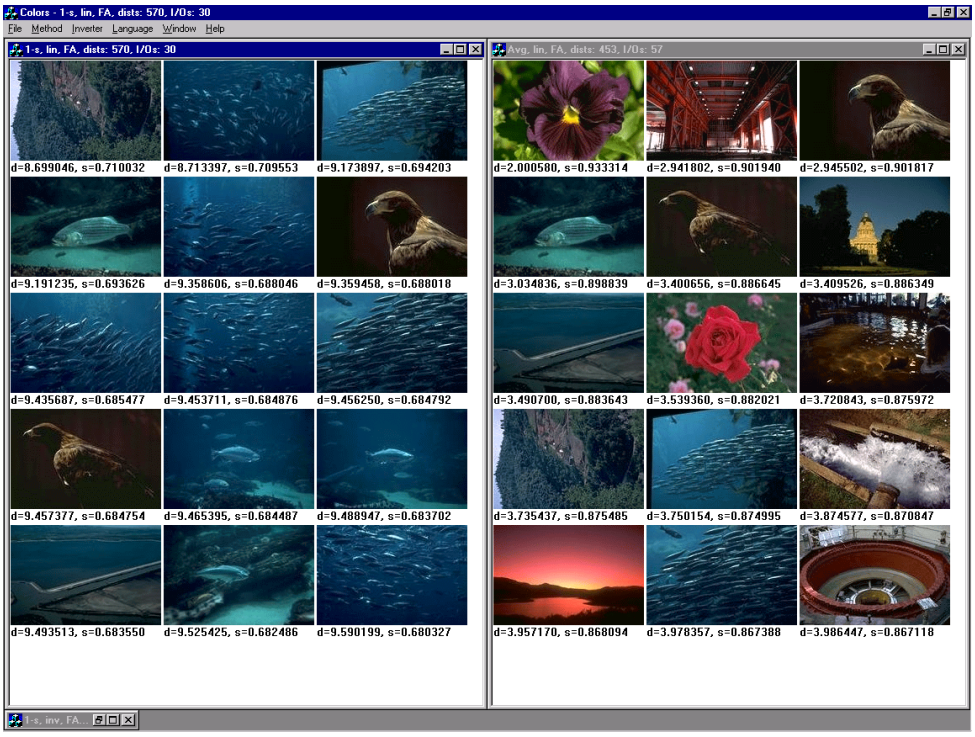

Figure B.7: Results obtained using the Average method (on the right) can be completely different with respect to those obtained with the other three methods (left) for the same query.

B.5 The Similarity Environment

In order to fully specify the similarity environment (Definition 7.4), the user has to specify the similarity language $\mathcal{L}$ and the correspondence function h. The similarity languages we implemented are $\mathcal{FS}$ and $\mathcal{FA}$ (Section 7.1.1), and the user can choose between them by using the **Language** menu. As to h, we implemented three different correpondence functions, that are specified through the **Inverter** menu:

1. **Linear** is a simple linear function, where $h(d) = 1 - d/d^+$,
2. **Exponential** is a simple exponential function, where $h(d) = e^{-d}$, and
3. **Distribution** is the 1-complement of the distance distribution between objects (see Section 7.5.1), $h(d) = 1 - G(d)$; $G(d)$ is estimated through a sample of the dataset and stored as an *equi-width* histogram with 100 bins.

Of course, changing either the similarity language or the correspondence function has an impact on the query result, both in the value of similarity between images and in the order in which images are sorted (see Section 7.1.1).

Bibliography

[AMN+94] Sunil Arya, David M. Mount, Nathan S. Netanyahu, Ruth Silverman, and Angela Y. Wu. An optimal algorithm for approximate nearest neighbor searching. In *Proceedings of the 5th Annual ACM-SIAM Symposium on Discrete Algorithms*, pages 573–582, Arlington, VA, January 1994.

[BBK98] Stefan Berchtold, Christian Böhm, and Hans-Peter Kriegel. The pyramid-technique: Towards breaking the curse of dimensionality. In *Proceedings of the 1998 ACM SIGMOD International Conference on Management of Data*, pages 142–153, Seattle, WA, June 1998.

[BBKK97] Stefan Berchtold, Christian Böhm, Daniel A. Keim, and Hans-Peter Kriegel. A cost model for nearest neighbor search in high-dimensional data space. In *Proceedings of the 16th ACM SIGACT-SIGMOD-SIGART Symposium on Principles of Database Systems (PODS'97)*, pages 78–86, Tucson, AZ, May 1997.

[BFM+96] Julio Barros, James French, Worthy Martin, Patrick Kelly, and Mike Cannon. Using the triangle inequality to reduce the number of comparisons required for similarity-based retrieval. In *Electronic Imaging '96, Storage and Retrieval for Still Image and Video Databases IV*, San Jose, CA, January 1996.

[BKK96] Stefan Berchtold, Daniel A. Keim, and Hans-Peter Kriegel. The X-tree: An index structure for high-dimensional data. In *Proceedings of the 22nd International Conference on Very Large Data Bases (VLDB'96)*, pages 28–39, Mumbai (Bombay), India, September 1996.

[BKSS90] Norbert Beckmann, Hans-Peter Kriegel, Ralf Schneider, and Bernhard Seeger. The R*-tree: An efficient and robust access method for points and rectangles. In *Proceedings of the 1990 ACM SIGMOD International Conference on Management of Data*, pages 322–331, Atlantic City, NJ, May 1990.

[BÖ97] Tolga Bozkaya and Meral Özsoyoglu. Distance-based indexing for high-dimensional metric spaces. In *Proceedings of the 1997 ACM SIGMOD International Conference on Management of Data*, pages 357–368, Tucson, AZ, May 1997.

[BP93] Roberto Brunelli and Tomaso Poggio. Face recognition: Features versus templates. *IEEE Transactions on Pattern Analysis and Machine Intelligence*, 15(10):1042–1052, 1993.

[Bri95] Sergey Brin. Near neighbor search in large metric spaces. In *Proceedings of the 21st International Conference on Very Large Data Bases (VLDB'95)*, pages 574–584, Zurich, Switzerland, September 1995.

[BYÖ97] Tolga Bozkaya, Nasser Yazdani, and Meral Özsoyoglu. Matching and indexing sequences of different lengths. In *Proceedings of the 6th International Conference on Information and Knowledge Management (CIKM'97)*, pages 128–135, Las Vegas, NE, November 1997.

[CA97] Weimin Chen and Karl Aberer. Efficient querying on genomic databases by using metric space indexing techniques. In *1st International Workshop on Query Processing and Multimedia Issues in Distributed Systems (PMIDS'97)*, Toulouse, France, September 1997.

[CG96] Surajit Chaudhuri and Luis Gravano. Optimizing queries over multimedia repositories. In *Proceedings 1996 ACM SIGMOD International Conference on Management of Data*, pages 91–102, Montreal, Canada, June 1996.

[Chi94] Tzi-cker Chiueh. Content-based image indexing. In *Proceedings of the 20th International Conference on Very Large Data Bases (VLDB'94)*, pages 582–593, Santiago, Chile, September 1994.

[Cia98] Paolo Ciaccia. An algebra for similarity queries and its index-based evaluation. Technical report, ESPRIT LTR Project HERMES (no. 9141), 1998. Available at URL `http://www.ced.tuc.gr/hermes/`.

[CNP99] Paolo Ciaccia, Alessandro Nanni, and Marco Patella. A query-sensitive cost model for similarity queries with M-tree. In *Proceedings of the 10th Australasian Database Conference (ADC'99)*, pages 65–76, Auckland, New Zealand, January 1999.

[CP98] Paolo Ciaccia and Marco Patella. Bulk loading the M-tree. In *Proceedings of the 9th Australasian Database Conference (ADC'98)*, pages 15–26, Perth, Australia, February 1998.

[CPZ97] Paolo Ciaccia, Marco Patella, and Pavel Zezula. M-tree: An efficient access method for similarity search in metric spaces. In *Proceedings of the 23rd International Conference on Very Large Data Bases (VLDB'97)*, pages 426–435, Athens, Greece, August 1997.

[CPZ98a] Paolo Ciaccia, Marco Patella, and Pavel Zezula. A cost model for similarity queries in metric spaces. In *Proceedings of the 16th ACM SIGACT-SIGMOD-SIGART Symposium on Principles of Database Systems (PODS'98)*, pages 59–68, Seattle, WA, June 1998.

[CPZ98b] Paolo Ciaccia, Marco Patella, and Pavel Zezula. Processing complex similarity queries with distance-based access methods. In *Proceedings of the 6th International Conference on Extending Database Technology (EDBT'98)*, pages 9–23, Valencia, Spain, March 1998.

[EKS+98] Martin Ester, Hans-Peter Kriegel, Jörg Sander, Michael Wimmer, and Xiaowei Xu. Incremental clustering for mining in a data warehousing environment. In *Proceedings of the 24th International Conference on Very Large Data Bases (VLDB'98)*, pages 323–333, New York City, NY, August 1998.

[Fag96] Ronald Fagin. Combining fuzzy information from multiple systems. In *Proceedings of the 15th ACM SIGACT-SIGMOD-SIGART Symposium on Principles of Database Systems (PODS'96)*, pages 216–226, Montreal, Canada, June 1996.

[FB74] Raphael A. Finkel and Jon Louis Bentley. Quad trees: A data structure for retrieval on composite keys. *Acta Informatica*, 4(1):1–9, 1974.

[FEF+94] Christos Faloutsos, Will Equitz, Myron Flickner, Wayne Niblack, Dragutin Petkovic, and Ron Barber. Efficient and effective querying by image content. *Journal of Intelligent Information Systems*, 3(3/4):231–262, July 1994.

[FK94] Christos Faloutsos and Ibrahim Kamel. Beyond uniformity and independence: Analysis of R-trees using the concept of fractal dimension. In *Proceedings of the 13th ACM SIGACT-SIGMOD-SIGART Symposium on Principles of Database Systems (PODS'94)*, pages 4–13, Minneapolis, MN, May 1994.

[FL95] Christos Faloutsos and King-Ip Lin. FastMap: A fast algorithm for indexing, data-mining and visualization of traditional and multimedia datasets. In *Proceedings of the 1995 ACM SIGMOD International Conference on Management of Data*, pages 163–174, San Jose, CA, June 1995.

[FSN+95] Myron Flickner, Harpreet Sawhney, Wayne Niblack, Jonathan Ashley, Qian Huang, Byron Dom, Monika Gorkani, Jim Hafner, Denis Lee, Dragutin Petkovic, David Steele, and Peter Yanker. Query by image and video content: The QBIC system. *IEEE Computer*, 28(9):23–32, September 1995. `http://wwwqbic.almaden.ibm.com/`.

[FW97] Ronald Fagin and Edward L. Wimmers. Incorporating user preferences in multimedia queries. In *Proceedings of the 6th International Conference on Database Theory (ICDT'97)*, pages 247–261, Delphi, Greece, January 1997.

[Gav94] D.M. Gavrila. R-tree index optimization. Technical Report CS-TR-3292, University of Maryland, College Park, 1994.

[GG96] Volker Gaede and Oliver Günther. Multidimensional access methods. Technical Report TR-96-043, International Computer Science Institute, Berkeley, CA, October 1996.

[Gut84] Antonin Guttman. R-trees: A dynamic index structure for spatial searching. In *Proceedings of the 1984 ACM SIGMOD International Conference on Management of Data*, pages 47–57, Boston, MA, June 1984.

[Har92] Donna Harman. Relevance feedback and other query modification techniques. In Williams B. Frakes and Ricardo A. Baeza-Yates, editors, *Information Retrieval: Data Structures and Algorithms*, chapter 11, pages 241–263. Prentice Hall PTR, 1992.

[HGH+96] Arun Hampapur, Amarnath Gupta, Bradley Horowitz, Chiao-Fe Shu, Charles Fuller, Jeffrey R. Bach, Monika Gorkani, and Ramesh Jain. Virage image search engine: An open framework for image management. In *Storage and Retrieval for Image and Video Databases SPIE*, volume 2670, pages 76–87, San Jose, CA, February 1996. `http://www.virage.com/`.

[HM95] Andreas Henrich and Jens-Uwe Möller. Extending a spatial access structure to support additional standard attributes. In *Proceedings of the 4th International Symposium on Advances in Spatial Databases (SSD'95)*, pages 132–151, Portland, ME, August 1995.

[HNP95] Joseph M. Hellerstein, Jeffrey F. Naughton, and Avi Pfeffer. Generalized search trees for database systems. In *Proceedings of the 21st International Conference on Very Large Data Bases (VLDB'95)*, pages 562–573, Zurich, Switzerland, September 1995. `http://gist.cs.berkeley.edu:8000/gist/`.

[Jai96] Ramesh Jain. Infoscopes: Multimedia information systems. In Borko Furht, editor, *Multimedia Systems and Techniques*, chapter 7, pages 217–253. Kluwer Academic Publishers, 1996.

[JD88] Anil K. Jain and Richard C. Dubes. *Algorithms for Clustering Data*. Prentice-Hall, 1988.

[Kan77] Takeo Kanade. *Computer Recognition of Human Faces*. Birkhauser, Basel and Stuttgart, 1977.

[KF93] Ibrahim Kamel and Christos Faloutsos. On packing R-trees. In *Proceedings of the 2nd International Conference on Information and Knowledge Management (CIKM'93)*, pages 490–499, Washington, DC, November 1993.

[KF94] Ibrahim Kamel and Christos Faloutsos. Hilbert R-tree: An improved R-tree using fractals. In *Proceedings of the 20th International Conference on Very Large Data Bases (VLDB'94)*, pages 500–509, Santiago, Chile, September 1994.

[KK72] Y. Kaya and K. Kobayashi. A basic study on human face recognition. In *Frontiers of Pattern Recognition*, pages 265–289. Academic Press, New York, 1972.

[KS97] Norio Katayama and Shin'ichi Satoh. The SR-tree: An index structure for high-dimensional nearest neighbor queries. In *Proceedings of the 1997 ACM SIGMOD International Conference on Management of Data*, pages 369–380, New York, NY, May 1997.

[KY95] Georg J. Klir and Baozung Yuan. *Fuzzy Sets and Fuzzy Logic; Theory and Applications*. Prentice Hall, 1995.

[LL91] Ki-Joune Li and Robert Laurini. The spatial locality and a spatial indexing method by dynamic clustering in hypermap systems. In *Proceedings of the 2nd International Symposium on Advances in Spatial Databases (SSD'91)*, pages 207–223, Zurich, Switzerland, August 1991.

[LLE97] Scott T. Leutenegger, Mario A. Lopez, and Jeffrey Edgington. STR: A simple and efficient algorithm for R-tree packing. In *Proceedings of the 13th International Conference on Data Engineering (ICDE'97)*, pages 497–506, Birmingham, UK, April 1997.

[LR94] Ming-Ling Lo and Chinya V. Ravishankar. Spatial joins using seeded trees. In *Proceedings of the 1994 ACM SIGMOD International Conference on Management of Data*, pages 209–220, Minneapolis, MN, June 1994.

[LR95] Ming-Ling Lo and Chinya V. Ravishankar. Generating seeded trees from data sets. In *Proceedings of the 4th International Symposium on Advances in Spatial Databases (SSD'95)*, pages 328–347, Portland, ME, August 1995.

[Man77] B. Mandelbrot. *The Fractal Geometry of Nature*. W.H.Freeman, New York, 1977.

[NHS84] Jürg Nievergelt, Hans Hinterberger, and Kenneth C. Sevcik. The grid file: An adaptable, symmetric multikey file structure. *ACM Transactions on Database Systems*, 9(1):38–71, March 1984.

[OS95] Virginia E. Ogle and Michael Stonebraker. Chabot: Retrieval from a relational database of images. *IEEE Computer*, 28(9):40–48, September 1995.

[PM97] Apostolos Papadopoulos and Yannis Manolopoulos. Performance of nearest-neighbor queries in R-trees. In *Proceedings of the 6th International Conference on Database Theory (ICDT'97)*, pages 394–408, Delphi, Greece, January 1997.

[PPS96] Alex Pentland, Rosalind W. Picard, and Stan Sclaroff. Photobook: Content-based manipulation of image databases. In Borko Furht, editor, *Multimedia Tools and Applications*, chapter 2, pages 43–80. Kluwer Academic Publishers, 1996.

[PTSE95] Dimitris Papadias, Yannis Theodoridis, Timos Sellis, and Max J. Egenhofer. Topological relations in the world of minimum bounding rectangles: a study with R-trees. In *Proceedings of the 1995 ACM SIGMOD International Conference on Management of Data*, pages 92–103, San Jose, CA, May 1995.

[RKV95] Nick Roussopoulos, Stephen Kelley, and Frédéric Vincent. Nearest neighbor queries. In *Proceedings of the 1995 ACM SIGMOD International Conference on Management of Data*, pages 71–79, San Jose, CA, May 1995.

[RL85] Nick Roussopoulos and Daniel Leifker. Direct spatial search on pictorial databases using packed R-trees. In *Proceedings of the 1985 ACM SIGMOD International Conference on Management of Data*, pages 17–31, Austin, TX, May 1985.

[Sam89] Hanan Samet. *The Design and Analysis of Spatial Data Structures*. Addison-Wesley, Redding, MA, 1989.

[SC96] John R. Smith and Shih-Fu Chang. VisualSEEk: A fully automated content-based image query system. In *Proceedings of the 4th ACM International Conference on Multimedia*, pages 87–98, Boston, MA, November 1996. `http://www.ctr.columbia.edu/visualseek/`.

[Sco92] David W. Scott. *Multivariate Density Estimation. Theory, Practice and Visualization*. Wiley-Interscience, New York, 1992.

[Sha77] Marvin Shapiro. The choice of reference points in best-match file searching. *Communications of the ACM*, 20(5):339–343, 1977.

[SJ98] Simone Santini and Ramesh Jain. Similarity matching. To appear in *IEEE Transactions on Pattern Analysis and Machine Intelligence*, 1998.

[SK88] Bernhard Seeger and Hans-Peter Kriegel. Techniques for design and implementation of efficient spatial access methods. In *Proceedings of the 14th International Conference on Very Large Data Bases (VLDB'88)*, pages 360–371, Los Angeles, CA, August 1988.

[SK97] Thomas Seidl and Hans-Peter Kriegel. Efficient user-adaptable similarity search in large multimedia databases. In *Proceedings of the 23rd International Conference on Very Large Data Bases (VLDB'97)*, pages 506–515, Athens, Greece, August 1997.

[SK98] Thomas Seidl and Hans-Peter Kriegel. Optimal multi-step k-nearest neighbor search. In *Proceedings of the 1998 ACM SIGMOD International Conference on Management of Data*, pages 154–165, Seattle, WA, June 1998.

[Smi97] John R. Smith. *Integrated Spatial and Feature Image Systems: Retrieval, Analysis and Compression*. PhD thesis, Columbia University, 1997.

[SO95] Markus Stricker and Markus Orengo. Similarity of color images. In *Storage and Retrieval for Image and Video Databases SPIE*, volume 2420, pages 381–392, San Jose, CA, February 1995.

[SRF87] Timos Sellis, Nick Roussopoulos, and Christos Faloutsos. The R+-tree: A dynamic index for multi-dimensional objects. In *Proceedings of the 13th International Conference on Very Large Data Bases (VLDB'87)*, pages 507–518, Brighton, England, September 1987.

[SZ+96] Avi Silberschatz, Stan Zdonik, et al. Strategic directions in database systems — breaking out of the box. *ACM Computing Surveys*, 28(4):764–778, December 1996.

[TP91] Matthew Turk and Alex Pentland. Eigenfaces for recognition. *Journal of Cognitive Neuroscience*, 3(1):71–87, 1991.

[TS96] Yannis Theodoridis and Timos Sellis. A model for the prediction of R-tree performance. In *Proceedings of the 15th ACM SIGACT-SIGMOD-SIGART Symposium on Principles of Database Systems (PODS'96)*, pages 161–171, Montreal, Canada, June 1996.

[Uhl91] Jeffrey K. Uhlmann. Satisfying general proximity/similarity queries with metric trees. *Information Processing Letters*, 40(4):175–179, November 1991.

[vdBSW97] Jochen van den Bercken, Bernhard Seeger, and Peter Widmayer. A generic approach to bulk loading multidimensional index structures. In *Proceedings of the 23rd International Conference on Very Large Data Bases (VLDB'97)*, pages 406–415, Athens, Greece, August 1997.

[Wal91] Gregory K. Wallace. The JPEG still picture compression standard. *Communications of the ACM*, 34(4):30–44, April 1991.

[WBKW96] Erling Wold, Thom Blum, Douglas Keislar, and James Wheaton. Content-based classification, search, and retrieval of audio. *IEEE Multimedia*, 3(3):27–36, 1996.

[WJ96] David A. White and Ramesh Jain. Similarity indexing with the SS-tree. In *Proceedings of the 12th International Conference on Data Engineering (ICDE'96)*, pages 516–523, New Orleans, LO, February 1996.

[WSB98] Roger Weber, Hans-Jörg Schek, and Stephen Blott. A quantitative analysis and performance study for similarity-search methods in high-dimensional spaces. In *Proceedings of the 24th International Conference on Very Large Data Bases (VLDB'98)*, pages 194–205, New York, NY, August 1998.

[WZ96] Hugh Williams and Justin Zobel. Indexing nucleotide databases for fast query evaluation. In *Proceedings of the 5th International Conference on Extending Database Technology (EDBT'96)*, pages 275–288, Avignon, France, March 1996.

[Yia93] Peter N. Yianilos. Data structures and algorithms for nearest neighbor search in general metric spaces. In *Proceedings of the 4th ACM-SIAM Symposium on Discrete Algorithms (SODA'93)*, pages 311–321, Austin, TX, January 1993.

[Zad65] Lotfi Asker Zadeh. Fuzzy sets. *Information and Control*, 8:338–353, 1965.

[ZCF+97] Carlo Zaniolo, Stefano Ceri, Christos Faloutsos, Richard T. Snodgrass, V.S. Subrahmanian, and Roberto Zicari, editors. *Advanced Database Systems*. Morgan Kaufmann, San Francisco, 1997.

[ZSAR98] Pavel Zezula, Pasquale Savino, Giuseppe Amato, and Fausto Rabitti. Approximate similarity retrieval with M-trees. *The VLDB Journal*, 7(4):275–293, 1998.

"In my end is my beginning"
Thomas Stearn Eliot